JOURNAL OF GEOPHYSICAL RESEARCH

The continuation of

TERRESTRIAL MAGNETISM AND ATMOSPHERIC ELECTRICITY

(1896-1948)

An International Quarterly

VOLUME 60 June, 1955 NUMBER 2

CONTENTS

(Contents concluded on outside back cover)

Published at

THE WILLIAM BYRD PRESS, INC.

P. O. BOX 2-W, SHERWOOD AVE. AND DURHAM ST.

RICHMOND 5, VIRGINIA

Address all correspondence to

JOURNAL OF GEOPHYSICAL RESEARCH

5241 BROAD BRANCH ROAD, NORTHWEST

WASHINGTON 15, D.C., U.S.A.

SIX DOLLARS A YEAR SINGLE NUMBERS, TWO DOLLARS

JOURNAL OF GEOPHYSICAL RESEARCH

The continuation of

Terrestrial Magnetism and Atmospheric Electricity

(1896-1948)

An International Quarterly

Founded 1896 by L. A. BAUER *Continued 1928-1948 by* J. A. FLEMING

Editor: MERLE A. TUVE *Editorial Assistant:* WALTER E. SCOTT

Honorary Editor: J. A. FLEMING

Fields of Interest

Terrestrial Magnetism
Atmospheric Electricity
The Ionosphere
Solar and Terrestrial Relationships
Aurora, Night Sky, and Zodiacal Light
The Ozone Layer
Meteorology of Highest Atmospheric Levels
The Constitution and Physical States of the Upper Atmosphere
Special Investigations of the Earth's Crust and Interior, including experimental seismic waves, physics of the deep ocean and ocean bottom, physics in geology
And similar topics

This Journal serves the interests of investigators concerned with terrestrial magnetism and electricity, the upper atmosphere, the earth's crust and interior by presenting papers of new analysis and interpretation or new experimental or observational approach, and contributions to international collaboration. It is not in a position to print, primarily for archive purposes, extensive tables of data from observatories or surveys, the significance of which has not been analyzed.

Forward *manuscripts* to one of the Associate Editors, or to the editorial office of the Journal at 5241 Broad Branch Road, Northwest, Washington 15, D. C., U. S. A. It is preferred that manuscripts be submitted in English, but communications in French, German, Italian, or Spanish are also acceptable. A brief abstract, preferably in English, must accompany each manuscript. A *publication charge* of $8 per page will be billed by the Editor to the institution which sponsors the work of any author; private individuals are not assessed page charges. Manuscripts from outside the United States are invited, and should not be withheld or delayed because of currency restrictions or other special difficulties relating to page charges. Costs of publication are roughly twice the total income from page charges and subscriptions, and are met by subsidies from the Carnegie Institution of Washington and international and private sources.

Back issues and *reprints* are handled by the Editorial Office, 5241 Broad Branch Road, N.W. Washington 15, D.C., U.S.A.

Subscriptions are handled by the Editorial Office, 5241 Broad Branch Road, N.W., Washington 15, D.C., U.S.A.

Entered as second-class matter at the Post Office at Richmond, Virginia, under the act of March 3, 1879.

Journal of

GEOPHYSICAL RESEARCH

The continuation of

Terrestrial Magnetism and Atmospheric Electricity

VOLUME 60 JUNE, 1955 No. 2

THE SUNSPOT CYCLE, 649 B.C. TO A.D. 2000

BY D. JUSTIN SCHOVE

St. David's College, Beckenham, Kent, England

(Received December 28, 1954)

ABSTRACT

Annual sunspot numbers since 1700 and the known maxima and minima since 1610 show a similarity of pattern from century to century. This suggests that the mean cycle is approximately 11-1/9 years.

The records of sunspots and aurorae enable magnitudes and dates of sunspot maxima since at least A.D. 300 to be estimated. The constancy of the mean cycle over long periods enables the number of missing maxima to be calculated, and, using certain general principles, a table of minima complete since at least 200 B.C. can be established. A 78-year cycle appears to exist in the length of the sunspot cycle and an irregular cycle of about 200 to 205 years may exist in auroral intensity. A characteristic pattern in even centuries enables some predictions to be made for the next 50 years. Intervals between intense maxima in the range 200 to 1,000 years apart show clusters at certain values; these values are close to multiples of 11.11. Intervals between well-dated maxima since A.D. 300 are often slightly less than such multiples, for example, 554 instead of 555; from B.C. 200 to A.D. 300, intervals are slightly greater. In classical and early medieval times the cycle was thus slightly less. The variability of the sunspot cycle is only apparent. The fundamental rhythm of 11.1 years (together with the 78-year cycle) is constant through the centuries; temporary aberrations are

partly due to variations in sunspot intensity, inasmuch as active cycles tend to become "early" and weak cycles "late."

1. *Introduction.*

Sunspot numbers form a long and reliable series since A.D. 1749, and using the calculations of Wolf [see 1 of "References" at end of paper] can be extended (Table 1), on an annual basis, back to A.D. 1700. The 11-year solar cycle has been

TABLE 1—*Annual sunspot numbers, A.D. 1700–1953 (information partly supplied by H. W. Newton)*
—Part *A*

Note: The value for 1700 was (6); values in parentheses are less certain than the others.

Period	Schove remainder										
	1	2	3	4	5	6	7	8	9	10	11/0
1701–1711	(12)	(19)	26	39	60	32	23	12	9	(3)	0
1712–1722	0	2	12	31	50	65	(62)	42	31	29	(25)
1723–1733	(12)	24	43	80	112	(100)	(75)	(50)	(31)	(12)	(6)
1734–1744	(20)	(37)	(72)	82	(106)	98	(75)	(44)	23	18	(6)
1745–1755	12	25	44	62	81	83	48	48	31	12	10
1756–1766	10	32	48	54	63	86	61	45	36	21	11
1767–1777	38	70	106	101	82	67	35	31	7	20	93
1778–1788	154	126	85	68	39	23	10	24	83	132	131
1789–1799	118	90	67	60	47	41	21	16	6	4	7
1800	15										
Mean.....	39	48	56	64	71	66	46	35	29	28	32
Smoothed mean	41	48	54	61	61	56	49	41	34	33	35

TABLE 1 (*Continued*)—Part *B*

Period	Schove remainder										
	1	2	3	4	5	6	7	8	9	10	11/0
1801–1811	34	45	43	47	42	28	10	8	3	0	1
1812–1822	5	12	14	35	46	41	30	24	16	7	4
1823–1833	2	9	17	36	50	63	67	71	48	27	9
1834–1844	13	57	121	138	103	86	63	37	24	11	15
1845–1855	40	61	99	124	96	67	65	54	39	21	7
1856–1866	4	23	55	94	96	77	59	44	47	31	16
1867–1877	7	37	74	139	111	102	66	45	17	11	12
1878–1888	3	6	32	54	60	64	63	52	25	13	7
1889–1899	6	7	36	73	85	78	64	42	26	27	12
1900	9										
Mean.....	12	29	55	82	77	67	54	42	27	16	9
Smoothed mean	24	37	51	62	67	64	53	41	30	21	19

TABLE 1 (*Concluded*)—Part C

Period	Schove remainder										
	1	2	3	4	5	6	7	8	9	10	11/0
1901–1911	3	5	24	42	63	54	62	49	44	19	6
1912–1922	4	1	10	47	57	104	81	64	38	26	14
1923–1933	6	17	44	64	69	78	65	36	21	11	6
1934–1944	9	36	80	114	110	88.8	67.8	47.5	30.6	16.3	9.6
1945–1955	33.2	92.6	151.6	136.3	134.7	83.9	69.4	31.5	13.9	( )	( )
Sum.....	55	152	310	403	434	409	345	228	148	.....	.....
Mean.....	11	30	62	81	87	82	69	46	30	.....	.....

reliably traced back to about 1610, when sunspots were discovered through the telescope. No explanation of the cycle has proved satisfactory, and current estimates of its mean length vary according to the period selected for investigation. Prediction of future sunspot numbers and cycles is important but harmonic analysis has proved unsuccessful and there has been little agreement among scientists as to a suitable basis for forecasting.

Records of aurorae and sunspots extend back to at least the fifth century B.C., and an attempt to trace the solar maxima of intervening centuries appears to offer a basis for theoretical and mathematical investigations.

2. *Sunspot Numbers since A.D.* 1700.

From A.D. 1749, the annual sunspot numbers in Table 1 are the unaltered Zurich figures as calculated by Wolf and his successors. It is not generally known that Wolf also extended his calculations back to 1700, and indeed his estimates [1] have suffered neglect, because they were never revised to the same basis as his later values. Thus, the values for 1749 and 1750 were given by Wolf in 1868 as 63.8 and 68.2. As these two years are now credited with sunspot numbers of 80.9 and 83.4, Wolf's earlier figures have likewise been increased by 24.4 per cent for tabulation here. Many values—here indicated by parentheses—were obtained by interpolation or data that Wolf considered inadequate; on the other hand, he indicated that his figures for certain years (1705, 1709, 1716, 1717, 1719, 1749, and 1750) were especially reliable.

The evidence of auroral observations suggests that these revised values are still too low in the 1720's and 1730's. At the same time, for many purposes the figures are useful, and in particular they show clearly the phase of the 11-year sunspot cycle.

3. *The Sunspot Cycle since A.D.* 1600.

Annual figures are not available for the seventeenth century, but the Zurich dates of maxima and minima from 1610 onwards have been calculated with fair reliability, and these dates have been included in my Tables 2 and 3.

4. *The Length of the Sunspot Cycle.*

The well-known 11-year cycle has varied in practice between 8 and 16 years; so far in the present century, it has been a cycle of 10 years. The length of the *mean* cycle is variously regarded by different authors as 10.83, 11.1 and 11.4 years. It certainly differs little from 11.11 or 100 divided by 9, because maxima and minima tend to occur within corresponding groups of years in each century. Thus, maxima occur in 16**39**, 17**38**, 18**37**, and 19**37**, whilst minima occur in 16**10**, 17**12**, 18**10**, and 19**13**.

5. *The Phase of the Sunspot Cycle.*

In accordance with the rule just indicated, the years of sunspot minima tend to be approximately divisible by 11. Examples are 16**55**, 16**66**, 17**55**, 18**33**, and 19**33**.

The phase of a particular cycle can be loosely defined by the *remainder* when multiples of 11 have been deducted from the last two digits of the years of minima. Thus, in the past three centuries, a remainder of 5 has been typical. The phase of a maximum near the turn of a century is ambiguous. Thus, 700 may be regarded as a seventh-century maximum with remainder 1 or an eighth-century maximum with remainder 0.

6. *Prediction of Future Cycles.*

Prediction of sunspot cycles is hampered by the variable length of the period between successive maxima. The last great maximum was expected by some scientists to fall in 1949, a year with a typical remainder of 5, but for some reason it arrived early, in 1947, a year with a remainder of 3 [2]. Some success is being achieved in the prediction of sunspot numbers from month to month and year to year [3]; Gleissberg has predicted that the next minimum will lie between March and July 1955 and will be followed by another intense maximum between August 1958 and August 1959.

The ultimate test of all theories and formulae must lie in prediction. A successful prediction of a single maximum would not be decisive; a formula relating to the maxima before A.D. 1600 would, however, be subject to proof or disproof, provided that the dates of early maxima can be determined from historical evidence.

7. *Sunspot Cycles before A.D.* 1600.

A preliminary attempt to determine the years of sunspot maxima was made in the nineteenth century by Fritz, whose results [4] are those generally quoted. His analysis was however somewhat uncritical, and the evidence was fitted rather arbitrarily into an 11-year scheme. (*a*) *Sunspots* and (*b*) *aurorae* are, of course, indicators of the cycle, but (*c*) *hail* and (*d*) *wine harvests* in Central Europe were also used in the analysis. It is now clear that no valid conclusions about sunspot cycles can be gleaned from references to weather and harvests. The results of (*e*) *tree-ring analysis* and (*f*) *earthquakes* may possibly prove useful eventually. The data from tropical trees used by de Boer [5] and from earthquakes in different parts of the world used by Davison [6] lead to maxima in the sixteenth century that are not inconsistent with those determined from auroral records and pre-

sented here. At the same time, my own investigations of tree-ring data do not give grounds for optimism [7].

The rather shaky foundations of the final table of Fritz must now be disregarded. On the other hand, his tables for sunspots and aurorae separately were recently combined and retabulated [8], because many of his results have been confirmed by the present extended investigation.

8. *Ancient Aurorae and Sunspots.*

There are numerous records of sunpots seen with the naked eye and of ancient displays of northern lights [9] in different parts of the world. These were collected initially as by-products of a collection of meteorological chronologies, chronologies which have been sent to me in connection with the so-called "Spectrum of Time" project [10].

9. *The Estimation of Years of Maxima.*

The evidence of aurorae and sunspots can be used to prepare a table of years of maxima subject to certain assumptions. Thus, in the preparation of Table 2, it has been assumed that

(*a*) The time between successive maxima was never less than 8 and never more than 16 years.
(*b*) There are 9 maxima in 100 years.

These two assumptions have proved valid since A.D. 1515 [8, 11]; indeed, despite the irregularity of individual cycles, large departures from eleven do not persist for many cycles. There are 30-year groups when the cycle is longer (for example, centred c. 1650/55, 1720, 1805/10, 1885/90) and intervening groups when it is shorter (for example, centred c. 1685, 1760/65, c. 1845, c. 1935). The mean length of seven cycles has lain between 10 and 12 years for at least two and one-half centuries.

These two generalizations, together with the principles outlined below, enabled the maxima of Table 2 to be determined. Some doubt still exists about the dates in parentheses; dates before 502 B.C. depend only on somewhat dubious evidence for aurorae in China, and dates from 502 to 460 on the B.C. dating implied by Livy. The Greek evidence for the fifth century B.C. has not been used, as it has not been possible to differentiate between comets and aurorae [12].

10. *The Numbering of Minima and Maxima.*

The system of numbering adopted is a decimal one, based on the phase-rule already indicated. Thus, in recent centuries, the year endings of sunspot minima tend to follow the pattern

'00 '11 '22 '33 . . . '88 '99/00

and they are indicated by

.0 .1 .2 .3 . . . .8 .0

An additional minimum involves the inclusion of a term ending in .9. The intervening maxima are thus denoted by decimals .05, .15, .25 . . . .85, .05. In early centuries, it is the maxima that follow the eleven-times table rule.

TABLE 2—*Sunspot cycles since B.C. 649* (November 1954)

Number of max.	Year of max.	Probable error	Remainder	Intensity of maximum	Years since p. max.	Years since p. min.	Min.	Rem.
−6.45	−648	3	8	S(?)	..	..	(−653)	3
−5.25	−522	3	12	S(?)	..	5	(−527)	7
−5.15	(−512)	4	11	..	(10)	4	(−516)	7
−5.05	−501	2	11	S(?)	(11)	4	(−505)	7
−4.85	(−491)	4	9	W–M	(10)	5	(−496)	4
−4.75	−481	2	8	S	10	5	−486	3
−4.65	−471	2	7	S	10	3	−474	4
−4.55	−461	2	6	S	10	4	−465	2
−3.85	−393	3	7	S	..	6	−397	3
−3.75	.....	..	..	..	..	..	−386	3
−3.65	.....	..	..	..	..	..	(−375)	..
−3.55	.....	..	..	..	..	..	(−365)	..
−3.45	−349	3	7	S	..	5	−354	2
−3.35	−340	3	5	S	9	4	−344	1
−3.25	.....	..	..	..	..	..	−332	2
−2.85	(−293)	4	9	..	..	..	(−298)	2
−2.75	(−283)	4	8	..	..	..	(−288)	1
−2.65	−272	3	6	X	..	(5)	−277	1
−2.55	(−261)	4	6	..	..	..	−266	1
−2.45	(−249)	4	7	..	..	..	(−254)	2
−2.35	−236	3	9	X	..	6	−243	3
−2.25	−223	3	11	X	13	7	−230	4
−2.15	−214	2	9	S	9	5	−219	4
−2.05	−205	2	7	S	9	5	−210	2
−1.85	−192	2	8	S	13	7	−199	2/1
−1.75	−182	3	7	WM	10	5	−187	2
−1.65	−172	3	6	WM	10	5	−177	1
−1.55	−163	3	4	S	9	4	−167	0
−1.45	(−149)	4	(7)	W	(14)	(5)	(−154)	2
−1.35	−135	3	10	M	(14)	6	−141	4
−1.25	−125	3	9	MS	10	4	−129	5
−1.15	−113	2	10	S	12	6	−119	4
−1.05	−104	2	8	S	9	4	−108	4
−0.85	−91	2	9	SS	13	5	−96	4
−0.75	(−82)	4	7	M	(9)	4	(−86)	3
−0.65	(−72)	3	6	WM	(10)	5	(−77)	1
−0.55	−62	2	5	SS	10	7	−69	−2
−0.45	−53	2	3	SS	9	5	−58	−2
−0.35	−42	3	3	MS	11	4	−46	−1
−0.25	−27	2	7	S	15	5	(−32)	2
−0.15	−16	3	7	WM	11	5	−21	2
−0.05	(− 5)	4	7	WM	(11)	(6)	−11	1

TABLE 2—*Sunspot cycles since B.C. 649*—Continued

Number of max.	Year of max.	Probable error	Remainder	Intensity of maximum	Years since p. max.	Years since p. min.	Min.	Rem.
+0.05	(A.D.8)	4	(8)	W or M	13	5	(3)	3
0.15	20	3	9	S	12	5	15	4
0.25	(31)	4	(9)	W or M	(11)	(5)	26	4
0.35	42	3	9	W or M	(11)	5	37	4
0.45	53	3	9	S	11	6	47	3
0.55	65	3	10	S	12	5	60	5
0.65	(76)	4	(10)	W or M	(11)	6	(70)	4
0.75	(86)	4	(9)	W or M	(10)	6	(80)	3
0.85	(96)	4	(8)	W or M	(10)	5	(91)	3
1.05	105	3	5	M or S	9	4	101	1
1.15	(118)	4	7	W or M	(13)	6	112	1
1.25	(130)	4	8	W or M	(12)	6	(124)	2
1.35	(141)	4	8	W or M	(11)	6	(135)	2
1.45	(152)	4	8	W or M	(11)	6	(146)	2
1.55	(163)	4	8	W or M	(11)	6	(157)	2
1.65	175	3	9	M or S	(12)	5	170	4
1.75	186	3	9	S	11	4	182	5
1.85	196	3	8	S	10	4	192	4
2.05	(208)	4	8	X	(12)	5	203	3
2.15	(219)	4	8	X	(11)	5	(214)	3
2.25	(230)	4	8	X	(11)	5	(225)	3
2.35	(240)	4	7	X	(10)	5	(235)	2
2.45	(252)	4	8	X	(12)	5	(247)	3
2.55	(265)	4	10	X	(13)	5	(260)	5
2.65	(277)	4	11	X	(12)	5	(272)	6
2.75	290	3	13	M or S	13	6	(284)	7
2.85	302	1	14/13	SS	12	6	296	8
2.85	302	1	13	See previous row				
3.05	311	1	11	M	9	4	307	7
3.15	321	1	10	M	10	4	317	6
3.25	330	3	8	W	9	4	326	4
3.35	342	2	9	W	12	6	336	3
3.45	354	2	10	S	12	6	348	4
3.55	362	3	7	S	8	4	358	3
3.65	372	1	6	SS	10	4	368	2
3.75	387	3	10	M	15	7	380	3
3.85	396	3	8	M	9	5	391	3
4.05	410	4	10	W	14	6	404	4
4.15	(421)	4	(10)	W	11	5	416	5
4.25	430	1	8	M or S	9	4	426	4
4.35	441	1	8	M or S	11	4	437	4
4.45	452	2	8	S	11	4	448	4
4.55	(465)	4	(10)	W	(13)	6	459	4
4.65	479	1	13	M or S	(14)	7	472	6
4.75	490	1	13	M	11	6	484	7
4.85	501	1	13/12	SS	11	6	495	7

TABLE 2—*Sunspot cycle since B.C. 649*—Continued

Number of max.	Year of max.	Probable error	Remainder	Intensity of maximum	Years since p. max.	Years since p. min.	Min.	Rem.
4.85	501	1	12	See previous row				
5.05	511	1	11	S	10	4	507	7
5.15	522	2	11	W or M	11	5	517	6
5.25	531	1	9	S	9	5	526	4
5.35	542	3	9	M	11	4	538	5
5.45	557	1	13	M	15	6	551	7
5.55	567	1	12	SS	10	5	562	7
5.65	578	2	12	M	11	5	573	7
5.75	585	3	8	S	7	3	582	5
5.85	597	2	9	W or M	12	5	592	4
6.05	(607)	4	(7)	W	10	5	(602)	2
6.15	618	2	7	M	11	5	613	2
6.25	628	3	6	W–M	10	5	623	1
6.35	642	2	9	M	14	5	637	4
6.45	654	2	10	M–S	12	5	649	5
6.55	665	2	10	M	11	5	660	6
6.65	677	2	10	S	12	6	671	5
6.75	(689)	4	13	W	12	5	684	7
6.85	(699)	4	12	W	10	6	(693)	5
7.05	714	1	14	S	15	7	(707)	7
7.15	724	1	13	S	10	5	719	8
7.25	735	3	13	W	11	5	730	8
7.35	745	1	12	SS	10	6	739	6
7.45	754	2	10	M	9	5	(749)	5
7.55	765	1	10	SS	11	4	761	6
7.65	(776)	4	10	MS	(11)	6	(770)	4
7.75	(787)	4	10	W	(11)	5	(782)	5
7.85	(798)	4	10	MS	(11)	5	(793)	5
8.05	809	1	9	S	11	5	804	4
8.15	821	3	10	W	12	6	815	4
8.25	829	2	8	S	8	4	825	4
8.35	840	1	7	SS	11	4	836	3
8.45	850	1	6	MS	10	4	846	2
8.55	862	1	7	M	12	6	856	1
8.65	872	3	6	S	10	4	868	2
8.75	887	3	10	M	15	5	882	5
8.85	898	3	10	W	11	5	893	5
9.05	907	2	7	W	8	5	902	2
9.15	917	2	6	M	11	5	912	1
9.25	926	1	4	SS	9	5	921	−1
9.35	938	2	5	MS	12	4	934	1
9.45	(950)	3	6	WM	12	5	(945)	1
9.55	963	2	8	SS	13	4	959	4
9.65	974	3	8	SS	11	4	970	4
9.75	986	2	9	M	12	4	982	5
9.85	(994)	2	6	W	8	(4)	(990)	2

TABLE 2—*Sunspot cycles since B.C. 649*—Continued

Number of max.	Year of max.	Probable error	Remainder	Intensity of maximum	Years since p. max.	Years since p. min.	Min.	Rem.
10.05	1003	1	3	S	9	(5)	(998)	−1/−2
10.15	1016	1	5	M	13	5	1010	−1
10.25	1027	1	5	M	11	5	1022	0
10.35	1038	3	5	W	11	4	1034	+1
10.45	(1052)	4	8	WW	14	5	(1047)	3
10.55	1067	4	12	M	15	7	(1060)	5
10.65	1078	2	12	M	11	7	1071	5
10.75	1088	1	11	M	10	6	1082	5
10.85	1098	1	10	SS	10	6	1092	4
11.05	(1110)	3	10	WM	12	4	1106	6
11.15	1118	1	7	SS	8	3	1115	4
11.25	1129	1	7	S	11	5	1124	2
11.35	1138	1	5	SS	9	4	1134	1
11.45	1151	1	7	S	13	6	1145	1
11.55	1160	2	4	WM	9	5	1155	0
11.65	1173	1	7	MS	13	6	1167	1
11.75	1185	1	8	MS	12	5	1180	3
11.85	1193	1	5	M	8	3	1190	2
12.05	1202	1	2	SS	9	3	1199	0/−1
12.15	1219	3	8	M	17	7	1212	1
12.25	1228	1	6	M	9	4	1224	2
12.35	1239	3	6	M	11	6	1233	0
12.45	1249	3	5	WM	10	5	1244	0
12.55	1259	2	4	M	10	3	1256	1
12.65	1276	3	10	M	17	7	(1269)	3
12.75	1288	1	11	M	12	6	1282	5
12.85	1296	3	8	W	8	5	(1291)	3
13.05	1308	2	8	M	12	7	1301	1
13.15	1316	2	5	M	8	5	1311	0
13.25	1324	2	2	M	8	5	1319	−3
13.35	1337	3	4	W	13	5	1332	−1
13.45	1353	2	9	WM	16	7	1346	+2
13.55	1362	2	7	SS	9	4	1358	3
13.65	1372	1	6	SSS	10	4	1368	2
13.75	1382	2	5	MS	10	4	1378	1
13.85	1391	3	3	M	9	5	1386	−2
14.05	1402	1	2	M	11	6	1396	−3/−4
14.15	(1413)	3	2	WW	11	6	1407	−4
14.25	(1429)	4	7	WM	16	8	(1421)	−1
14.35	(1439)	3	6	WM	10	5	1434	+1
14.45	1449	4	5	WM	10	6	1443	−1
14.55	1461	3	6	WM	12	4	1457	2
14.65	(1472)	4	6	WW	11	4	1468	2
14.75	(1480)	4	3	WW	8	4	(1476)	−1
14.85	1492	4	4	WM	12	4	(1488)	0

TABLE 2—*Sunspot cycles since B.C. 649*—Concluded

Number of max.	Year of max.	Probable error	Remainder	Estimated sunspot number	Intensity of max.	Years since p. max.	Years since p. min.	Min.	Rem.
15.05	1505	3	5	(60)	W	13	7	1498	−1/−2
15.15	1519	1	8	(80)	M	14	7	1512	+1
15.25	1528	1	6	(150)	SS	9	3	1525	+3
15.35	1539	1	6	(130)	S	11	4	1535	+2
15.45	1548	1	4	(120)	S	9	5	1543	−1
15.55	1558	1	3	(160)	SS	10	5	1553	−2
15.65	1572	1	6	(150)	SS	14	5	1567	+1
15.75	1581	1	4	(130)	S	9	3	1578	+1
15.85	1591	2	3	(70)	WM	10	4	1587	−1
16.05	1604.5	2	4	(80)	WM	13	5	1599.5	0/−1
16.15	1615.5	1	4	(90)	M	11	4.7	1610.8	−0.7
16.25	1626.0	1	3.5	(100)	MS	10.5	7	1619.0	−3.5
16.35	1639.5	1	6	(70)	WM	13.5	5.5	1634.0	+0.5
16.45	1649.0	1	4.5	(40)	WW	9.5	4	1645.0	+0.5
16.55	1660.0	1	4.5	(50)	WW	11.0	5	1655.0	−0.5
16.65	1675.0	1	8.5	(60)	W	15.0	9	1666.0	−0.5
16.75	1685.0	1	7.5	(50)	WW	10.0	5.5	1679.5	+2
16.85	1693.0	1	4.5	(30)	WWW	8.0	3.5	1689.5	+1
17.05	1705.5	1	5.0	(50)	WW	12.5	7.5	1698.0	−1.5/−2.5
17.15	1718.2	1	6.7	(130)	S	12.7	6.2	1712.0	+0.5
17.25	1727.5	1	5.0	(140)	SS	9.3	4.0	1723.5	+1.0
17.35	1738.7	1	5.2	(110)	S	11.2	4.7	1734.0	+0.5
17.45	1750.3	..	5.8	80	M	11.6	5.3	1745.0	+0.5
17.55	1761.5	..	6.0	90	M	11.2	6.3	1755.2	−0.3
17.65	1769.7	..	3.2	110	S	8.2	3.2	1766.5	0
17.75	1778.4	..	+0.9	150	SS	8.7	2.9	1775.5	−2.0
17.85	1788.1	..	−0.4	130	S	9.7	3.4	1784.7	−3.8
18.05	1805.2	..	+4.7	50	WW	17.1	6.9	1798.3	−1.2/−2.2
18.15	1816.4	..	4.9	50	WW	11.2	5.8	1810.6	−0.9
18.25	1829.9	..	7.4	70	WM	13.5	6.6	1823.3	−0.8
18.35	1837.2	..	3.7	140	SS	7.3	3.3	1833.9	+0.4
18.45	1848.1	..	3.6	120	S	10.9	4.6	1843.5	−1.0
18.55	1860.1	..	4.6	100	MS	12.0	4.1	1856.0	+0.5
18.65	1870.6	..	4.1	140	SS	10.5	3.4	1867.2	+0.7
18.75	1883.9	..	6.4	60	W	13.3	5.0	1878.9	+1.4
18.85	1894.1	..	5.6	90	M	10.2	4.5	1889.6	+1.1
19.05	1907.0	..	6.5	60	W	12.9	5.3	1901.7	+1.2
19.15	1917.6	..	6.1	100	MS	10.6	4.0	1913.6	+2.1
19.25	1928.4	..	5.9	80	WM	10.8	4.8	1923.6	+1.1
19.35	1937.4	..	2.9	110	S	9.0	3.6	1933.8	+0.3
19.45	1947.5	..	3.0	150	SS	10.1	3.3	1944.2	−0.2
19.55	(1958.5)	2	(3)	...	SS	....	(4)	(1954.5)	(−1)
19.65	(1972.5)	2	(6)	...	M/S	....	(6)	(1966.5)	(0)
19.75	(1984.5)	2	(7)	...	SS	....	(6)	(1978.5)	(+1)
19.85	(1994.5)	2	(6)	...	S	....	(5)	(1989.5)	(+1)
20.05	(2004.5)	2	(5/4)	...	M/S	....	(4)	(2000.5)	(1/0)
20.15	(2014.5)	2	(3)	...	M	....	(5)	(2009.5)	(−2)
20.25	(2025.5)	2	(4)	...	..	....	...	.....	.....

11. *Probable Error.*

Wherever a sunspot cycle has been interpolated without definite evidence, the year has been indicated in parentheses and the probable error has been regarded as 4. A probable error of 3 indicates ambiguity in the interpretation. For purposes of mathematical analysis, the dates of cycles of both these kinds should be excluded.

Modern investigations suggest that the phase of the auroral cycle is slightly later than the sunspot cycle [12], and the great aurorae associated with intense maxima (S) occur between $S - 2$ and $S + 3$ years. On the other hand, sunspot maxima that are weak or "late" (that is, with high remainders), or those near the onset of an aurorally weak period, often appear to be associated with double or diffuse auroral maxima, and in these cycles the minima are more readily dated than the maxima. There may be persistent bias in our dating of ± 0.3 year either for these reasons or for the inevitable personal equation.

12. *Remainders.*

In order to avoid minus signs, the "remainders" in Table 2 have been expressed as follows:

(*a*) Up to A.D. 800 on a scale from 5 to 15 (instead of -6 to $+4$)
(*b*) After A.D. 800 on a scale from 1 to 13

13. *Strength.*

The strength of each cycle can be readily gauged from the evidence for aurorae considered in relation to other observations of natural phenomena in the historical sources.

	Annual mean sunspot number
SSS = Extremely strong	> 160
SS = Very strong (150, 140, 140)	145
S = Strong (110, 130, 120, 110)	120
MS = Moderately strong (100, 100)	100
M = Moderate (90, 90, 80)	85
WM = Moderately weak (70)	70
W = Weak (60, 60)	60
WW = Very weak (50, 50)	50
WWW = Extremely weak	< 45
X = Unknown	

The figures in parentheses are corresponding sunspot numbers of maxima since 1750, and the figures at the right-hand side are the equivalent auroral numbers used in the curve (Fig. 1) for the earlier period.

14. *The Calculation of Years of Minima.*

In aurorally rich periods, such as the sixteenth century, the years of sunspot minima are defined by groups of years without notable displays, as extensive aurorae do not occur within two years of sunspot minimum [14].

In aurorally weaker periods, the position of a minimum in relation to the dates of neighbouring maxima can be estimated from certain rules, based on the behaviour of the sunspot cycle since 1610. Thus,

(*a*) The *minimum preceding* a given *maximum* usually occurs

4 years before, if the maximum is to be strong or very strong,
5 years before, if it is to be moderate or moderately strong, and
6 years before other (that is, weaker) maxima.

TABLE 3—*Sunspot minima arranged by centuries* (November 1954)

Period	.1	.2	.3	.4	.5	.6	.7	.8	.0
−700+	..	..	..	(47)	(57)	..	..	..	...
−600+	..	..	..	..	..	(73)	(84)	(95)	(104) i.e., 497 B.C. (Livy)
−500+	14	26	35	46	..	..	..	..	103 i.e., 398 B.C.
−400+	14	(25)	(35)	46	56	68	(..)	(..)	(102)
−300+	(12)	23	34	(46)	57	70	81	90	101 i.e., 200 B.C.
−200+	13	23	33	(46)	59	71	81	92	104 i.e., 97 B.C.
−100+	14	23	31	42	54	68	79	(91)	(103) i.e., A.D.3
0+	15	26	37	47	60	(70)	(80)	91	101
100+	12	(24)	(35)	(46)	(57)	70	82	92	203
200+	(14)	(25)	(35)	(47)	(60)	(72)	(84)	96	307
300+	17	26	36	48	58	68	80	91	404
400+	16	26	37	48	59	72	84	95	507
500+	17	26	38	51	62	73	82	92	(602)
600+	13	23	37	49	60	71	84	(93)	(707)
700+	19	30	39	(49)	61	(70)	(82)	(93)	804
800+	15	25	36	46	56	68	82	93	902
900+	12	21	34	(45)	59	70	82	(90)	(998)
1000+	10	22	34	(47)	(60)	71	82	(92)	1106
1100+	15	24	34	45	55	67	80	90	1199
1200+	12	24	33	44	56	(69)	82	(91)	1301
1300+	11	19	32	46	58	68	78	86	1396
1400+	7	(21)	34	43	57	68	(76)	(88)	1498
1500+	12	25	35	43	53	67	78	87	1599
1600+	10.8	19.0	34.0	45.0	55.0	66.5	79.5	89.5	1698.0
1700+	12.0	23.5	34.0	45.0	55.2	66.5	75.5	84.7	1798.3
1800+	10.6	23.3	33.9	43.5	56.0	67.2	78.9	89.6	1901.7
1900+	13.6	23.6	33.8	44.2	(54)	(66)	(78)	(89)	(2000)

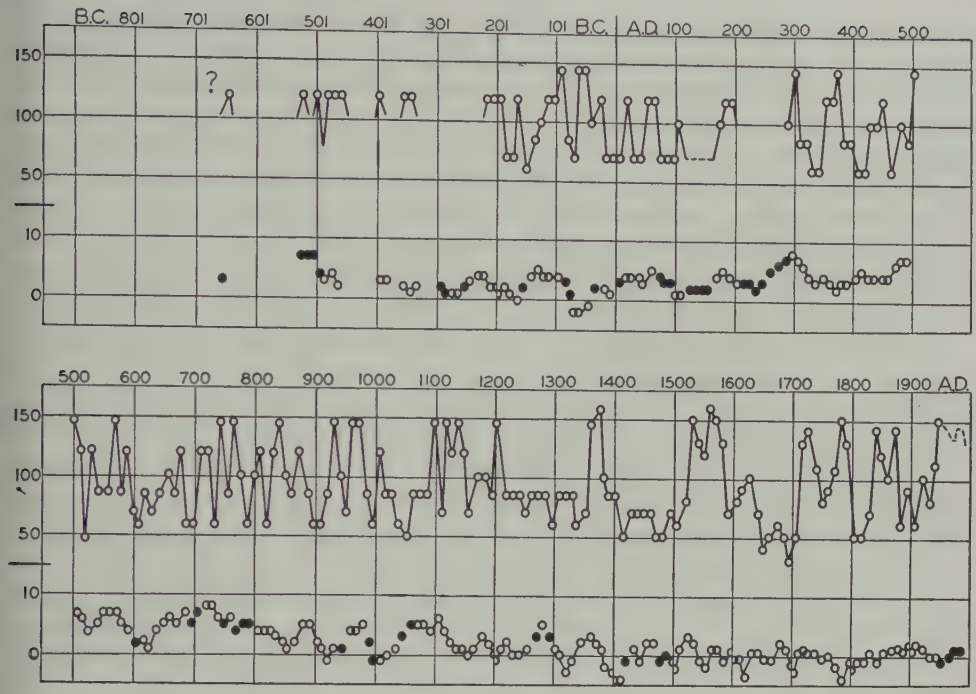

FIG. 1—Curves showing intensity and phase, B.C. 650 to A.D. 2000
Upper curve: Auroral intensity (sunspot numbers from A.D. 1750) of maxima
Lower curve: Phase (remainder) of minima; ○ = reliable, ● = uncertain

The formula $7 - (0.03)n$, where n is the sunspot number at maximum, holds for the strictly-dated intervals from minima to maximum since 1850.

(*b*) The intervals indicated by the preceding rule should nevertheless be increased by 1 to 1-1/2 years near the transition from an aurorally weak to an aurorally rich series of cycles.

(*c*) The minimum *following* a *weak* maximum often occurs about six years afterwards. The minimum following a *strong* maximum often occurs about seven years afterwards.

(*d*) The period from maximum to the following minimum is nevertheless only about five years near the transition from an aurorally weak to an aurorally rich group of cycles.

(*e*) The period of the sunspot cycle measured from one minimum to the next behaves with much more regularity than the period between consecutive maxima. Since 1715, it has invariably lain between 13.6 and 9.0 and, if—as seems possible—the Zurich minima at present dated 1634 and 1698 could be redated 1633 and 1699, these limits would have been valid since 1610. It is reasonable in any case to assume as a first approximation that the "remainders" of the consecutive minima do not differ by more than 3.

The minima can by these rules be dated with some precision back to 1512; intermittently they can be traced back to c. 500 B.C.

The presence of a great cycle of 78 years or seven sunspot cycles has been

postulated by Gleissberg and is certainly apparent in the data since 1610. Its presence in a preliminary table of the medieval data came to me as a surprise, but its phase in classical times helped to confirm the rule—implied by the table—of 90 to 91 cycles to a millenium. Nevertheless, before this cycle was taken for granted, the time occupied by 7 or 14 consecutive cycles was investigated, with results (since 1512) as follows:

(*f*) Seven cycles, measured from minimum to minimum, usually occupy between 77 and 79, but always more than 72 and less than 83 years.

(*g*) Fourteen cycles, measured from minimum to minimum, usually occupy between 154 and 158 years, but always more than 150 and less than 162 years.

(*h*) The longer values mentioned in the two preceding rules, that is, 83 and 162 years, are approached in periods measured forwards from the conclusion of an aurorally rich period. The length of 14 cycles in the Zurich figures thus reached its maximum (159.5 years) when measured from 1785 to 1944.

(*i*) The shorter values, 72 and 150 years, are conversely approached in periods which end near the conclusion of an aurorally rich period. Minima such as 1586 and 1785 are thus "early" and 1679 and 1712 are "late." The sunspot cycle is longer in aurorally weak periods and shorter in very active periods.

(*j*) The mean sunspot cycle for periods of the order of 500 years has varied between 11.03 and 11.14, and, since 200 B.C., there have been between 90 and 91 cycles to a thousand years. The justification for these statements is given below (§20).

The following series of dates, based on means of three successive minima in Table 3, is thus considered in relation to an arithmetical progression of the form

$$1932 - (155.2)n$$

Mean minimum	*Arithmetical progression*	*Observed minus formula*
(−)	−551.2	( )
(−397)	−396.0	+1
−241	−240.8	+1
− 86	− 85.6	0
+ 70	+ 69.6	0
(225)	224.8	(0)
380	380.0	0
538	535.2	+3
(695)?	690.4	(−5)
846	845.6	0
999	1000.8	+2
1156	1156.0	0
1310	1311.2	+1
(1467)	1466.4	(−1)
1621.3	1621.6	+0.3
1775.6	1776.8	+0.8
1933.9	1932.0	−1.9

The differences are remarkably small, and the positive signs are usually associated with active "early" maxima.

These rules made possible the calculation of the *number* of minima missing

at the various breaks. Table 3 seems to offer a unique and correct solution of the number of cycles since at least 250 B.C. It may be noted that identical totals are obtained from applying the same rules to the various maxima listed by Fritz [8], Kanda [15], and Nicolini [16]. It must also be added that, although the total *number* of cycles can be ascertained in this way, some of the more anomalous cycles—as in the mid-first century B.C. or the seventh to eighth centuries A.D.—may have been "smoothed" or wrongly placed in an attempt to keep within the limits obtaining since 1610. Errors of about 11 in certain remainders may thus occur, and the dates of maxima tabulated with probable errors 3 or 4 in Table 2 should be omitted in rigorous analysis.

15. *The Mean Cycle.*

The last two digits of years of *minima* have roughly followed the eleven-times table since cycle A.D. 800 [8], and before A.D. 800 the *maxima* behaved in the same way. Thus, except at the transition, the mean cycle has been approximately 11.11. We have seen that the length of 14 cycles appears to be 155.2, corresponding to a mean cycle (since B.C. 398) of 11.09, so that it may be supposed that near the transition at A.D. 800 the sunspot cycle was shorter than usual.

The mean values of the "remainders," as divided into centuries in Table 2, are set out in Table 4. The impression is given of a cycle slightly greater than 11.11 up to A.D. 800, followed by a cycle somewhat less. The mean length is calculated from the final maxima of each century (605 B.C. . . . A.D. 1894); a deviation from the nine-cycle pattern in a particular century would introduce a ten per cent error in the mean.

16. *The 78-year Cycle.*

The 78-year cycle [17] is clearly shown since 1610 by an alternation of periods of shortening (c. 1650-1700, c. 1725-65, c. 1890-1930) and lengthening cycles (c. 1700-25, c. 1765-1810, c. 1845-90). The half-amplitude of this "Gleissberg" cycle is about ± 1 year measured by "remainders," and the extreme values of the length of the ordinary sunspot cycle measured from minimum to minimum are close to the minimum remainders of this 78-year cycle. Preliminary investigations revealed that this greater period of seven ordinary cycles was in existence before 1610, and these principles were therefore utilized in the final Tables 2 and 3.

In addition to the 78-year cycle, a more important longer cycle of about 160 to 170 years could fit well the known changes in cycle length *since* c. 1510. Thus, the mean cycle has been

10 years from 1560 to 1590
1750 to 1790
1900 to 1950
but 12 years from 1600 to 1670
and 1780 to 1820

This alternation appears, however, to arise indirectly from the two-century cycle in auroral *activity* mentioned below, and late maxima (high remainders) at about A.D. 300, 495, 690, 890, 1080, 1290, 1520, 1680, 1830 (and 1900) follow the longer cycles of the weaker periods. No cycle of 160 to 170 years is evident before c. 1510,

TABLE 4—*The sunspot phase through the centuries*

Century	Remainder		Difference	Cycle length implied in Table 2
	Maximum	Minimum		
7th B.C.	(8)	(3)	(5)	....
6th B.C.	(11)	(7)	(4)	(11.4)
5th B.C.	(7)	(3)	(4)	(10.8)
4th B.C.	(6)	(2)	(4)	(11.1)
3rd B.C.	(7)	(3)	(4)	(11.0)
2nd B.C.	7.7	(2.5)	5.1	11.2
1st B.C.	(6)	(0.9)	5.1	(11.0)
1st A.D.	9.0	(3.7)	5.3	(11.2)
2nd A.D.	(7.8)	(2.5)	(5.2)	(11.1)
3rd A.D.	(9.7)	(4.4)	(5.2)	11.8
4th A.D.	8.8	3.9	4.9	10.4
5th A.D.	10.3	(5.0)	5.2	11.7
6th A.D.	10.4	5.8	4.7	10.7
7th A.D.	9.3	(4.3)	5.2	(11.3)
8th A.D.	(11.3)	(6.0)	5.3	(11.0)
9th A.D.	8.1	3.3	4.8	(11.1)
10th A.D.	6.5	2.1	4.4	(10.7)
11th A.D.	(7.9)	(2.3)	(5.5)	(11.5)
12th A.D.	6.8	2.2	4.5	10.5
13th A.D.	6.7	1.5	5.1	11.4
14th A.D.	5.4	+0.3	5.1	10.5
15th A.D.	(4.5)	(−0.6)	(5.2)	11.2
16th A.D.	5.0	+0.2	4.8	11.0
17th A.D.	5.2	−0.2	5.4	11.3
18th A.D.	4.1	−0.6	4.8	10.5
19th A.D.	5.0	−0.1	4.9	11.8
20th A.D.	(5.2)	(+0.7)	(4.5)	(11.1)

but, if our placing of the cycles is correct, the sunspot period has been shorter in the even centuries.

17. *Fluctuations in Auroral Activity.*

The fluctuations between aurorally rich and aurorally weak periods follow sunspot fluctuations closely, and in Figure 1 and the last part of Table 2 have been interpreted numerically. No cycle of the length of 78 years could be traced in auroral *intensity*, although periodicities about 85 and perhaps 65 years were vaguely indicated.

A more definite cycle of two centuries may be inferred from the rule that *activity has been greater in even than in odd centuries.* This rule is indicated in the number of dates of maxima of either sunspots or aurorae which Fritz was able to

determine before 1610. Seventy-eight belonged to even and only 41 to odd centuries [8]. Since the beginning of the Christian era, the ninth century forms the only odd century in which activity was as intense as in the centuries immediately preceding and following.

18. *The Active Periods of Even Centuries.*

The aurorally rich periods of the even centuries characteristically have two maxima with a short intervening lull. Central dates of such maxima—which correspond to the short lull—can be identified as follows: A.D. 1755, 1555, 1350, 1160, 955, 755, 540, 340 . . . . The cycle of auroral activity thus appears to be 200 to 205 years in length. The dates of the two major peaks are often about a half-century apart, and, although irregularities exist, they can be traced as follows:

Earlier peak	*Later peak*	*Difference*	
(?) 520 B.C.	(?) 460 B.C.	Unknown	
(310 B.C.)	(260 B.C.)	No evidence	
92 B.C.	54 B.C.	(4 × 9.5)	38 years
2nd century A.D.	....	Unknown	
A.D. 302	372	(7 × 10)	70 years
A.D. 511	567	(6 × 9)	56 years
A.D. 724?	765	(5 × 10)	51 years
A.D. 926	974	(4 × 12)	48 years
A.D. 1118	1173	(5 × 11)	55 years
A.D. 1324	1372	(4 × 12)	48 years
A.D. 1528	1572	(4 × 11)	44 years
A.D. 1727	1778	(5 × 10)	51 years
A.D. 1947	(1995?)	(5 × 10)	c.50 years

These double maxima appear to be the only basis for the cycle of 55-56 years conceived by Fritz [18].

The mean behaviour of the sunspot cycle in even centuries provides a clue to prediction of future cycles. The pattern since A.D. 900 has been

Year	(*Rem.*)	*Typical intensity*	*Years since previous maximum*
'07	(7)	Weak	..
'17	(6)	Strong	10
'27	(5)	Strong	10
'38	(5)	Strong	11
'50	(6)	Moderate	12
'61	(6)	Strong	11
'72	(6)	Very strong	11
'82	(5)	Strong	11
'91	(3)	Weak Moderate	8
'03	(4/3)	Weak Moderate	12

The probable error in the dating is less than two years; the intensity pattern progresses slowly forward and is subject to much irregularity. Table 1 has been continued on Gleissberg's assumption that a third intense and early maximum will shortly occur. The weak "central" maximum has thus been dated c. 1970 instead of c. 1960. The effect of the 78-year cycle has also been included.

The dates of aurorally rich periods—in both odd and even centuries—may be summarized as follows:

(?) c. 649 B.C.	651– 682
(?) c. 523 B.C.	743– 772
(?) 502–455 B.C.	826– 880
(?) 395–340 B.C.	920– 930
217–162 B.C.	961– 979
113– 89 B.C.	1000–1018
66– 43 B.C.	1095–1152 V. strong
c. A.D. 20 (?)	1200–1205
A.D. 43–68	1245–1264
Early 2nd cent. A.D.(?)	1307–1325
A.D. 174–196	1352–1393 V. strong
Third century A.D.(?)	1520–1582 V. strong
299–322	1616–1640 Relatively strong
351–375	1716–1746 V. strong
430–458	1770–1789 V. strong
499–514	1830–1880
565–586	1930–1960(?) V. strong
c. 620(?)	

19. *Quiescent Periods of the Odd Centuries.*

Since A.D. 200, long periods with very little auroral activity have occurred in the odd centuries only, notably in the third, eleventh, fifteenth, and seventeenth. The high remainders at the conclusion of some of these cycles have already (§16) been noted in relation to the two-century cycle. No regular pattern can be discerned as typical of odd centuries. Aurorally weak periods can be dated as follows:

c.440–400 B.C.		1037–1066	Very weak
160–135 B.C.		1279–1306	
1st, 2nd, 3rd cents. A.D.	Exact limits unknown	1326–1351	
401–428		1404–1431	Very weak
458–477		1468–1516	Very weak
601–615		1641–1670	Very weak
683–713	Very weak	1681–1715	Very weak
813–825		1791–1816	
891–916		1883–1908	

20. *Intervals between Intense Maxima.*

The dating of the major maxima is clearly established, and, pending harmonic analysis of the intensity curve, the intervals between the great peaks have been studied. No obvious periodicities are apparent, but clusters occur at particular values such as 244 and 353. As an example, we may consider 554.

A.D. 501– 54 B.C.	= 554 years
A.D. 926–372	= 554 "
A.D. 1117–566	= 551 "
A.D. 1527–974	= 553 "
[Cf. also A.D. 1938–1382	= 556 "
and A.D. 54–(?)502 B.C.	= 555 "]

That this was significant and not accidental was shown by the calculation of "remainders," defined in the sense of §5, but applied to the intervals. Their distribution was not accidental. In the range 200 to 300 years, there were actually ten

instances like 244 with zero remainder but only one (247) leaving a remainder 3.

The explanation can only lie in the constancy of the mean cycle over long periods. The intervals noted must correspond to integral numbers of "mean cycles" and may be split up as follows:

244 = 22 × 11.09	Rem. 0
353 = 32 × 11.03	Rem. −2
375 = 34 × 11.03	Rem. −2
480 = 43 × 11.16	Rem. +3
554 = 50 × 11.08	Rem. −1
632 = 57 × 11.09	Rem. −1
743 = 67 × 11.09	Rem. −1
763 = 69 × 11.06	Rem. −3
1005 = 91 × 11.04	Rem. −6

Similar clusters were noted at 93 (94?), 109 (110?), 115 (116?), and 117 (118?) cycles. Considering all intervals from 200 to 1,000, those yielding remainders 8, 9, 10, 0, and 2 were most frequent and those yielding remainder 3 least frequent. In this way, the value of the mean cycle as 11.1 and the assumption of between 90 and 91 cycles per millenium were confirmed.

An independent check on this was provided by intervals (200 to 1,000 years) of the main maxima selected by Fritz. The dates are less reliable, but have the merit of being more evenly distributed. Moreover, Fritz himself believed that the mean cycle was greater than 11.1 and that there were 120 (not 122) cycles between A.D. 503 and 1848. However, even in the dates selected by Fritz, remainders of 9, 10, 0, and 1 were the most frequent and clusters could be identified as follows:

Years	*Remainder*	*Number of cycles*	*Mean period*
309	9	28	11.04
410	10	37	11.08
475	9	43	11.05
542	9	49	11.06
720	9	65	11.08
854	10	77	11.09
898	10	81	11.09
911	0	82	11.11

A separate examination was made of the probable and established maxima between B.C. 649 and A.D. 302. The remainder 0 was then the most frequent and the tendency for cycles slightly greater than 11.11 was noted. The following results seemed most probable.

649 B.C. to 215 B.C. = 434 years = (?) 39 × 11.13
215 B.C. to A.D. 196 = 410 years = 37 × 11.08
A.D. 196 to 302 = 106 years = 9 × 11.8 (*sic*)
(N.B. Not 10 × 10.6)

We thus have

649 B.C. to A.D. 1947 = 2595 years = 234 × 11.09
215 B.C. to A.D. 1947 = 2161 years = 195 × 11.08

The integral numbers (that is, of cycles 11.1 years) which had appeared in these three investigations themselves showed a tendency to clusters—in this

case, near multiples of seven. This was independent evidence of the 78-year cycle, but no evidence of longer cycles was apparent.

21. *Conclusion.*

There is thus a fundamental rhythm involved in the production of sunspot cycles. The mean period of this rhythm is 11.1, and the rhythm itself is subject to a major cycle of seven sunspot cycles (77-1/2 or 78 years). Individual cycles in active periods tend to appear earlier in relation to the fundamental period. This is especially true of maxima, but is also true of minima. Conversely, the length of the cycle is longer in aurorally weak periods.

22. *Acknowledgments.*

I should like to thank all those who have kindly sent or translated the historical records of aurorae that form the basis of this paper. Many of these collaborators—in the so-called "Spectrum of Time" project—are named in previous articles. Prof. S. Chapman kindly read the typescript and made some helpful suggestions.

References

[1] R. Wolf, Astron. Mitt., Zurich, **24**, 111 (1868).
[2] D. J. Schove, The sunspot-cycle before 1750, Terr. Mag., **52**, 233-238 (1947).
[3] A. F. Cook, On the mathematical characteristics of sunspot-variations, J. Geophys. Res., **54**, 347-353 (1949); W. Gleissberg, The predictability of the probable features of the sunspot cycle, Astroph. J., **109**, 321-326 (1949); W. Gleissberg, Zs. Astroph., Berlin, **29**, 1-8 (1951); A. G. McNish and J. V. Lincoln, Prediction of annual sunspot numbers, Washington, D.C., U.S. Dept. of Comm., Nat. Bur. Stan., Central Radio Prop. Lab., CRPL Rep. No. 1-1 (1947).
[4] H. Fritz, The periods of solar and terrestrial phenomena, translation by W. W. Reed, Mon. Weath. Rev., **56**, 401-407 (1928). [Published originally in Vierteljahrsch. Natf. Ges., Zürich, Heft 1, 1893.]
[5] H. J. de Boer, Tree-ring measurements and weather fluctuations in Java from A.D. 1512, Proc. Kon. Nederland. Akad. Wetensch., Amsterdam, Ser. B, Vol. LIV, No. 3, 194-209 (1951) and Vol. LV, 386-394 (1952).
[6] C. Davison, Studies in the periodicity of earthquakes, London (1938).
[7] D. J. Schove, Geog. Ann., Stockholm, **36**, 40-80 (1954).
[8] D. J. Schove, Sunspot epochs, A.D. 188-1610, Pop. Astr., **56**, 247-252 (1948); see Table 1.
[9] D. J. Schove, J. Brit. Astr. Assn., **61**, 22-25, 126-128 (1951); **62**, 38-43, 63-66 (1952); and **63**, 266-270, 321-325 (1953); also J. Brit. Archaeol. Assn., 3rd Ser., No. 13, 34-49 (1950).
[10] D. J. Schove, Sunspots, aurorae and blood rain, Isis, **42**, 133-138 (1951).
[11] D. J. Schove, The auroral cycle in the 16th century (not yet published).
[12] D. J. Schove, Sunspots and aurorae (500-250 B.C.), J. Brit. Astr. Assn., **58**, 178-190 (1947).
[13] L. Harang, The aurora, New York, John Wiley and Sons, Inc. (1951). [Vol. I, International Astrophysical Series.]
[14] H. W. Newton and A. S. Milsom, The distribution of great and small geomagnetic storms in the sunspot cycle, J. Geophys. Res., **59**, 203-214 (1954).
[15] S. Kanda, Ancient records and sunspots and auroras in the Far East and the variation of the period of solar activity, Proc. Imp. Acad. Tokyo, **9**, No. 7, 293-296 (1933).
[16] T. Nicolini, Il periodo medio dell'attività solare in relazione alle osservazioni antiche e moderne, R. Oss. Astrofs. di Capodimonte, Napoli, Contributi Astronomici, Ser. 11, Vol. 11, No. 7, 79-88 (1942).
[17] W. Gleissberg, Terr. Mag., **49**, 243-244 (1944).
[18] H. Fritz, Das Polarlicht, Leipzig, Brockhaus, p. 161 (1881).

TIME RELATIONSHIP OF SMALL MAGNETIC DISTURBANCES IN ARCTIC AND ANTARCTIC

BY S. J. AHMED

Geophysical Observatory, Quetta, Pakistan

and

W. E. SCOTT

Department of Terrestrial Magnetism, Carnegie Institution of Washington, Washington 15, D. C.

(Received October 14, 1954)

ABSTRACT

Magnetograph records for February and March 1934 from Little America and College-Fairbanks (Alaska) were examined for conspicuous disturbance movements with respect to their parallelism in time of occurrence. The study, although based on only a few available records, is unique, in that the two stations lie in about the same geographical meridian and each is located in respective northern and southern auroral zones. It was found that the time difference between the occurrences at the two stations is often small (a matter of minutes or less).

INTRODUCTION

It is known that there is a great difference magnetically between time fluctuations measured at stations in moderate and high latitudes. At arctic and antarctic stations, magnetic disturbances usually show a persistence and amplitude an order of magnitude or more intense than in temperate or torrid zones.

Around the turn of the century, Birkeland attempted to explain these magnetic changes in terms of surges of electric currents flowing in the upper atmosphere [see 1 of "References" at end of paper]. Birkeland thought that the sun emits cathode rays, or some other similar form of radiation, which when passing near the earth are drawn into its magnetic field and tend to run along lines of magnetic force. These streams of rays give rise to electric currents that circulate in the upper atmosphere, starting in general in the auroral zones of polar regions where they may also cause aurora. The atmospheric current enters the auroral zone at a height of about 100 km or so, where it divides, one part flowing east and the other west, until at the opposite side of the auroral zone it may flow upwards along the lines of magnetic force. According to Birkeland, both large and small perturbations in the earth's magnetism are due to this current. Birkeland, in the discussion of the results obtained on the Norwegian Expedition, 1899-1900, compared certain selected disturbances, using magnetograph records in some instances from Potsdam only and in others from the observatories at Pavlovsk, Copenhagen, Potsdam, Greenwich, and Toronto, along with his own observations at Haldde (on the fringe of the northern auroral zone). From the comparisons of Haldde and

Potsdam high-speed records, he found that the time of occurrence of small disturbances [see Fig. 1 and Pls. III-VII, reference 1] was practically simultaneous at the two stations. Birkeland's model is still often referred to, but it has been shown that its magnetic field fails to reproduce observed magnetic changes near the center of the auroral zone [2].

In 1921, Chree [3] published the valuable magnetic data obtained on the British (Terra Nova) Antarctic Expedition, 1910-1913, at Cape Evans (below the southern auroral zone). Six chapters are devoted to the study of simultaneous magnetic disturbances at different parts of the earth, besides a chapter dealing with the comparison of magnetic disturbance and aurora. His Chapter XI deals with short-period disturbances, examples of which and comparisons with other observatories being given. He classified these disturbances into normal and special types. Among his many conclusions, Chree [3] mentions the following: "The examination of the short-period disturbances . . . shows that except in the Antarctic the disturbances were all essentially of the same kind."

Prior to his volume of results on the British Antarctic Expedition, Chree [4] published his "Studies in terrestrial magnetism," which contains a chapter on arctic and antarctic disturbances. On page 156 of his book he states:

> "Disturbed conditions being practically chronic in high latitudes, whether northern or southern, it was inevitable that the Antarctic curves would show sensible disturbance during the disturbance shown by the curves of Birkeland's Arctic stations. To establish any real connection, it is necessary to show that more than ordinarily disturbed conditions tend to prevail simultaneously in the Arctic and the Antarctic. It can hardly be claimed that the times indicated on the two sets of curves are of such accuracy as to justify the positive assertion that prominent peaks in them answer to absolutely identical times. Our examination, however, . . . has shown that in a number of cases when conspicuous isolated movements presented themselves in the Arctic curves, conspicuous isolated movements also presented themselves in the Antarctic curves, the time difference between the two events being if not zero at least too small to be measured. This, taken in conjunction with the fact that sudden movements to all appearance simultaneous could be recognized at all the intermediate stations, is at least very strong evidence of a fundamental connection between the phenomena in north and south."

Our studies bore out that there is a general correspondence in times rather than simultaneity. It is believed that Chree was referring to small magnetic storms, where the possibility of simultaneity of commencement is greatest. It should be remarked that the use of synonymous terms (for example, magnetic fluctuations or variations, short-period disturbances, brief storms, conspicuous isolated movements, etc.) is often ambiguous or confusing, and has no doubt occasioned in the past some unwarranted disagreement between investigators. It is by reference to the traces or reproductions of them and a knowledge of the ordinate scales that the events can best be appraised.

PRESENT INVESTIGATION

While disturbances of a world-wide character have been found to affect the traces of the different observatories of the world nearly simultaneously, it was believed that examination might reveal local effects, especially of interest if for

a pair of stations located nearly along the same line of force of the geomagnetic field. These conditions are at least crudely fulfilled for College, Alaska (lat. 64° 51′ north, long. 147° 50′ west) and Little America II (lat. 78° 34′ south, long. 163° 56′ west), with data available for a period of nearly two months during the Second International Polar Year. These records have been examined with the view to ascertaining whether disturbances can be singled out as affecting the field in the two polar regions at about the same time. For this purpose, only those cases of magnetic disturbances, whether composed of large or small variations, preceded by more or less steady or quiet periods at both the stations were examined. Fifteen disturbed periods are listed in Table 1, together with their Greenwich mean times

TABLE 1—*Times of commencement in Greenwich mean time of disturbances in Z, H, and D*

Date	Station	*Z*	*H*	*D*	Mean for *Z*, *H*, and *D*	Time diff.
1934		*h m*	*h m*	*h m*	*h m*	*m*
Feb. 21	College	06 34	06 36	06 34	06 35	
	L. America	06 37	06 37	06 35	06 36	−1
Feb. 26	College	06 37	06 34	06 36	06 36	
	L. America	06 36	06 36	06 38	06 37	−1
March 10	College	08 32	08 31	08 30	08 31	
	L. America	No trace	08 27	08 27	08 27	+4
March 11	College	11 06	11 04	11 05	11 05	
	L. America	No trace	11 06	11 06	11 06	−1
March 11	College	18 30	18 29	18 29	18 29	
	L. America	No trace	18 29	18 30	18 30	−1
March 12	College	06 39	06 38	06 37	06 38	
	L. America	06 37	06 37	06 37	06 37	+1
March 13	College	14 00	14 01	14 00	14 00	
	L. America	14 01	14 01	14 00	14 01	−1
March 16	College	07 24	07 24	07 25	07 24	
	L. America	07 25	07 25	07 25	07 25	−1
March 18	College	06 57	06 57	06 57	06 57	
	L. America	07 01	07 01	07 00	07 01	−4
March 18	College	09 54	09 54	09 53	09 54	
	L. America	09 57	09 56	09 56	09 56	−2
March 19	College	05 33	05 33	05 33	05 33	
	L. America	05 33	05 33	05 34	05 33	0
March 22	College	03 43	03 40	03 40	03 41	
	L. America	03 45	03 40	03 40	03 42	−1
March 22	College	12 40	12 40	12 40	12 40	
	L. America	12 39	12 40	12 40	12 40	0
March 25	College	08 38	08 39	08 38	08 38	
	L. America	08 40	08 40	08 40	08 40	−2
March 27	College	13 43	13 43	13 46	13 44	
	L. America	13 41	13 44	13 40	13 42	+2

of commencement in declination (*D*), horizontal intensity (*H*), and vertical intensity (*Z*). The portions of the magnetograms showing these fluctuations at College and Little America, respectively, are shown in Figure 1 (*A* and *B*). Upward

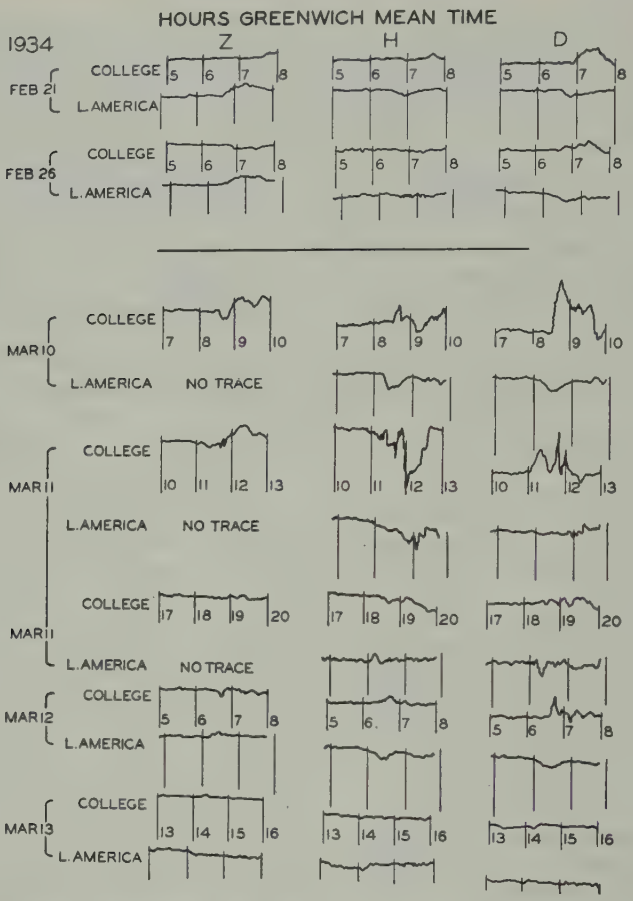

FIG. 1A—Portions of magnetograms showing fluctuations at College and Little America

motion on the traces means an increase in component, except for College where downward motion of the Z trace denotes an increase. The traces at both stations were obtained at approximately 15 mm per hour (paper speed). The scale values are as follows: *College*—$Z = 20.44\ \gamma$/mm, $H = 15.10\ \gamma$/mm, $D = 2.46\ '$/mm; and *Little America*—$Z = 26.62\ \gamma$/mm, $H = 21.22\ \gamma$/mm, $D = 7.57\ '$/mm. Reversals sometimes appear in each of the elements. The movements at College are generally of a less simple type than at Little America.

Considering the mean times of commencement of the disturbances, it is seen that the disturbances started earlier at Little America on three occasions as against ten at College, while on two occasions their starts were simultaneous. Taken together, the disturbances affected the two stations within less than five minutes of one another. As the errors of reading the times from the traces can in themselves be of the order of one to two minutes, it may be reasonable to infer that the two stations were affected in these disturbances almost simultaneously. Also, the time differences may arise also in part from effects of induced earth currents.

While the meagerness of the data prevents one from drawing too precise a conclusion that magnetic disturbances of a world-wide character, whenever they

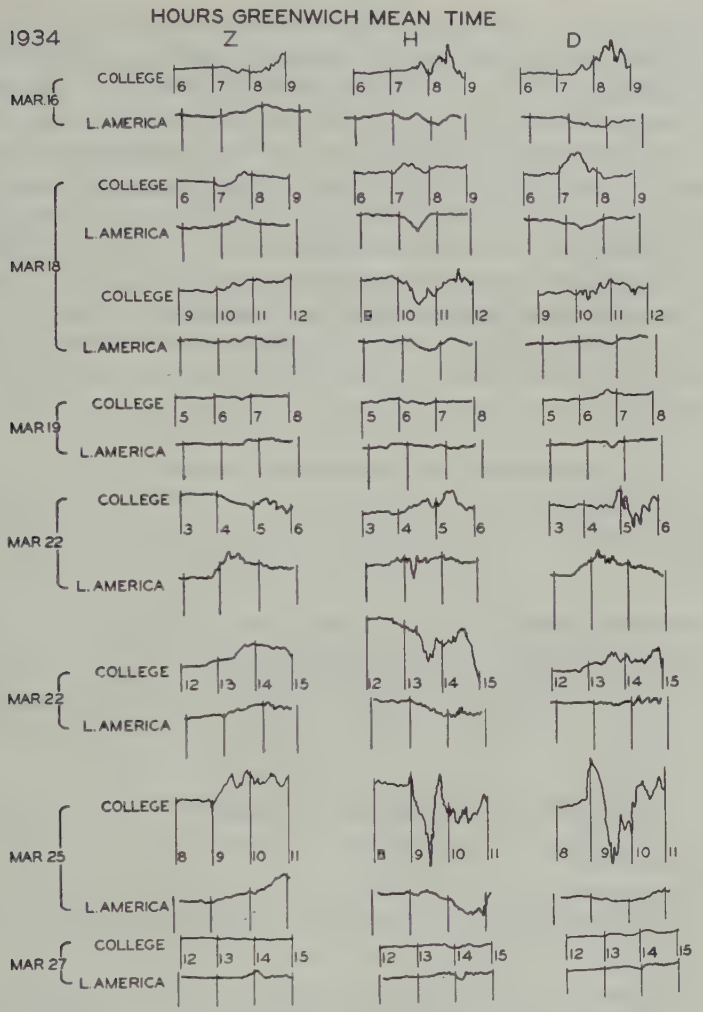

FIG. 1*B*—Portions of magnetograms showing fluctuations at College and Little America

can be singled out, can be recognized as affecting the magnetic fields at the two polar regions more or less at the same time, the necessity to look for a more reliable mode of identifying variations of the two fields was felt. This led us into examining the traces of Little America and College for locating reasonably small intervals of the order of one hour or so containing micropulsations that can, by virtue of the closeness of their periods and amplitudes, be identified as stemming from any single source of disturbance. Some 40 years ago, Angenheister [5] showed that pulsations in a number of cases were of about the same magnitude at different places on the earth. The few cases which appeared to us vaguely to satisfy this criterion, however, on closer examination disclosed varying sizes of time displacements, of amplitude, of frequency, and other deformations, indicating that the recordings were not simple harmonic. This would seem to be due to the fact that other forces besides the single one contemplated must have been affecting the

fields, at least subsequent to the first pulse, if not from the very beginning. Indeed, it is not quite appropriate to call the pulsations on these traces "micropulsations," as their amplitudes were on an average of the order of about 50γ—a situation hardly comparable to the "micropulsations" of the middle or low latitudes.

For the purpose of comparing similar events, the horizontal-intensity records of the Huancayo Magnetic Observatory, located close to the geomagnetic equator and more or less on the same lines of force passing through College and Little America, were examined. It was found that at these times there appeared recognizable or conspicuous irregularities, particularly micropulsations, which can be related to the disturbances studied in the two polar regions. Out of the 15 cases examined, it seems that incidence of micropulsations on the traces was conspicuous by being present on 13 occasions. This, as may be seen from Table 2, does not seem purely accidental.

TABLE 2—*Huancayo H-traces (all times are GMT)*

Date	Remarks regarding *H*-traces
1934	
Feb. 21	At $06^h\ 30^m$, there is a small peak, followed by three micropulsations ending at $06^h\ 34^m$.
Feb. 26	A series of micropulsations commenced at $06^h\ 37^m$.
Mar. 10	At $08^h\ 32^m$, there is a trough, followed immediately by four micropulsations.
Mar. 11	At $11^h\ 06^m$, a small gradual trough commenced, followed by micropulsations beginning at $11^h\ 12^m$. At $18^h\ 30^m$, there is a trough.
Mar. 12	At $06^h\ 37^m$, there is a small sharp rise, immediately followed by a couple of micropulsations.
Mar. 13	At $14^h\ 00^m$, there is a small but sharp rise, followed by a few micropulsations.
Mar. 16	At $07^h\ 24^m$, a series of micropulsations commenced, with *H* increasing with every pulsation.
Mar. 18	Micropulsations, which had commenced at $06^h\ 36^m$ with increasing *H*, doubled in amplitude at $06^h\ 58^m$, and remained so until $07^h\ 03^m$. At $09^h\ 54^m$, four micropulsations commenced.
Mar. 19	At $05^h\ 30^m$, there is a peak.
Mar. 22	At $03^h\ 40^m$, a series of micropulsations commenced, the amplitude of which attained a maximum at $03^h\ 46^m$. At $12^h\ 40^m$, there is a sudden, though small, drop in *H*.
Mar. 25	At $08^h\ 33^m$, there is a small peak, with a small trough occurring at $08^h\ 37^m$.
Mar. 27	There is a long series of micropulsations with increasing *H*; a peak was attained at $13^h\ 45^m$, around which oscillations occurred until $14^h\ 00^m$.

It is generally accepted that there is a certain connection between the phenomenon of terrestrial magnetism and the occurrence of sunspots and aurorae but the nature of the connection and the relation between these natural phenomena have not yet been definitely determined. Dungey [6] has discussed the theories of magnetic storms and aurorae. There is only the possibility of aurorae australis and borealis occurring simultaneously. In recent years, a statistical study of the correlation of auroral observations in the northern and southern hemispheres was made by Little and Shrum [7]. They found that parallel analyses of coincident aurorae, on an intensity basis, failed to reveal a marked connection between great displays in north and south auroral zones.

DISCUSSION

According to the Chapman-Ferraro-Martyn theory [8, 9], some magnetic disturbances at the ground are ascribed to effects of charged particles entering the polar regions along lines of magnetic force. These particles presumably start mainly from ionized solar streams at an equatorial distance of a few earth radii, or from an equatorial current-ring there. If this theory were correct, and magnetic changes in polar regions directly associated in time with the entry there of charged particles, geomagnetic disturbances should often probably appear simultaneously in north and south polar regions. If a dynamo theory based on the wind-motion of electrically conducting air of the ionosphere in the presence of the earth's magnetic field gives rise to these changes, it is difficult to postulate simultaneous changes in air flow in north and south polar regions, unless the air flow is an immediate effect of suddenly applied solar radiation, or alternately of solar corpuscular radiation in some way [10, 11]. Finally, regular trains of electromagnetic waves of a period a minute or so are known to occur; a difference in phase between north and south polar regions might then suggest that these are due to hydromagnetic waves [12, 13], propagated mainly along lines of force of the geomagnetic field, possibly with some evidence of dispersion. To test this possibility, it is conceivably preferable to have a north and south polar station located about on the same line of force of the geomagnetic field. While the stations Little America and College (Alaska) only crudely approximate this condition, and simultaneous records at the two stations exist for less than two months, it has seemed of interest to try to assess factual possibilities in at least a preliminary way here.

TABLE 3—*Micropulsations in the H trace*

Date	Time GMT (between)	Period of micropulsations		
		College	Huancayo	L. America
1934	*hours*	*minutes*	*minutes*	*minutes*
Feb. 21	16–17	5.5	1.3	3.2
Feb. 22	8–9	3.1	1.4	4.0
Feb. 23	8–9	2.7	1.6	4.1
Feb. 25	20–21	3.1	1.9	2.9
Feb. 26	12–13	2.9	1.3	5.0
Mar. 4	11–12	7.0	2.0	5.9
Mar. 6	1–2	4.3	1.0	4.0
Mar. 9	1–2	3.9	1.0	2.8
Mar. 11	11–12	3.8	2.0	3.7
Mar. 12	10–11	3.2	1.9	3.9
Mar. 13	10–11	4.1	1.0	5.7
Mar. 16	7–8	2.8	1.2	3.8
Mar. 17	10–11	3.0	1.3	3.1
Mar. 18	6–7	3.5	1.5	3.4
Mar. 21	6–7	3.1	1.9	3.2
Mar. 28	12–13	3.3	1.1	2.0
Mar. 28	16–17	4.0	2.0	3.9
Means.....		3.72	1.49	3.80

In order to see what other aspects of the magnetic phenomena are comparable between the polar regions and the other regions, the H traces of Little America and College were compared in regard to the periods of the micropulsations with the H traces of Huancayo, the magnetic observatory previously referred to as being very close to the magnetic equator and to the lines of force passing through Little America and College. The Z and D traces were not examined because of the rarity of the recognizable micropulsations on them. Given above is Table 3 showing the result of the study of 17 cases.

As the number of cases is not large enough to give statistical results, the approximation of the relationships in the periods of the micropulsations between the equatorial region and the polar regions, namely, 2:5, needs examination using more data. An interesting thought is that the periods within polar regions are perhaps compatible with the supposition of an equatorial source with propagation towards the poles, the increase in the period being due to dispersion of the waves during their transit. However, it does not seem possible for dispersion alone to increase the period to 2.5 times that at the equator.

ACKNOWLEDGMENT

The writers are indebted to Dr. E. H. Vestine for suggestions and discussions. They also wish to express their thanks to Dr. M. A. Tuve, the Director of the Department of Terrestrial Magnetism, Carnegie Institution of Washington, for his kind arrangements by which this work was done.

References

[1] Kr. Birkeland, Expédition Norvégienne de 1899-1900 pour l'étude des aurores boréales. Résultats des recherches magnétiques, Kristiania, Skr. Vid. selsk., 1. Math.-naturv. Kl. No. 1 (1901).

[2] E. H. Vestine and S. Chapman, The electric current-system of geomagnetic disturbance, Terr. Mag., **43**, 351-382 (1938).

[3] C. Chree, Terrestrial magnetism, British (Terra Nova) Antarctic Expedition, 1910-1913, London, Harrison and Sons, Ltd. (1921).

[4] C. Chree, Studies in terrestrial magnetism, London, Macmillan and Co., Ltd. (1912).

[5] G. Angenheister, Ueber die Fortpflanzungsgeschwindigkeit magnetischer Störungen und Pulsationen, Bericht über die erdmagnetischen Schnellregistrierungen in Apia (Samoa), Batavia, Cheltenham und Tsingtau im September 1911, Göttingen, Nachr. Ges. Wiss. Math.-physik. Kl., 565-581 (1913).

[6] J. W. Dungey, Theories of magnetic storms and aurora, Nature, **170**, 795 (1952).

[7] D. E. Little and G. M. Shrum, Correlation of auroral observations in the northern and southern hemispheres, Trans. R. Soc. Can., **44**, 51-56 (1950).

[8] S. Chapman and V. C. A. Ferraro, Terr. Mag., **36**, 77-97, 171-186 (1931); **37**, 147-156, 421-429 (1932); **38**, 79-96 (1933); S. Chapman, J. Geophys. Res., **55**, 361-372 (1950); V. C. A. Ferraro, J. Geophys. Res., **57**, 15-79 (1952).

[9] D. F. Martyn, The theory of magnetic storms and auroras, Nature, **167**, 92-94 (1951).

[10] O. R. Wulf, On the relation between geomagnetism and the circulatory motions of the air in the atmosphere, Terr. Mag., **50**, 185-197, 259-278 (1945).

[11] E. H. Vestine, Winds in the upper atmosphere deduced from the dynamo theory of geomagnetic disturbances, J. Geophys. Res., **59**, 93-128 (1954).

[12] H. Alfvén, Cosmical electrodynamics, Oxford, Clarendon Press (1950).

[13] C. O. Hines, Generalized magneto-hydrodynamic formulae, Proc. Cambridge Phil. Soc. **49**, Pt. 2, 299-307 (1953).

ON AN INTERPLANETARY MAGNETIC FIELD*

BY ARTHUR BEISER

New York University, University Heights, New York 53, New York

(Original manuscript received December 30, 1954; revised February 10, 1955)

ABSTRACT

Considerations suggesting the existence of an interplanetary magnetic field are presented. Such a field would not exceed about 5×10^{-8} gauss, and its presence can explain the observed cutoff in the primary cosmic-ray momentum spectrum. A field existing within the earth's orbit can account for all or part of the observed solar-terrestrial time delays in aurorae and magnetic storms. The time required for the formation of a magnetic field pervading the solar system is less than 10^3 years, and its lifetime against decay is probably more than 10^{10} years.

INTRODUCTION

Recent work in magnetohydrodynamics has shown that, in general, magnetic fields are associated with the motion of ionized gases in the universe. These cosmic fluids are highly turbulent, and, if a small magnetic field is present initially, kinetic energy from the fluid motion is converted to magnetic energy until an equilibrium situation is established. When this occurs, the magnetic field is "frozen in" the fluid, that is, the lines of force are tied to, and move with, the fluid particles. These results are well known, and have been applied to such phenomena as sunspots and magnetized galactic clouds.

If this picture of the behavior of cosmic fluids is correct, interplanetary space should be in a state of magnetohydrodynamic turbulence. It is the purpose of this paper to consider quantitatively the properties of the magnetic fields associated with the interplanetary matter and some of their consequences.

SOME RESULTS OF MAGNETOHYDRODYNAMICS

We start by sketching the derivation [see 1 of "References" at end of paper] of the magnetohydrodynamic relations that will be employed subsequently. This is done here for convenience and so that the degree of approximation involved (which is considerable) shall be clear. CGS electromagnetic units are used throughout, with μ assumed to be unity.

Neglecting the displacement current, Maxwell's equations for a cosmic fluid are

$$\text{curl } \mathbf{E} = -\partial \mathbf{H}/\partial t \quad (1)$$

$$\text{div } \mathbf{H} = 0 \quad (2)$$

*This work was assisted by the joint program of the U.S. Office of Naval Research and the U.S. Atomic Energy Commission.

and

$$\text{curl } \mathbf{H} = 4\pi\mathbf{J} \quad (3)$$

Inserting

$$\mathbf{J} = \sigma\mathbf{E} + \sigma\mathbf{v} \times \mathbf{H}$$

where $\mathbf{v}$ refers to the fluid motion, in (3), taking the curl of both sides, and making use of (1),

$$\frac{\partial \mathbf{H}}{\partial t} = \text{curl } \mathbf{v} \times \mathbf{H} - \frac{1}{4\pi\sigma} \text{curl curl } \mathbf{H}$$

Expanding the last term of the above, we have, in view of (2),

$$\frac{\partial \mathbf{H}}{\partial t} = \text{curl } \mathbf{v} \times \mathbf{H} + \frac{1}{4\pi\sigma} \nabla^2\mathbf{H} \quad (4)$$

For high conductivities, such as those typical of cosmic fluids, the last term of (4) may be omitted. Hence

$$\partial\mathbf{H}/\partial t = \text{curl } \mathbf{v} \times \mathbf{H} \quad (5)$$

From (5) it follows that for a steady state $\mathbf{v}$ must be parallel (or antiparallel) to $\mathbf{H}$, with the magnetic lines of force frozen in the fluid and carried along in its motion. When this is not true, the interaction between the fluid motion and the magnetic fluid is such as to align $\mathbf{v}$ and $\mathbf{H}$. To obtain the rate of increase of the field we expand (5) into

$$\partial\mathbf{H}/\partial t = (\mathbf{H}\cdot\text{grad})\mathbf{v} - (\mathbf{v}\cdot\text{grad})\mathbf{H} + \mathbf{v} \text{ div } \mathbf{H} - \mathbf{H} \text{ div } \mathbf{v}$$

Since div $\mathbf{H} = 0$ from (2) and div $\mathbf{v} = 0$ if the fluid is incompressible, which we assume,

$$\partial\mathbf{H}/\partial t + (\mathbf{v}\cdot\text{grad})\mathbf{H} = (\mathbf{H}\cdot\text{grad})\mathbf{v}$$

or

$$d\mathbf{H}/dt = (\mathbf{H}\cdot\text{grad})\mathbf{v} \quad (6)$$

This is equivalent to

$$\mathrm{d}H/\mathrm{d}t = Hv/L$$

where v and L are a "representative" velocity and length in the fluid. Integrating,

$$H = H_0 \exp(vt/L) \quad (7)$$

This expression governs the growth of the magnetic field in the turbulent fluid. No lower limit to H_0, the "seed" field, appears and so even a small stray field will do.

The relation between the magnetic and kinetic energy densities at equilibrium is a matter of some controversy. A plausible argument can be made for equipartition, that is, that

$$H^2/8\pi = \rho v^2/2 \quad (8)$$

at least on an average basis. On the other hand, from (7) we see that H increases more rapidly for the large wave-number ($1/L$) components of the turbulent fluid, which therefore preempt the supply of kinetic energy. Thus, H would vary with the size of the eddy. In general, a safe statement is that H does not exceed the value given by (8).

Returning to (4), when the field has been frozen in the fluid, the first term on the right-hand side vanishes and

$$\partial \mathbf{H}/\partial t = \nabla^2 \mathbf{H}/4\pi\sigma$$

which is equivalent to

$$H/\tau = H/4\pi\sigma L^2$$

Hence τ, the time required for the decay of H by magnetohydrodynamic viscosity, is

$$\tau = 4\pi\sigma L^2 \quad \ldots\ldots\ldots\ldots\ldots\ldots\ldots\ldots\ldots\ldots (9)$$

in the present degree of approximation.

THE INTERPLANETARY FIELD

We now apply the above results to the interplanetary fluid. Ideally, a cosmic fluid subject to no outside influences will have no net magnetic field because of the random distribution of the turbulent elements. The interplanetary fluid, however, is affected by the magnetic moment of the sun (and by the smaller ones of the planets) and presumably partakes of the general rotational motion of the solar system as well. Two consequences of these departures from the ideal case are the possibility of a general magnetic field pervading the interplanetary fluid, and a specific orientation of lines of force near the sun.

An upper limit to the magnitude of the general field follows from (8). Assuming that ρ corresponds to 10 hydrogen atoms per cm^3 and that $v = 10^6$ cm sec^{-1},

$$H < 10^{-5} \text{ gauss} \quad \ldots\ldots\ldots\ldots\ldots\ldots\ldots\ldots\ldots\ldots (10)$$

This figure corresponds to the strongest local fields possible, and the general field might be several orders of magnitude smaller. So small a field does not permit direct measurement, but may give rise to certain phenomena, which are discussed below, that serve to fix its magnitude more precisely than (10).

The effect of the solar magnetic dipole on magnetohydrodynamic fields in its vicinity follows from (5), with the result that the fluid motion is coerced by the dipole field, so that $\mathbf{v}$ is aligned with the dipole lines of force. Since the lines of force carried by the fluid are parallel to $\mathbf{v}$ (by the same reasoning), they must follow those of the dipole. Hence, ion streams originating in the sun can reach the earth without being deflected outside the plane of the ecliptic, since the axis of the solar dipole is certainly at least approximately normal to this plane.

We now inquire whether the time needed for the formation of a magnetic field in the interplanetary fluid and its lifetime against decay are such as to make the current existence of the field plausible. If $L = 5 \times 10^{14}$ cm (slightly smaller than Pluto's orbital radius) and $v = 10^5$ cm sec^{-1}, then, from (7), H attained its equili-

brium value in at most a few hundred years. For the lifetime of the field, we require the conductivity, given by the usual formula

$$\sigma = N\lambda e^2/mv \quad (11)$$

where the symbols have their customary meanings and refer to the electrons of the interplanetary matter. For complete ionization, σ is independent of the electron density and is proportional to $T^{3/2}$, with T the absolute kinetic temperature of the electrons. If T has the very low value of 10°, $\sigma = 10^{-13}$ sec^{-1}, which, in (9), yields $\tau = 10^{10}$ years. This is longer than the age of the universe. If the electron temperature is higher, as seems likely, then the decay time of the field is even greater than 10^{10} years.

COSMIC-RAY CUTOFF

The integral momentum spectrum of the primary cosmic radiation is of the form

$$J(P) = KP^{-a},\ a \sim 1.1 \quad (12)$$

At low momenta, (12) predicts far more primaries than are actually observed, and the shape of the spectrum in this region has accordingly been the subject of much study.

The most recent experimental results [2] for primary protons and alpha particles indicate that a marked "cutoff" in the spectrum occurs at a magnetic rigidity pc/ze of about 1.5×10^9 volts, with primaries having rigidities below this figure almost entirely absent. Furthermore, a cutoff at the same rigidity is observed in the heavy nuclei ($z > 2$) of the cosmic radiation. It can be concluded from these results that the cutoff is a function of rigidity and not of velocity. Hence, the cutoff cannot be due to an absorption process involving ionization loss, but must rather be of a magnetic nature.

Several authors in the past have invoked a solar magnetic field to account for the cutoff [3]. Their calculations require a value for the dipole magnetic moment of the sun (6×10^{33} gauss cm^3) at least an order of magnitude greater than can be reconciled with direct measurements of solar surface fields [4]. As far as is known, no other explanation for the magnetic cutoff has been advanced seriously.

The hypothesis of an interplanetary magnetic field leads naturally to a cosmic-ray cutoff, however. An ion of rigidity pc/ze entering a magnetic field H is deflected into a helical path of radius

$$R = pc/300zeH \quad (13)$$

For the interplanetary field, an estimate of the smallest radius of curvature that can penetrate as far as the earth might be 10^{14} cm. In that case, the observed cutoff at 1.5×10^9 volts gives $H = 5 \times 10^{-8}$ gauss, which is entirely consistent with (10). If the field were larger in extent than the solar system, which is not too unlikely, H could be lower than 10^{-8} gauss and still produce the cutoff.

Should the lifetime of the field be smaller than 10^{10} years, or if it came into being an appreciable time after the origin of the universe, then H was larger formerly than it is now. In this event, the cosmic-ray cutoff was also higher, and since the primaries obey (12) above the cutoff, even a slight increase in the cutoff

would cause a considerable reduction in cosmic-ray intensity. This possibility is mentioned because it is commonly assumed that cosmic radiation was more intense in the past if there were any difference at all.

SOLAR-TERRESTRIAL TIME DELAYS

An interplanetary magnetic field will have consequences other than a cosmic-ray cutoff. In particular, it will interact with ion streams originating in the sun that cause aurorae and magnetic storms.

It is well known that a delay of about a day takes place between the meridian passage of a particular sunspot or flare and the start of a magnetic storm or auroral display correlated with it [5]. If the ions travel in straight paths, the time lag suggests velocities of about 10^8 cm sec^{-1}, and this effect has been used as evidence for such velocities. However, recent work [6] indicates that the streams are actually composed of fast protons with velocities of perhaps 10^{10} cm sec^{-1}, accompanied by slow electrons, so that the streams as a whole are electrically neutral. Therefore the time lags require a different explanation.

If a magnetic field exists within the earth's orbit normal to the plane of the orbit, the protons are deflected in their passage from the sun, but can still reach the earth if their momenta are sufficiently large. The neutralizing electrons come from the interplanetary matter and follow the proton beam. The radius of curvature of the beam that gives rise to a time delay t is, from the geometry of the situation,

$$R = r/2 \sin (2\pi t/T) \quad (14)$$

where r is the orbital radius of the earth and T the synodic solar rotation period. For $t = 1$ day and $T = 27$ days, $R = 3 \times 10^{13}$ cm. The magnetic rigidity of protons moving at 10^{10} cm sec^{-1} is approximately 4×10^8 volts. The corresponding H is 4×10^{-8} gauss from (13), in remarkable agreement with the value found in the previous section.

In the above calculation, the solar magnetic dipole was considered negligible. However, the field of this dipole will cause a deflection in the proton beams even if the moment is quite small, thus contributing to the time lags or even being entirely responsible for them [7]. Until the exact magnitude of the solar dipole moment is determined, the lags only provide an upper limit of 4×10^{-8} gauss to the interplanetary field near the sun.

I wish to thank S. A. Korff and G. Beiser for their helpful comments.

References

[1] For example, W. M. Elsasser, Revs. Mod. Phys., **22**, 1 (1950); Phys. Rev., **95**, 1 (1954); L. Biermann, Ann. Rev. Nuclear Sci., **2**, 335 (1953); and references therein.
[2] R. A. Ellis, M. B. Gottlieb, and J. A. Van Allen, Phys. Rev., **95**, 147 (1954).
[3] L. Janossy, Zs. Physik, **104**, 430 (1937); P. S. Epstein, Phys. Rev., 53, 862 (1938).
[4] H. W. Babcock and T. G. Cowling, Mon. Not. R. Astr. Soc., **113**, 357 (1953).
[5] L. Harang, The aurorae, John Wiley and Sons, Inc., New York (1951), Chapter 7 and references therein.
[6] W. H. Bennett and E. O. Hulburt, Phys. Rev., **95**, 315 (1954); J. Atmos. Terr. Phys., **5**, 211 (1954).
[7] A. Beiser, J. Geophys. Res., **60**, 161 (1955).

SOLAR-TERRESTRIAL TIME DELAYS*

BY ARTHUR BEISER

New York University, University Heights, New York 53, New York

(Received December 30, 1954)

ABSTRACT

The observed delay of about 24 hours between the meridian passage of a sunspot or flare and the onset of an associated magnetic storm or aurora is shown to originate in the magnetic deflection of the ion streams involved. If a solar magnetic dipole is exclusively responsible, its moment must be between 6×10^{27} and 10^{29} gauss cm^3. If an interplanetary magnetic field is involved, its magnitude is about 4×10^{-8} gauss. Should both fields act, which is likely, then the above figures represent maxima.

INTRODUCTION

Considerable data exist correlating the times of onset of magnetic storms and aurorae with the meridian passage of certain solar phenomena [see 1 of "References" at end of paper]. In most of the cases studied, a delay of about a day is found to be present between the time a sunspot or flare passes the central meridian and the start of a particular storm or auroral display. If the latter are caused by ion streams originating in the sun, as is generally believed, then this time lag implies stream velocities of about 1.5×10^8 cm sec^{-1}. However, convincing evidence [2] has been presented in favor of the hypothesis that the streams actually consist of fast (10^{10} cm sec^{-1}) protons accompanied by slow electrons to provide electrical neutrality. In this event, the time lags must be accounted for on some basis other than travel time.

It is the purpose of this note to show that these lags can arise from the magnetic deflection of the proton beam in either (or both) the solar magnetic dipole field or a weak interplanetary field. Furthermore, the duration of the time lags provides upper limits to the magnitudes of the solar dipole and of the interplanetary field.

EFFECT OF THE SOLAR DIPOLE

If the sun has a dipole magnetic moment M apart from the random multipolar fields that are observed on its surface [3], the resulting field will deflect a proton beam in its passage out to the earth. The word "beam" is used in view of the self-focusing action that can be expected in a current of fast protons [2]. Since the neutralizing electrons come from the interplanetary matter, they will follow

*This work was assisted by the joint program of the U.S. Office of Naval Research and the U.S. Atomic Energy Commission.

the proton beam in its vicissitudes. For convenience, it is assumed here that the magnetic equatorial plane of the sun coincides with the plane of the ecliptic.

A proton emitted from the sun with a sufficiently large momentum will spiral outward with a rapidly increasing radius of curvature R. To obtain the equation $r = r(\theta)$ describing this spiral, we note that R for a proton of magnetic rigidity pc/e in a magnetic field H normal to its direction of motion is given by

$$R = pc/300eH \quad (1)$$

The equatorial field of a magnetic dipole is

$$H = M/r^3 \quad (2)$$

and so

$$R = pcr^3/300eM \quad (3)$$

Now the radius of curvature corresponding to $r(\theta)$ is

$$R = \frac{(r^2 + r'^2)^{3/2}}{r^2 + 2r'^2 - rr''} \quad (4)$$

where the primes refer to differentiations with respect to θ. This equation must agree with (3) when the ratio of the magnetic rigidity of the protons to the dipole moment of the sun is large enough. The simplest spiral that satisfies this requirement is

$$r^2\theta = a^2 \quad (5)$$

Substituting (5) in (4) yields

$$R = \frac{[r^2 + (r^6/4a^4)]^{3/2}}{r^2 - (r^6/2a^4)} \quad (6)$$

We note the following:

(a) If $r < a$, $R = r$, that is, the proton describes a circle.
(b) If $r > a$, $R = r^3/4a^2$, which corresponds to (3). Hence the proton follows a spiral trajectory which rapidly approaches a straight line. The minus sign refers to the direction of the curvature and will be omitted henceforth.
(c) If $r \approx a$, $R = \infty$, which represents the transition between the circular orbits of trapped protons and the outward spirals.

In view of (3), the equation describing the proton paths becomes

$$r^2\theta = 75eM/pc \quad (7)$$

We can now compute the value of M, the solar dipole moment, needed to give the observed time lags. From (7),

$$\theta_0 - \theta_e = \frac{75eM}{pc}\left[\frac{1}{r_0^2} - \frac{1}{r_e^2}\right] \quad (8)$$

Here $\theta_0 - \theta_e$, the angular difference between the solar location at which th

proton beam is emitted and the position of the earth when it intersects the beam, is given by

$$\theta_0 - \theta_e = 2\pi t/T \quad (9)$$

with t the observed time lag and T the synodic solar rotation period. For a 10^{10} cm sec^{-1} proton, pc/e is about 4×10^8 volts; r_0 is the radial distance from the solar axis at which the protons emerge into the dipole field, and r_e is the radius of the earth's orbit. Clearly, $r_e^2 \gg r_0^2$, and so the last term in the brackets of (8) is negligible. Thus, since $t/T = 1/27$,

$$M = 1.2 \times 10^6 r_0^2 \quad (10)$$

If $r_0 = 7 \times 10^{10}$ cm, the radius of the photosphere, $M = 6 \times 10^{27}$ gauss cm^3. However, it is more reasonable to suppose that the proton beams originate in the corona. Furthermore, "tunnels" which shield the protons from the dipole field may well exist for some distance outward from their production region, due perhaps to local fields associated with the acceleration process [4]. It is hard to imagine such a tunnel extending more than five solar radii through the corona; if that long, $M \approx 10^{29}$ gauss cm^3.

Recent measurements [3] of solar surface fields place an upper limit to the dipole moment of about 10^{32} gauss cm^3. This maximum also follows from various cosmic-ray data [5]. No lower limit to M is implied by the above work, and therefore $6 \times 10^{27} \leq M \leq 10^{29}$ gauss cm^3 seems reasonable.

EFFECT OF AN INTERPLANETARY FIELD

Considerations indicating the existence of a weak magnetic field pervading the solar system were presented in another communication [6]. The radius of curvature of a proton in a uniform field H that gives rise to a time delay t is

$$R = r_e/2 \sin (2\pi t/T) \quad (11)$$

Hence, making use of (1) with $pc/e = 4 \times 10^8$ volts, $r_e = 1.5 \times 10^{13}$ cm, and $t/T = 1/27$, we find $H = 4 \times 10^{-8}$ gauss. This is the same value of H required to account for the primary cosmic-ray cutoff, and is entirely plausible on the basis of magnetohydrodynamic reasoning [6].

Any interplanetary field must be normal to the plane of the ecliptic in the vicinity of that plane in order that the protons not be deflected in such a way as to miss the earth's orbit. This condition is always fulfilled near the sun, since the lines of magnetic force carried by the interplanetary field will be forced by the presence of a permanent field to line up with it. The dipole field of the sun, even if small, therefore compels the interplanetary field to have the proper orientation for ion streams propagated in the plane of the ecliptic.

It is tempting to ignore a hypothecated interplanetary field and to assume that the solar dipole field is alone responsible for the time lags. However, while a field of $< 10^{-7}$ gauss is hardly subject to direct confirmation, the evidence in favor of its existence does not permit it to be dismissed. Of course, both an interplanetary field and the solar dipole can act simultaneously, and this may well be the case. All that can be said at the moment, then, is that $M < 10^{29}$ gauss cm^3

for the solar dipole and that $H < 4 \times 10^{-8}$ gauss for the interplanetary field. In any event, a magnetic origin for the time delays seems reasonable.

References

[1] L. Harang, The aurorae, John Wiley and Sons, Inc., New York (1951), Chapter 7.
[2] W. H. Bennett and E. O. Hulburt, Phys. Res., **95**, 315 (1954); J. Atmos. Terr. Phys., **5**, 211 (1954).
[3] H. W. Babcock and T. G. Cowling, Mon. Not. R. Astr. Soc., **113**, 357 (1953).
[4] A. Beiser, to be published.
[5] W. P. Staker, M. Pavalow, and S. A. Korff, Phys. Rev., **81**, 889 (1951); J. Firor, F. Jory, and S. B. Treiman, Phys. Rev., **93**, 551 (1954).
[6] A. Beiser, J. Geophys. Res., **60**, 155 (1955).

VOLCANIC ACTIVITY AND CHANGES IN GEOMAGNETISM

By Tsuneji Rikitake and Izumi Yokoyama

Earthquake Research Institute, Tokyo University, Tokyo, Japan

(Received February 21, 1955)

ABSTRACT

Geomagnetic works have been conducted on Volcano Mihara since its great eruption in 1950. As a result of repeated magnetic surveys marked changes in the geomagnetic field have been found. A continuous recording also proves the occurrence of anomalous changes in geomagnetic declination in connection with development and subsidence of the volcanic activity. It seems likely that the main parts of the geomagnetic changes thus found are caused by the demagnetization and magnetization within the volcano, which is composed of basaltic rocks containing a large amount of magnetite. Geomagnetic studies will be useful for inferring the internal state of certain volcanoes and sometimes even for the prediction of their eruptions.

1. INTRODUCTION

A number of field-studies have been hitherto made in order to see whether or not anomalous changes in the geomagnetic field take place on occasions of volcanic eruption and earthquake occurrence. Although it has been sometimes reported that we find geomagnetic changes which seem to be accompanied by volcanic or seismic activity, they are not always reliable because of various difficulties in field-studies. Actually, we have not yet been able to discover the general nature of supposed local anomalous changes, even if they did occur. Consequently, it has been almost impossible to presume internal state under emergency area from this sort of work.

In 1950, a violent eruption occurred at Volcano Mihara on Ooshima Island, which is situated about 100 km south of Tokyo. Magnetic dip-surveys were carried out by one of the writers over the volcano at the early and the most violent stages of the eruption. On comparing the first survey to the second one, it was found that geomagnetic dip-angle decreases everywhere during a two-month period. The decrease was systematically distributed, being large in the central part of the island and becoming smaller as the distance from the centre increased. The maximum decrease amounted to as much as 30 minutes of arc. Being encouraged by the success, the writers afterwards frequently repeated dip-surveys, as well as high accuracy surveys for three geomagnetic elements. A temporary station for continuous recording of changes in geomagnetic declination has also been set up at the western foot of the volcano since 1951. The result of the recording shows a general eastward drift of 5 minutes of arc, superposed by undulatory oscillations

with a few months period. As will be seen in the following paragraph, the former drift may be caused by the internal magnetization acquired during the gradual cooling after the violent activity. However, the undulations seem to correspond to the heating and cooling associated with the intermittent activities. Since the variometer has often been calibrated by absolute measurements and the influences of magnetic storms and daily variations are eliminated by comparison with the standard magnetic observation, the results are quite reliable.

Volcano Mihara had a minor eruption on October 5, 1953. Just before the eruption, we had made a magnetic survey of three components. The difference between this survey and the one which was carried out soon after the eruption clearly shows decreases in geomagnetic dip-angle around the central part of the island. Although the amount of decrease is smaller than that which was found in 1950, the way of the distribution is quite similar to the previous one. Since the two surveys were conducted with a magnetometer of high accuracy, the anomalous change mentioned above is reliable within an accuracy of approximately 0.1 minute of arc. We also found a corresponding westward drift of declination during the same period at the temporary station.

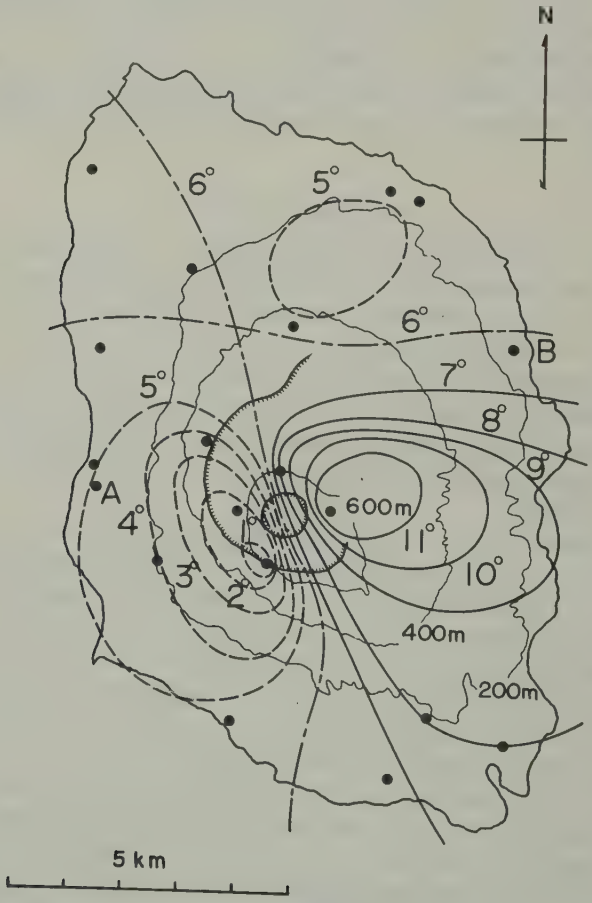

FIG. 1—The distribution of westerly declination on Ooshima Island for 1951.4

Judging from the results of the studies stated above, we can definitely say that local anomalous changes in geomagnetic field take place in relation to the volcanic activity of Volcano Mihara.

From our experiences with intermittent activities of the volcano, a rough idea of the general characteristics of the changes can be obtained. If we analyse those changes, we may be able to get some information concerning the interior of an active volcano. All those studies have been published in a series of papers [see 1 of "References" at end of paper], the present article being a brief summary of the work.

2. GEOMAGNETIC FIELD ON VOLCANO MIHARA

Volcano Mihara is composed of basaltic rocks with high natural remanent magnetization [2], the mean intensity of magnetization being estimated at 0.03 emu from the results of the magnetic survey. Accordingly, we find a large anomaly in geomagnetic field over the volcano. Figure 1 shows the distribution of westerly declination there. The anomalous distribution of declination, as well as the other

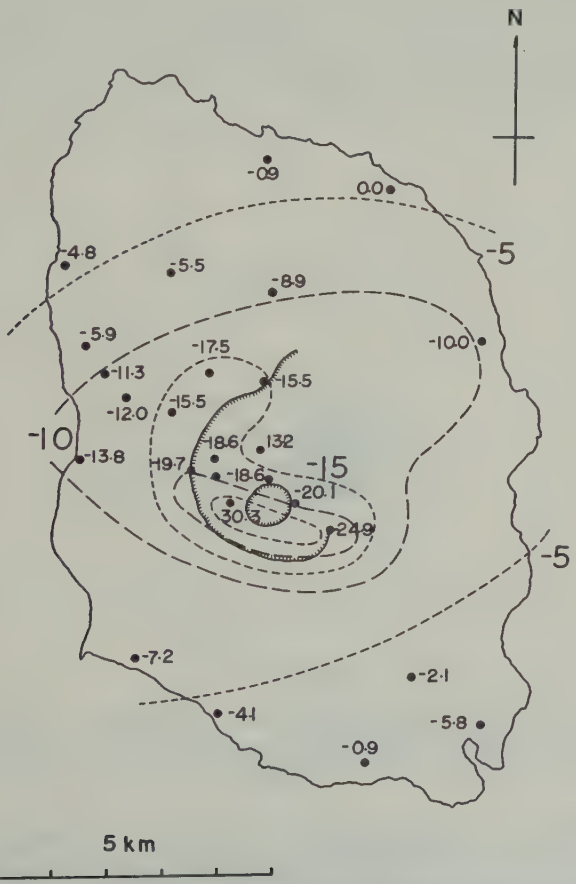

FIG. 2—The distribution of changes in geomagnetic dip associated with the 1950 eruption (Unit: minute of arc)

geomagnetic components, can be attributed to the strong magnetization of the volcano in the direction of the general geomagnetic field.

3. THE 1950 ERUPTION

After ten years of quiescence, Volcano Mihara resumed its eruptive activity on July 16, 1950. The eruption apparently ceased on September 23. The lava ejected during the period amounted to 4×10^7 metric tons altogether. Soon after the outbreak of the eruption, a geomagnetic dip-survey was carried out over the volcano with a miniature earth-inductor [3], while another survey was also made during the period from September 22 to 25. The differences between the two surveys are shown in Figure 2. The errors due to transient magnetic disturbances, such as magnetic storms and daily variations, are eliminated with the aid of the observations at Kakioka Magnetic Observatory, which is situated at a distance of about 150 km from the volcano.

It is noticeable that dip-angle decreases at almost all stations. The amount of decrease becomes larger and larger as the stations approach the central area of the volcano, reaching almost 30 minutes of arc at its maximum. If we approximate the distribution of the decrease with a magnetic field of an underground magnetic dipole, it is most probable that the dipole is situated at a depth of 5 km under the point as shown in Figure 3. The polarization of the dipole seems to be almost

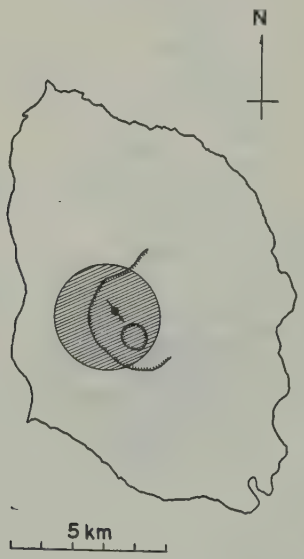

FIG. 3—The hypothetical dipole corresponding to the geomagnetic changes; the hatched area shows the horizontal projection of the supposed region in which the temperature exceeds the Curie point

reversed to the general geomagnetic field there, while its strength is estimated at 6.3×10^{14} emu. If we assume that the change is caused by the demagnetization probably due to the temperature rise in the interior of the volcano, the demagnetized region is obtained as a sphere with a radius of 2 km for the first approxi-

mation. The projection of the sphere to the horizontal plane is also shown in Figure 3. Since we have no other plausible reason for the demagnetization, the possible heating in the volcano would be the only reasonable interpretation at the present stage. But it is not clear how such a rapid heating can occur in the above-mentioned region in which the temperature seems to exceed the Curie point.

4. THE MINOR ACTIVITY IN 1953

The violent activity mentioned in Section 3 continued until the end of 1951, repeating intermittent eruptions. After that, the volcano did not show any apparent activity. During the period, the writers conducted two dip-surveys and two surveys for three components. From these, it was found that the great change in the geomagnetic field at the early stage of the activity had been gradually recovering during the period. However, the volcano erupted again, ejecting volcanic bombs and ashes on October 5, 1953. The activity continued intermittently until the beginning of the next year, while no appreciable amount of new lava welled up in the course of the minor activities.

Soon after the commencement of the new eruption, a survey was carried out with a GSI (Geographical Survey Institute) type of magnetometer on October 7 and 8. Comparing the results with those of the previous survey, which was carried out during the period from July 30 to August 12, 1953, we detected a systematic change in geomagnetic field around the crater, as shown in Figure 4, with respect

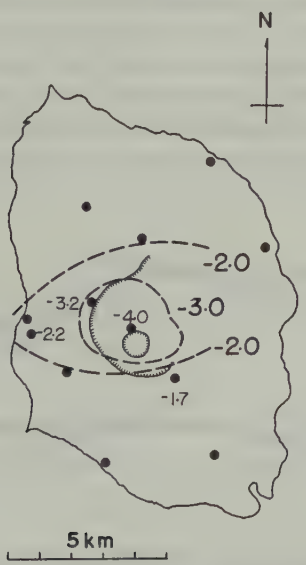

FIG. 4—The distribution of changes in geomagnetic dip associated with the 1953 eruption (Unit: minute of arc)

to geomagnetic dip. Although the amount of the changes is not so large as that described in the preceding section, the results are of high accuracy, 0.1 minute of arc in dip-measurements, because both the surveys were carried out with the same magnetometer of great accuracy. The mode of the distribution is of similar

type in both cases. So we may presume that the magnetization in the volcano also decreases in connection with the minor activity. This means that the internal temperature goes up with the development of volcanic activity, provided we adopt the same viewpoint as before. It will be quite natural that the smaller the activity, the smaller the geomagnetic change.

A similar decrease in geomagnetic dip was also reported at the beginning of the 1940 eruption of Volcano Miyakeshima [4], which is also composed of basaltic rocks. From these examples, we may get some idea of local anomalous changes in geomagnetic field over volcanoes of this sort.

5. CONTINUOUS OBSERVATION

Although the writers could prove the occurrence of special change in geomagnetic field in relation to the volcanic activity by repeating magnetic surveys, it is not clear how the field changes during a rather short period. In order to trace geomagnetic change in detail, a continuous recording has been undertaken since April, 1951, when the first activity reached its final stage. On Ooshima Island we have commercial electric supply only during the evening and that only along the coast. Under those circumstances, it will be of great difficulty to keep a magnetic variometer in good condition over a long period if we install it at a point very far from the inhabited area. On the basis of the declination chart in Figure 1 the writers decided to set up a temporary station for the observation of declination at A-point in Figure 1, where they could find a small cave suitable for setting a variometer, because the point would be sensitive to changes in geomagnetic declination, provided the changes are caused by increase or decrease of the magnetization of the volcano. The variometer is of the usual type, having a small magnet suspended by a fine phosphor-bronze ribbon. In order to avoid artificial drift, absolute measurements are occasionally carried out just in front of the cave

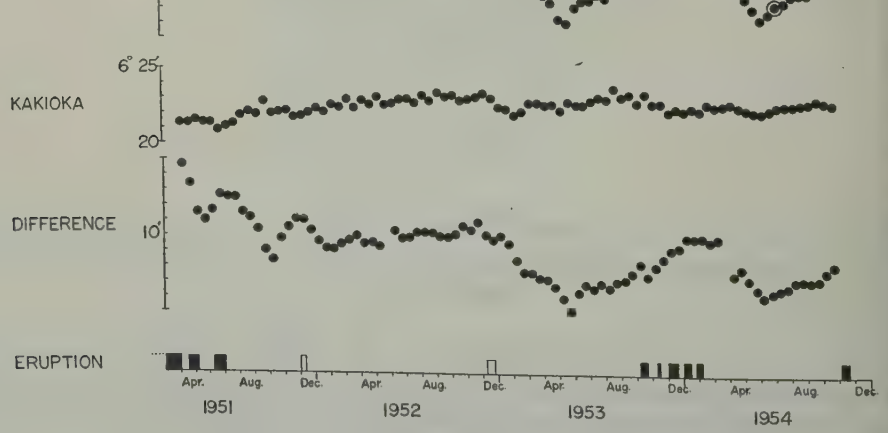

FIG. 5—The changes in 15-day mean of geomagnetic declination

From the record, hourly values are read off, from which daily means are obtained. In order to show gradual changes, 15-day means are plotted in Figure 5, together with those of Kakioka Magnetic Observatory. The difference between the two curves is also shown in the Figure. The difference curve should be approximately free from transient magnetic disturbances. Those points surrounded with big circles show that the base-line value is checked by absolute measurements. In the lower part of Figure 5, the activities of the volcano are also shown in a rather arbitrary way. The period during which eruptions were observed on the summit is shown with black column, while white one shows the period during which we observed pulsatory ground-motion or earthquakes of volcanic origin and topographical deformation in the crater, though no eruption was reported. As is clearly seen in the Figure, the declination at *A* tends towards the west whenever the volcano becomes active. After activities have subsided, eastward drifts of the declination are observed. The general tendency, however, shows a gradual eastward drift of several minutes of arc. If the magnetization of the volcano becomes weak or strong, or, physically speaking, if the internal temperature goes up or down, the declination at *A* should tend towards the west or east, respectively, as is shown in Figure 1. Therefore, the change observed here is compatible with the physical interpretation concerning the relation between magnetization and internal temperature. It is also pointed out that the changes in the declination mentioned here are in harmony with those in any geomagnetic components which are obtained by examining the repeated geomagnetic surveys.

T. Nagata suggested that we should observe changes in declination in the opposite direction on the east side of the island provided the physical theory is plausible. It would be quite a job to add a new station on the opposite side of the island. But the writers have managed to make absolute measurements on both sides since 1954. Although we have very few observations available for the comparison, the changes are plotted in Figure 6, in which the results for *B*-point in

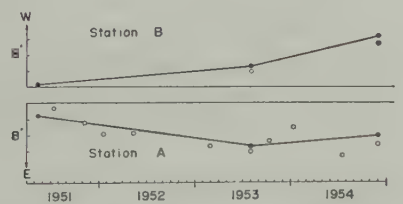

FIG. 6—The changes in geomagnetic declination at stations *A* and *B*, corrected for influence of the general secular variation

Figure 1 are given, together with those for *A*-point at the same epoch. It is noticeable that the declination has been drifting to the opposite direction at both stations, so the proposed physical mechanism would be approximately acceptable.

6. DISCUSSIONS AND CONCLUSIONS

From the geomagnetic studies mentioned above, we can definitely say that local anomalous changes of a particular type take place in relation to the volcanic activity of Volcano Mihara. As a less reliable example of similar change was

reported at the time of the 1940 eruption of Volcano Miyakeshima, we may imagine that this sort of change will be expected on any active volcanoes which are composed of basaltic rocks, as is the case for Mihara and Miyakeshima. The characteristics of the changes found at Volcano Mihara are as follows: (1) Changes corresponding to development or subsidence of activities can be explained, respectively, by apparent demagnetization or magnetization in the interior. (2) There is no relation between an individual eruption and a geomagnetic change. (3) The greater the activities are, the larger the local anomalous changes. (4) It is likely that recovery from the change after a violently active period is very slow.

As for the explanation of apparent demagnetization or magnetization, it seems most probable to suppose that heating and cooling within the volcano are responsible. If this view is accepted, we can estimate the rough extent of the region in which the temperature exceeds the Curie point. According to the opinion of some geologists, the extent of high-temperature region thus obtained seems to be acceptable from the geological point of view. However, it is no easy matter to understand such rapid changes in temperature. The heating may be explained by injection of high-temperature gas. However, the cooling at such a rate would not be possible if we take into account only heat conduction through rocks. Therefore, we do not say that the geomagnetic phenomena related to active volcanoes are wholly understood at the present stage of investigation.

The writers believe that they can presume the internal state of certain active volcanoes to some extent by the magnetic method. If we accumulate observations over a long period, we might be able to predict occurrences of eruptions by applying this method. It will be of great interest and importance to make similar studies on other volcanoes composed of rocks with high magnetization.

In conclusion, the writers are very grateful to Prof. T. Nagata for his helpful advice in the course of this study, and are also greatly indebted to Miss Y. Hishiyama, who assisted them both in field and laboratory.

References

[1] T. Rikitake, Bull. Earthquake Res. Inst., Tokyo Univ., **29**, 161, 499 (1951); T. Rikitake, I. Yokoyama, A. Okada, and Y. Hishiyama, Bull. Earthquake Res. Inst., Tokyo Univ., **29**, 583 (1951); and I. Yokoyama, Bull. Earthquake Res. Inst., Tokyo Univ., **32**, 17, 169 (1954).

[2] T. Nagata, Bull. Earthquake Res. Inst., Tokyo Univ., **21**, 1 (1943).

[3] T. Rikitake, Bull. Earthquake Res. Inst., Tokyo Univ., **29**, 147 (1951).

[4] R. Takahasi and K. Hirano, Bull. Earthquake Res. Inst., Tokyo Univ., **19**, 82, 373 (1941); T. Minakami, Bull. Earthquake Res. Inst., Tokyo Univ., **19**, 356 (1941); T. Nagata, Bull. Earthquake Res. Inst., Tokyo Univ., **19**, 335 (1941); and Y. Kato, Proc. Imp. Acad. Japan, **16**, 440 (1940).

NOTES ON CORRELATION METHODS FOR EVALUATING IONOSPHERIC WINDS FROM RADIO FADING RECORDS*

BY DONALD G. YERG

College of Agriculture and Mechanic Arts, University of Puerto Rico, Mayaguez, Puerto Rico

(Received October 14, 1954)

ABSTRACT

A correlation method requiring six values of the correlation coefficient is developed. Expressions for the drift velocity, fading velocity, and characteristic velocity are obtained from a correlation theory extended to include an elliptical contour in the horizontal plane.

The physical significance of the derived velocities is considered. Preliminary data indicate that the correlation ellipse exhibits a preferred orientation and that fading associated with random changes is as important as fading associated with a drifting pattern.

I. INTRODUCTION

Ionospheric winds may be obtained from signal intensity *vs* time records [see 1 of "References" at end of paper]. One method consists of determining the times of corresponding maxima and/or minima on three records originating at three spaced receivers. It is assumed that corresponding points in an interference pattern moving across the receiving stations may be connected by a straight line at right-angles to the direction of motion, so that the relative times of occurrence of maxima and minima are sufficient to determine the velocity and direction of the drifting pattern. This procedure may be termed the method of similar fades.

It has been shown by Briggs, Phillips, and Shinn [2] that the method of similar fades also assumes that random fluctuations of the signal intensity may be neglected. The correlation method developed by these investigators for the evaluation of the drift velocity, V, of the ground pattern also yields a velocity defined as the characteristic velocity, V_c , which is a measure of the contribution of random fluctuations. The method of similar fades is valid when the ratio V_c/V is small compared to unity and produces excessively large velocities if the ratio indicates that random fluctuations influence the relative time differences of maxima and minima.

The correlation method involves graphs of the auto-correlation function and the two cross-correlation functions taken with respect to the station at the origin. The computation of all the required correlation coefficients, perhaps 24 or more, is

*The research reported in this paper has been sponsored by the Geophysics Research Division of the Air Force Cambridge Research Center, Air Research and Development Command, under contract AF 19(122)-476.

rather laborious, so that the method has not been adopted generally as a routine procedure. Sample calculations with correlation methods have compared favorably with the results of the method of similar fades when the fading on each of the three records could be recognized as similar [3, 4, 5]. The validity of subsequent evaluations is to be judged by visual inspection of the records.

The lack of numerical criteria as a basis for this judgement suggests that careful attention should be given to the correlation method until considerable confidence has been gained or until appropriate criteria can be established for the validity of the much shorter method. The theoretical possibilities of correlation techniques appear so promising that the physical implications of the longer statistical procedure and methods for reducing the computational labor merit additional study. Such study is undertaken in this paper.

II. THE DEVELOPMENT OF A SIX-POINT CORRELATION METHOD

The normalized correlation function may be defined by

$$\rho(s,\tau) = \frac{\overline{[R(0,t) - \bar{R}(0,t)][R(s,t+\tau) - \bar{R}(s,t)]}}{\{\overline{[R(0,t) - \bar{R}(0,t)]^2}\}^{1/2}\{\overline{[R(s,t+\tau) - \bar{R}(s,t)]^2}\}^{1/2}} \quad \ldots\ldots(1)$$

Here, $R(0, t)$ represents the ordinate of the fading curve given as a function of time at a receiver site selected as the origin, and $R(s, t)$ represents a record obtained at a second station at a distance s from the first receiver site. If the second station may be located at any point in a horizontal plane, the notation $\rho(\xi, \eta, \tau)$ signifies the correlation coefficient between a second record at the position (ξ, η) and a record obtained at the origin, if the second record has been displaced by time τ relative to the first. In particular, $\rho(0, 0, \tau)$ represents the normalized auto-correlation function, and $\rho(0, 0, 0) = 1$.

If records are obtained at all points in the ξ, η-plane, $\rho(\xi, \eta, \tau)$ is found as a function of time and space. Let it be assumed that this function may be represented as a Taylor's series in three variables. Let it further be assumed that near the origin only first and second order terms need be retained. Since $\rho(\xi, \eta, \tau)$ is equal to one and is a maximum at the origin, the series becomes

$$\rho(\xi,\eta,\tau) = 1 + A\xi^2 + B\tau^2 + C\eta^2 + 2H\xi\tau + 2M\eta\tau + 2N\xi\eta \quad \ldots\ldots(2)$$

The remaining six coefficients may be evaluated from experimental data. If one receiver is at the origin and a second is at the point $(\xi_0, 0)$, the value of $\rho(\xi_0, 0, 0)$ may be determined. Substitution of these data in (2) shows that

$$A = \xi_0^{-2}[-1 + \rho(\xi_0,0,0)] \quad \ldots\ldots(3)$$

In a similar manner it may be found that

$$C = \eta_0^{-2}[-1 + \rho(0,\eta_0,0)] \quad \ldots\ldots(4)$$

$$B = \tau_i^{-2}[-1 + \rho(0,0,\tau_i)] \quad \ldots\ldots(5)$$

where τ_i is a particular value of τ.

If the above three equations are used to simplify the algebra, it also may be found from (2) that

$$H = (2\xi_0\tau_i)^{-1}[1 + \rho(\xi_0,0,\tau_i) - \rho(\xi_0,0,0) - \rho(0,0,\tau_i)] \quad (6)$$

$$M = (2\eta_0\tau_i)^{-1}[1 + \rho(0,\eta_0,\tau_i) - \rho(0,\eta_0,0) - \rho(0,0,\tau_i)] \quad (7)$$

$$N = -(2\xi_0\eta_0)^{-1}[1 + \rho(-\xi_0,\eta_0,0) - \rho(\xi_0,0,0) - \rho(0,\eta_0,0)] \quad (8)$$

In the development of these equations, receivers were located at (0, 0), (ξ_0 , 0), (0, η_0), and ($-\xi_0$, η_0). The correlation between records obtained at any two stations should depend upon the separation and the orientation of the connecting line relative to a fixed coordinate system and should not be greatly influenced by a small lateral displacement. It seems reasonable to assume that $\rho(-\xi_0 , \eta_0 , 0)$ is equal to the correlation between the records at (0, η_0) and (ξ_0 , 0). Then, only three receivers are required to evaluate the six coefficients of (2).

III. COMPARISON OF THE SIX-POINT AND GRAPHICAL CORRELATION METHODS

Briggs, Phillips, and Shinn [2] assume that the surfaces of constant correlation are concentric ellipsoids centered on the origin. Thus, in the ξ, τ-plane, the trace of a surface of constant values of $\rho(\xi, \eta, \tau)$ would be an ellipse of the form

$$A'\xi^2 + B'\tau^2 + 2H'\xi\tau = 1 \quad (9)$$

It is shown that these coefficients may be evaluated in terms of the receiver separations and any two of the three times, τ_0 , t_0 , and τ_s . Here, τ_0 is the time shift necessary to produce a maximum in the correlation between two records at a separation equal to ξ_0 , and "t_0 is the time lag for auto-correlation required to give a value of correlation equal to this maximum cross-correlation corresponding to a lag τ_0 ." The time τ_s is defined as the value of τ which satisfies the equality

$$\rho(\xi_0,0,0) = \rho(0,0,\tau_s) \quad (10)$$

These times may be obtained from graphs of the auto- and cross-correlation functions. In the development of the equations for the evaluation of A', *et al.*, the required constant value of the correlation contour is that value for which $\rho(\xi_0 , 0, \tau)$ is a maximum. Then, comparison of (9) with (2) shows that

$$A' = A[-1 + \rho(\xi_0,0,\tau)_{max}] \quad (11)$$

Similar relations exist for the other coefficients. The graphical method may be extended to include elliptical contours in horizontal planes, and a coefficient N' may be found from a third curve of a cross-correlation function [6].

A comparison of the two methods was undertaken using records published by Millman [7, 8]. The record for 24 February 1952 is representative of fading produced by ionospheric winds. The record for 20 November 1951 is representative of fading produced by a mixture of ionospheric winds and random variations or turbulence, and the record of 18 March 1952 is indicative of random variations or turbulence. The coefficients were evaluated by using each of the three possible combinations of times in the graphical method and by the six-point method. The results compared favorably [6]. These coefficients were used to find the wind velocity and direction (Table 1). The directions are given in parentheses and are measured counter-clockwise from north to the vector in the direction of the wind.

It may be noted that all the directions for any one record lie within an interval smaller than 22°.5, the angular spread corresponding to one direction of a 16-point compass. The velocities exhibit a larger variation, but are comparable. The results of either method are somewhat doubtful for the highly irregular curve.

TABLE 1—*Wind velocities and directions obtained by grqphical and six-point correlation methods*

Date	Graphical method			Six-point method	
	$t_o\ \tau_o$	$\tau_s\ \tau_o$	$t_o\ \tau_s$	$\tau_i = 6$	$\tau_i = 18$
Feb. 24, 1952	(286)– 86	(285)– 91	(289)–97	(286)–90	(281)–90
Nov. 20, 1951	(287)– 33	(287)– 38	(286)–35	(291)–27	(276)–36
Mar. 8, 1952	(260)–103	(260)–132	(252)–98	(266)–98	(252)–81

Since the graphical method requires three cross-correlation curves and one auto-correlation curve, perhaps 24 or more values of the correlation coefficient are necessary. The six-point method requires six values of the correlation coefficient and represents a great reduction in labor.

IV. EVALUATION OF WINDS FROM THE CORRELATION SURFACE

Briggs, Phillips, and Shinn [2] define the speed of fading, S, as follows:

$$S = \overline{|\partial R/\partial t|}\,\overline{R}^{-1} \qquad (12)$$

Then, the drift velocity, V, is defined in terms of the speed of fading. The drift velocity is "the velocity of an observer who has so adjusted his motion over the ground that he experiences the slowest possible speed of fading." If signal amplitudes are compared at times τ_1 apart, the displacement of the observer must be adjusted until $\rho(\xi_1, \tau_1)$ is a maximum. Then,

$$V = \xi_1/\tau_1 \qquad (13)$$

This is the drift velocity of the pattern on the ground.

For two dimensions, the drift velocity may be determined from the surfaces of constant correlation, assumed to be concentric ellipsoids centered on the origin. A plane $\tau = \tau_2$ is tangent to one of the concentric ellipsoids. The value of the correlation coefficient associated with this ellipsoid is the maximum value of $\rho(\xi, \eta, \tau_2)$ resulting from a displacement in the direction of drift. If the coordinates corresponding to the point of tangency (ξ_2, η_2, τ_2) are determined, the displacement may be found, and the drift velocity may be found from (13). It is shown that the components of the drift are

$$V_\xi = \xi_2/\tau_2\ ; \qquad V_\eta = \eta_2/\tau_2 \qquad (14)$$

It may be demonstrated further that the assumption of a circular contour in the ξ, η-plane leads to the equalities

$$\xi_2/\tau_2 = \xi_1/\tau_{1\xi}\ ; \qquad \eta_2/\tau_2 = \eta_1/\tau_{1\eta} \qquad (15)$$

where $(\xi_1 , \tau_{1\xi})$ and $(\eta_1 , \tau_{1\eta})$ are the coordinates of the tangent point of horizontal planes to the contours in the ξ, τ- and η, τ-planes. These tangent points may be found from equations of the form of (9). It follows that

$$V_\xi = -H'/A'; \qquad V_\eta = -M'/C' \ldots\ldots\ldots\ldots\ldots\ldots (16)$$

If the contour in the ξ, η-plane is elliptical, relation (15) is not valid. However, the component drift velocities may be obtained by direct application of the definition. In (2), let $\tau = \tau_2 =$ constant. The necessary conditions for $\rho(\xi, \eta, \tau_2)$ to be a maximum are that $\partial\rho/\partial\xi$ and $\partial\rho/\partial\eta$ are equal to zero. These conditions are satisfied at the point of tangency $(\xi_2 , \eta_2 , \tau_2)$. The results of differentiating (2) may be combined to solve for the ratios ξ_2/τ_2 and η_2/τ_2 . It follows that

$$V_\xi = [-H/A + MN/AC][1 - N^2/AC]^{-1} \ldots\ldots\ldots\ldots\ldots (17)$$

$$V_\eta = [-M/C + HN/AC][1 - N^2/AC]^{-1} \ldots\ldots\ldots\ldots\ldots (18)$$

If the contour in the ξ, η-plane is a circle, $A = C$, and $N = 0$, so that these equations reduce to (16), since by (11) $H'/A' = H/A$. If $A \neq C$, but $N = 0$, the equations still reduce to (16).

Assume, for convenience, that the wind is parallel to the ξ-axis. Then $V_\eta = 0$, and (18) becomes

$$-M/C + (H/A)(N/C) = 0 \ldots\ldots\ldots\ldots\ldots\ldots (19)$$

After appropriate rearrangement of (19), substitution in (17) shows that the wind is again given by (16).

In general, the wind results of the circular assumption will agree with those of the elliptical assumption, unless both the wind and the axes of the elliptical correlation contour are inclined to the coordinate axes.

V. THE EVALUATION OF SUPPLEMENTARY VELOCITIES

The radio fading has been represented by a drifting interference pattern on the ground. Then

$$dR/dt = \partial R/\partial t + V\, \partial R/\partial W \ldots\ldots\ldots\ldots\ldots\ldots (20)$$

Here $\partial R/\partial t$ is the variation of R observed at a fixed point on the ground, dR/dt is the change in R resulting from a change in ionospheric structure, and $V\, \partial R/\partial W$ is the variation associated with the drift. Also, $\partial R/\partial W$ is the spatial derivative on the ground in the direction of drift.

In a coordinate system moving in the direction of drift,

$$dR/dt = \delta R/\delta t + V_i\, \partial R/\partial W \ldots\ldots\ldots\ldots\ldots\ldots (21)$$

where $\delta R/\delta t$ is the variation in R observed at a fixed point in the moving coordinates, and V_i is the drift velocity relative to the moving system.

Subtracting (20) from (21) yields,

$$\delta R/\delta t = \partial R/\partial t + (V - V_i)\, \partial R/\partial W \ldots\ldots\ldots\ldots\ldots\ldots (22)$$

If

$$V_L = V - V_i \quad (23)$$

then V_L is the velocity of the moving coordinate system.

If the origin of the moving coordinates is held on a particular isopleth of R, then, V_L is the velocity of this isopleth. It follows that $\delta R/\delta t = 0$. When this result is substituted in (21) and (22), it is found that

$$V_i = (\mathrm{d}R/\mathrm{d}t)(\partial R/\partial W)^{-1} \quad (24)$$

$$V_L = (\partial R/\partial t)(\partial R/\partial W)^{-1} \quad (25)$$

These are instantaneous velocities. Since $\mathrm{d}R/\mathrm{d}t$ is known as the individual change and $\partial R/\partial t$ is the local change, the associated velocities may be called the individual velocity, V_i , and the local velocity V_L . The above procedure is equivalent to that applied to moving pressure systems [9]. If $\partial R/\partial W$ is replaced in (25) by $\partial R/\partial s$, the derivative in any direction, the definition of V_L is made more general. Then, V_L is a velocity that would produce the instantaneous observed fading by the drift of an isopleth towards the prescribed direction.

For an evaluation of V_L , consider two receiver stations, one to be selected as the origin. Each station provides a record of the signal as a function of time. If $R_{0,t}$ is the ordinate, at any given time, of the curve obtained at the station designated as the origin, the ordinate to the second curve at the same time is given by

$$R_{s,t} = R_{0,t} + (\partial R/\partial s)\ \Delta s \quad (26)$$

where s refers to the two stations which may have any orientation in a given coordinate system. The ordinate to the curve obtained at the origin at a time Δt after any given time is

$$R_{0,t+\Delta t} = R_{0,t} + (\partial R/\partial t)\ \Delta t \quad (27)$$

The ordinates given by (26) and (27) will always be equal if

$$\Delta s/\Delta t = (\Delta\xi^2 + \Delta\eta^2)^{1/2}/\Delta t = (\partial R/\partial t)(\partial R/\partial s)^{-1} = -V_L \quad (28)$$

In theory, it is possible to have a movable receiver station which could be positioned along a given direction so that (28) would always be satisfied. Then the record obtained at the movable station would be identical with the record of the fixed station, but would be displaced in time by Δt, so that

$$\rho(\Delta s,0) = \rho(\Delta\xi,\Delta\eta,0) = \rho(0,0,\Delta t) \quad (29)$$

Equation (29) may be used to find an average value of V_L , if it is implied that the average value is given by

$$\overline{V}_L = \overline{|\ \partial R/\partial t\ |}\ \overline{|\ \partial R/\partial s\ |}^{-1} = \overline{|\ \Delta s\ |}\ \overline{|\ \Delta t\ |}^{-1} \quad (30)$$

Application of (29) to (2) yields

$$A\ \Delta\xi^2 + C\ \Delta\eta^2 + 2N\ \Delta\xi\ \Delta\eta = B\ \Delta t^2 \quad (31)$$

From this equation, it may be shown that

$$\overline{V}_L^2 = B(1 + \tan^2 \theta)(A + C \tan^2 \theta + 2N \tan \theta)^{-1} \quad (32)$$

where θ is the direction of $\overline{V}_L$ with respect to the ξ-axis.

It may be noted that the definition and condition for evaluation of $\overline{V}_L$ are equivalent to those given for the fading velocity, V_c', by Briggs, Phillips, and Shinn [2]. If circular correlation contours are assumed, $A = C$ and $N = 0$, so that (32) becomes

$$\overline{V}_L^2 = B/A = B/C \quad (33)$$

If the contours are elliptical, $\overline{V}_L^2 = B/A$ when $\theta = 0$, and $\overline{V}_L^2 = B/C$ when $\theta = \pi/2$, but $B/A \neq B/C$.

A similar derivation for the average value of V_i leads to the conditions

$$\overline{V}_i = \overline{|\, dR/dt \,|}\ \overline{|\, \partial R/\partial W \,|}^{-1} = \overline{|\, \Delta W \,|}\ \overline{|\, \Delta t \,|}^{-1} \quad (34)$$

$$\rho(\Delta W, 0) = \rho(V\, \Delta t, \Delta t) \quad (35)$$

It is convenient to select the ξ-axis in the direction of the wind. Then from (2) and (35), it follows that

$$A\, \Delta W^2 = A V^2\, \Delta t^2 + B\, \Delta t^2 + 2HV\, \Delta t^2 \quad (36)$$

Division by Δt^2 and use of (30) and (34) and the equivalent of (16) yields

$$V_i^2 = \overline{V}_L^2 - V^2 \quad (37)$$

It may be noted that the definition and condition for evaluation of the average value of V_i are those given by Briggs, Phillips, and Shinn for the characteristic velocity, V_c [2]. Also, the result of (37) implies that all velocities are evaluated in the direction of the wind.

Equation (37) should be compared with (23). Also, reference should be made to the defining equations for the instantaneous and average velocities. It may be noted that

$$\overline{|\, (\partial R/\partial t)(\partial R/\partial s)^{-1} \,|} \neq \overline{|\, \partial R/\partial t \,|}\ \overline{|\, \partial R/\partial s \,|}^{-1} \quad (38)$$

Thus, the complete physical sense of the instantaneous relations is not necessarily carried over to the statistical evaluations. The instantaneous velocities do indicate the physical origins of the average quantities. In this respect, it should be noted that V_i and V_L were referred to the motion of a single isopleth. If the pattern does not change in size and shape, the speed of all isopleths is the same, and V_L is representative of the motion of the pattern.

Reference to (20) shows that the observed fading, $\partial R/\partial t$, results from a change in structure, dR/dt, and advection by the wind. If the change in structure is such that the pattern does not change its configuration but moves with a direction and/or velocity other than that of the wind, the fading results from a wave motion. The definition of the drift velocity would no longer be valid, because the slowest possible speed of fading would be observed by moving with the speed and direction of the unchanging pattern.

In practice, it is assumed that $V_L = V$, which implies that the unchanging pattern is drifting with twice the speed of the ionospheric wind and in the direction of the wind. That this assumption requires the pattern to be unchanging and drifting may be seen by substituting $V_L = V$ in (23) and subsequently $V_i = 0$ in (24) to show that $dR/dt = 0$. Then (20) shows that the observed fading may be attributed entirely to the drift.

Of course, random fluctuations may occur, so that the above statements apply to the average values of the instantaneous quantities, and dR/dt represents the fading resulting from random changes in structure. The inequality (38) and equation (30) indicate that the absolute values of random fluctuations are included in the evaluation of $\overline{V}_L$, the fading velocity. However, the definition of V assumes a steady drift and is not affected by the random fluctuations. Consequently, the fading velocity is not equal to the drift velocity, but is a combined measure of drift and random fluctuations. The characteristic velocity $\overline{V}_i$ involves only the fading represented by dR/dt and is a measure of the random fluctuations.

If the center of a closed system of isopleths is drifting with velocity V, but the pattern is expanding or contracting during the period of observation, the velocities of points on any two contours need not be the same, and the value of V_L given by (25) does not represent the velocity of the center. An average value, such as $\overline{V}_L$, could be obtained but would represent the combined effects of drift, expansion and random changes.

Also, the average speed that an observer should move to observe a minimum speed of fading would not be equal to the speed of the center, and the value of V would include the combined effects of drift and expansion.

VI. THE PHYSICAL SIGNIFICANCE OF THE SPATIAL CORRELATION

The correlation contour is assumed to be representative of the average distribution of the interference pattern. The orientation and eccentricity of an elliptical contour is expected to be associated with an average elliptical isopleth in the interference pattern. This may be further illustrated by considering the fading velocity as given by (30). Since $\overline{|\partial R/\partial t|}$ is a constant for all directions to be selected in the evaluation of $\overline{V}_L$, then, $|\partial R/\partial s|$ and the distribution of an average isopleth $\overline{R}$ depends on the distribution of $\overline{V}_L$. If (ξ, η) designates the coordinates of the tip of a radius vector with a magnitude $\overline{V}_L$, it may be shown that

$$A\xi^2 + 2N\xi\eta + C\eta^2 = B \qquad (39)$$

Thus, the locus of $\overline{V}_L$ is an ellipse concentric with the correlation ellipse in the ξ, η-plane. It follows that the correlation contour determines the orientation and shape of the average interference pattern.

The above statements include the assumption that the random fluctuations are independent of direction, so that the distribution of $\overline{V}_L$ is supposed to be influenced only by the space variations of the interference pattern. This assumption may not be true. Since the electrons move more freely along the magnetic field, fluctuations of the wind components parallel to the magnetic field may not have the same effect as the fluctuations perpendicular to the field. The effects of isotropic turbulence in the magnetic field may produce a directional dependence of dR/dt

so that the distribution of $\overline{V}_L$ and the correlation contour would combine these effects with the space variation of the interference pattern. The physical significance of the correlation contour may not be uniquely determined by the average shape of the interference pattern.

VII. PRELIMINARY DATA

Observations of radio fading on three receivers positioned at the corners of a right-triangle were begun in January, 1954, using a transmitter frequency of 2.3 Mc/sec. Three observations made during a half-hour interval and 28 observations made at two-hour intervals during the daytime in February were subjected to correlation analysis [6]. An example of the data is given in Table 2.

TABLE 2—*Ionospheric wind data for February 10, 1954*

Particulars	Two-hour intervals				
	$08^h\ 00^m$	$10^h\ 00^m$	$12^h\ 00^m$	$14^h\ 00^m$	$16^h\ 00^m$
Similar fades	(90)–215	(106)–92	(115)–101	(83)–65	(152)–321
Correlation (circle)	(109)– 32	(34)–26	(88)– 54	(70)–47	(345)– 12
Correlation (ellipse)	(141)– 29	(34)–20	(108)– 60	(106)–48	(342)– 14
$\overline{V}_i/V$	1.8	1.4	1.0	0.9	4.1
V	58	39	121	97	28
$\overline{V}_L$	118	66	167	131	117
$\overline{V}_i$	103	53	115	88	114
a/b	1.3	1.4	4.6	1.8	2.4
ϕ	135	140	155	154	174

The ionospheric wind velocity and direction are given for the method of similar fades and for the correlation method, assuming circular and elliptical horizontal contours. The directions are given in parentheses in degrees measured counter-clockwise from north to the vector pointing in the direction of drift and the velocities are in meters per second. The ratio a/b is the ratio of the major axis to the minor axis of the correlation ellipse in the ξ, η-plane, and the angle ϕ is measured counter-clockwise from north to the major axis.

Examination of all the data indicated that, in general, close agreement existed between the correlation methods using the circular and elliptical assumption. The two principal exceptions occurred when the major axis and the wind vector made angles between 30° and 40° with one of the coordinate axes.

The average velocity obtained by the method of similar fades was 92 m/sec, which may be compared to 27 m/sec obtained for the same observations by the correlation method. The observation at $14^h\ 00^m$ of 10 February 1954 represents the closest agreement found for the two methods. The two methods are expected to agree only when the ratio $\overline{V}_i/V$ is small compared to unity. The tabulation of these ratios indicates that in 25 of the 31 observations the ratio was greater than one. Of the remaining six observations, four were of doubtful accuracy. For this particular series of 31 observations, no agreement should have been expected.

Nevertheless, 21 of the 31 records were considered sufficiently similar to allow the determination of corresponding maxima and minima. The study suggests that it is not possible to judge the validity of the method of similar fades by a simple qualitative inspection of the records. In particular, the observations indicate that, in Puerto Rico, the fading caused by random changes is of the same order of importance as that caused by a drifting ionosphere.

For 11 of 18 observations, the wind direction given by the method of similar fades differs from that of the correlation method by less than 45°. Four others differ by less than 90°. The three remaining observations resulted from doubtful records. It would appear that the method of similar fades may be used to give an approximation to the direction of the wind under conditions which make the method invalid for the determination of velocities.

If values of $a/b \leq 1.5$ are considered too small to clearly designate an ellipse, 11 observations represent circles and 20 represent ellipses. A polar diagram of ϕ and $\overline{V}_i$ as the radius vector is given in Figure 1. All the values of ϕ are in the

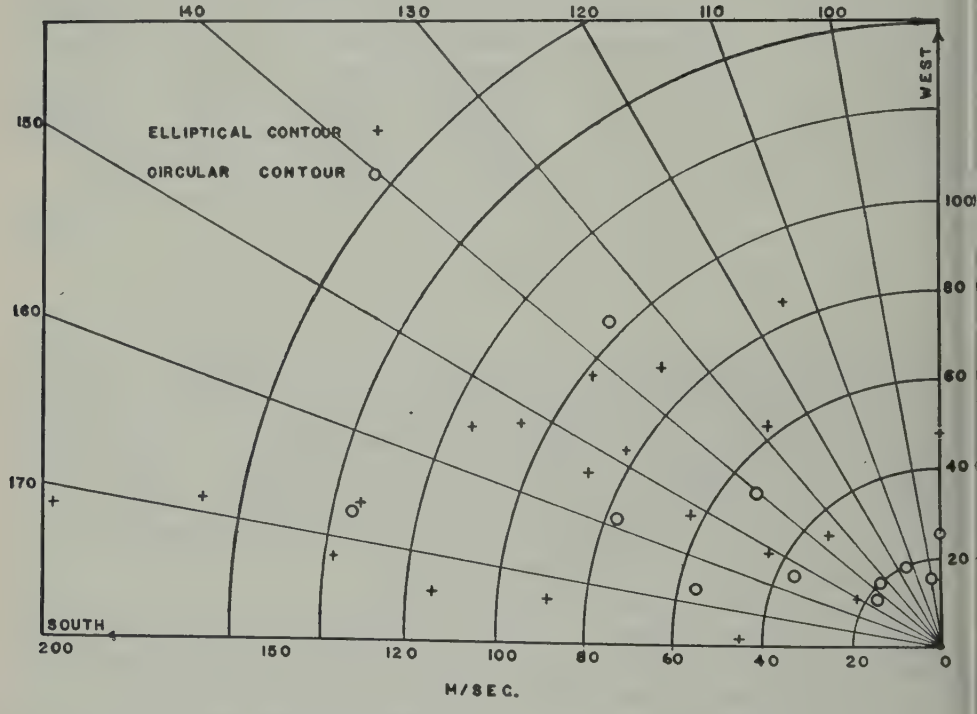

FIG. 1—Polar diagram for ϕ and $\overline{V}_i$ for ellipses and circles

second quadrant, so that the major axis is positioned in the NE and SW quadrants, a result also found from an evaluation of the three records published by Millman [7, 8]. It was found that 17 of the ellipses were oriented with the major axis between 130° and 180°. The median for these points is 152°. The marked orientation of the ellipse suggests a geomagnetic control.

The polar diagram also shows that 13 of the 20 ellipses correspond to values

of $\overline{V}_i$ greater than the average value of 78 m/sec and that 9 of the 11 circles correspond to values of $\overline{V}_i$ less than the average. The ellipses appear to be associated with the presence of turbulence.

Although the data are preliminary, the statistical distributions of wind velocities and directions are of interest. A histogram of velocity is given in Figure 2. The

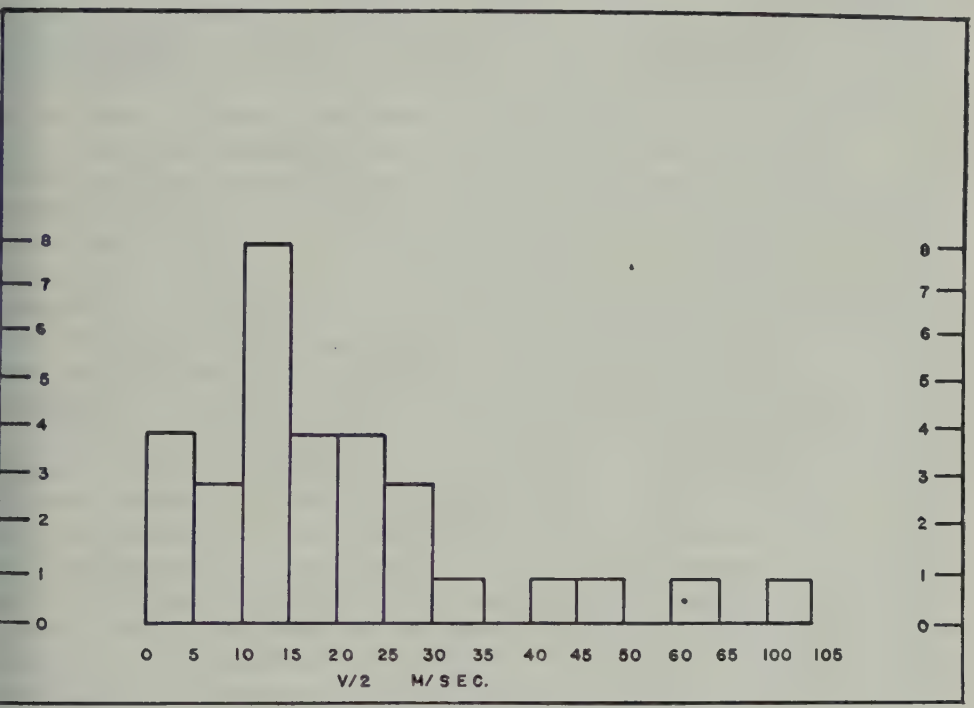

FIG. 2—Histogram for ionospheric wind velocities

average velocity is 19 m/sec and the median velocity is 16 m/sec, if the extreme value of 103 m/sec is rejected as unreliable. A polar frequency diagram of wind directions is given in Figure 3. The most preferred direction is a wind towards

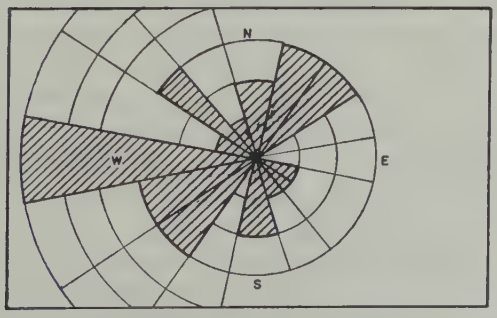

FIG. 3—Polar frequency diagram for ionospheric wind directions (reported as direction towards which wind is moving)

the west. Only six observations indicate winds moving towards directions below a NE to SW line.

VII. SUMMARY AND CONCLUSIONS

Ionospheric wind directions and velocities may be evaluated by the method of similar fades or by the longer statistical procedures of the correlation method. The comparatively short method of comparing times of maxima and minima is valid when random fading is small. A comparison of the two methods suggests that a simple visual inspection of the records is inadequate for the determination of the validity of the method of similar fades. This short method is found to give approximate directions under conditions of random fluctuations which render the velocity computation invalid. In particular, the preliminary data suggest that the random fluctuations are always of importance during daylight hours in Puerto Rico, so that the correlation method is necessary if the winds are to be evaluated on a routine basis.

A correlation method has been developed which requires only six values of the correlation coefficient. The results of this method are essentially equivalent to those of the much longer technique requiring graphs of the cross-correlation and auto-correlation functions. In addition, the six-point method readily determines the correlation ellipse in the horizontal plane.

Expressions for the drift velocity, fading velocity, and characteristic velocity have been derived from the correlation theory, extended to include the elliptical contour in the horizontal plane. The wind velocities will be comparable to those found under the assumption of a circular contour, unless both the wind and the major axis of the ellipse make large angles with both the coordinate axes. The physical origins of the evaluated velocities are associated with a local velocity and an individual velocity related to the local and individual change of signal intensity at a point in the interference pattern. The assumption that the interference pattern is unchanging except for random fluctuations and is drifting with the speed of the wind is shown to be necessary, if the evaluated velocities are to retain their intended physical meaning.

If this assumption is accepted, the correlation ellipse in the horizontal plane will indicate the shape and orientation of the average irregularity in the interference pattern, provided that it is further assumed that the random fluctuations are independent of direction. The possibility that the effects of isotropic turbulence on the random fluctuations may not be the same parallel or perpendicular to the magnetic field is noted. Preliminary data indicate a marked tendency for the major axis of the ellipse to lie in the northeast-southwest quadrants within 50° of north. The occurrence of the ellipse appears to be associated with larger than average values of the characteristic velocity, a measure of the random fluctuations. If the preferred orientation is a result of a geomagnetic control, it would seem that the effects of turbulence are not isotropic. Then, the assumption that the correlation ellipse is a measure of the shape of the interference pattern is not valid. The problem requires further study.

The preliminary data indicate that the *E*-region wind averages 19 m/sec in February. The most preferred direction is towards the west. Twenty-five of 31

observations showed winds moving towards directions above a line drawn from NE to SW. All observations were made during the daylight hours, $08^h\ 00^m$ to $16^h\ 00^m$ LMT.

VIII. ACKNOWLEDGMENT

Sincere appreciation is extended to Dr. Miguel Wiewall, Jr., Dean of the Faculty of Science, under whose direction the observational records were obtained. The author's gratitude also is expressed to Mr. Luis Escabí and Mr. Willie Ocasio for their considerable assistance in the evaluation of the experimental records.

References

[1] S. N. Mitra, Proc. Inst. Elec. Eng (London), **96**, Pt. 3, 441-446 (1949).
[2] B. H. Briggs, G. J. Phillips, and D. H. Shinn, Proc. R. Soc. (London), B, **63**, 106-121 (1950).
[3] J. H. Chapman, Can. J. Phys., **31**, 120-131 (1953).
[4] C. D. Salzberg and R. Greenstone, J. Geophys. Res., **56**, 521-533 (1951).
[5] B. H. Briggs and G. J. Phillips, Proc. Phys. Soc. (London), B, **63**, 907-923 (1950).
[6] D. G. Yerg, Sci. Rep. No. 2, Faculty of Science, College of Agriculture and Mechanic Arts, University of Puerto Rico (August, 1954).
[7] G. H. Millman, Ann. Géophys., **8**, 365-384 (1952).
[8] G. H. Millman, Sci. Rep. No. 37, Ionosphere Res. Lab., Pennsylvania State University (May, 1952).
[9] S. Petterssen, Weather Analysis and Forecasting New York, McGraw-Hill Book Co., Inc., 505 pp. (1940).

THE PRESSURE EFFECT ON THE ELECTRICAL CONDUCTIVITY OF PERIDOT*

By Harry Hughes

Dunbar Laboratory, Harvard University, Cambridge, Massachusetts

(Received February 12, 1955)

ABSTRACT

The effect of pressure on the ionic conductivity of peridot is measured and its influence on the electrical conductivity and temperature of the earth's mantle discussed.

The electrical conductivity throughout the earth's mantle can be inferred from various aspects of the geomagnetic field. The conductivity distribution found suggests that the mantle is a semiconductor, the rapid increase of conductivity observed being then attributable simply to the rise of temperature with depth. Measurements on the olivine and pyroxene series have shown that their conductivity does increase rapidly with temperature in the manner required (Hughes, 1953; Price, 1953). Above about 1100°C, they are ionic semiconductors; below this, electrons appear to be the current carriers and the increase of conductivity with temperature is more gradual. Before a revealing comparison between the observations and the measured conductivities can be made, it is necessary to determine how the measurements are affected by pressure.

The pressure apparatus used generates pressures up to 10,000 kg/cm^2 within a long cylinder, 4 cm in internal diameter, using compressed nitrogen as the pressure medium. The specimens to be measured have a very high impedance, so that a highly insulating medium was required to prevent short circuiting, and the leak resistance at the leads into the pressure chamber was kept above 10 megohms. The high temperature was produced by a platinum wire wound electric furnace placed inside the pressure chamber. Its length was 9 cm, its internal diameter 0.4 cm, and the power needed to reach 1600°K was about 0.6 kw. In the first thousand atmospheres, the density of the nitrogen increased to about unity and convection became the chief means of heat loss, resulting in a change in the temperature distribution in the furnace. Measurements were not attempted in this region of rapid change, but were confined to the range 10^3 to 10^4 bars.

The temperature of the specimen had to be accurately measured, as the conductivity depends so sensitively on it (the percentage change in conductivity was about 20 times the percentage change in temperature). However, the temperature need only be held constant for the short time required to make a conductivity measurement, and a small departure from a chosen fixed temperature could be readily allowed for. It was found sufficient simply to apply the approximate power

*Paper No. 139, published under the auspices of the Committee on Experimental Geology and Geophysics and the Division of Geological Sciences at Harvard University.

needed through a Variac, and make simultaneous conductivity and temperature measurements a minute or two later. Various thermostats were tried, but none was sufficiently good to simplify the above procedure.

The specimen used was a small cylinder of peridot, the gem-stone variety of olivine from the Red Sea, 0.35 cm long and 0.17 cm in diameter. It was held between two ceramic tubes of similar diameter, which were themselves supported in cylindrical steel blocks forming the ends of the furnace. Each tube carried a Pt/10%Rh:Pt thermocouple, whose junction touched the specimen. Good electrical contact was made by coating the ends of the specimen and tubes with platinum, formed by firing platinum paste. By firing with the specimen in place on one of the tubes, it could be firmly attached; this made for ease of assembly.

The thermocouples served as leads for the conductivity measurements, which were made by an A.C. bridge method to prevent the specimen polarising. An oscillator provided 50 volts, 400-cycle A.C.; the voltage had to be reduced at high conductivities to keep the Joule heating negligible, but was always large compared with the thermo-e.m.f.'s across the specimen. The detector used was a C.R.O., which, with amplification of 10^4, enabled the resistance to be measured to better than 2 per cent in the range 10^6 to 10^4 ohms.

The departures of temperature from a chosen value are of three kinds. One results from not attempting to adjust the temperature closer than ± 2 to 3°C to the desired value. Secondly, there are temperature gradients across the specimen which were particularly steep (5 to 10°C/mm) because of the small size of the furnace. It is this that necessitates using thermocouples touching each end of the specimen and taking the average temperature. The third error arises from the effect of pressure on the thermocouple readings. Only a thermometer utilising the the resistor noise from the electrons' random motion appears capable of giving temperatures on the thermodynamic scale under high pressures, and a practicable instrument has yet to be built (but see Garrison and Lawson, 1949). At moderate temperatures, the whole pressure chamber can be placed in a constant temperature bath and thermometers inside and outside the chamber compared. Using this method, Birch (1939) found the e.m.f. of a Pt/10%Rh:Pt couple decreased by 15μV at 470°C and 4100 kg/cm^2, the limits of his measurements. The effect, though small, introduces a considerable correction to the measurements described here, which were furthermore made at considerably higher temperatures and pressures.

Chemical change in the apparatus produced various difficulties. It prevented the use of tungsten or molybdenum furnace windings. Moisture had to be absorbed by silica gel to prevent short circuiting of the leads at the plug. Carbon was deposited on the hot portions of the apparatus and short circuited the specimen. Its source was probably the fine rubber dust produced by friction at the piston packings and carried into the furnace by the dense convecting fluid. Filters proved insufficient, so an auxiliary furnace was added which, heated to about 700°C for an hour after altering the pressure, fixed most of the carbon but was time consuming in use. The best solution was to heat the specimen quickly to the high temperatures at which measurements were made; the carbon would then deposit harmlessly in the cooler regions. A final difficulty was the susceptibility of hot iron-bearing

silicates to decompose, revealed by their progressively changing conductivity under constant conditions and by their blackened appearance found on dismantling. Neither effect was found on the peridot specimen finally used.

The direct measurement of the pressure effect requires measuring the conductivity as a function of pressure with the temperature held constant. Four runs were made at temperatures of 1333°K, 1429°K, 1513°K, and 1597°K, though the last was valueless, as the electrical contact with the specimen was poor. At each temperature, measurements were made at pressures of 1000, 2500, 4000, 5500, 7000, and 8500 kg/cm^2 in an ascending and descending cycle. The two readings at each pressure were averaged, a straight line relationship assumed, and the pressure effect determined from the slope. The method of reduction eliminates a uniform drift, though this was present only at the lowest temperature. Each conductivity reading had a correction of a few per cent to allow for the departure of the temperature from the chosen value. The three runs gave the decrease of conductivity with pressure as $(2.9 \pm 0.9)\%$, $(3.7 \pm 0.3)\%$, and $(2.3 \pm 0.6)\%$ per 1000 kg/cm^2, respectively, where the standard errors express the scatter of the points. The conductivities in the three runs, at three different temperatures, varied by a factor of 15, so evidently it is not the absolute but the percentage change of conductivity with pressure that is approximately constant; that is,

$$\frac{1}{\sigma}\frac{\partial \sigma}{\partial p} = \frac{\partial(\log \sigma)}{\partial p} \simeq \text{constant}$$

At a single temperature, the measurements were not sufficiently accurate to distinguish between $\sigma^{-1}\partial\sigma/\partial p$ and $\partial\sigma/\partial p$. The total change in conductivity with

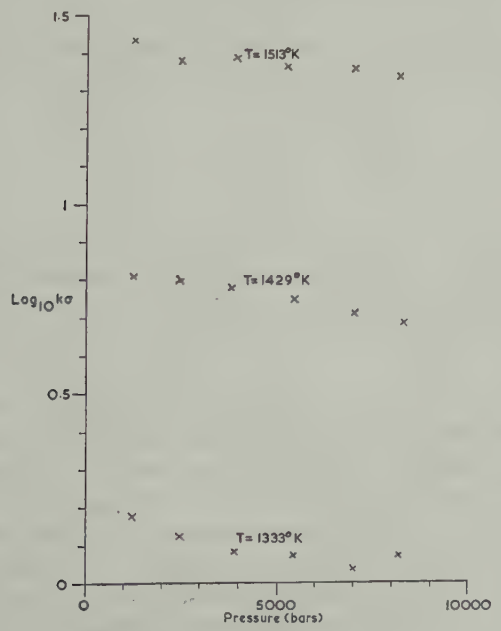

Fig. 1—Conductivity-pressure measurements on peridot

pressure was about 20 per cent, equal to that produced by a temperature change of 14°C. Figure 1 illustrates the scatter of the measurements and the relative magnitudes of the changes of conductivity with temperature and pressure.

The pressure effect on the thermocouples, extrapolating Birch's measurements, results in the measured temperature being 0.7°C lower than the true temperature for each 1000 kg/cm^2 pressure. This would cause an apparent increase of conductivity of 1.1 per cent per 1000 kg/cm^2. Thus, the true decrease of conductivity is $(4.0 \pm 0.9)\%$, $(4.8 \pm 0.3)\%$, and $(3.4 \pm 0.6)\%$ per 1000 kg/cm^2; that is, $\partial \log \sigma/\partial p \simeq 4 \times 10^{-5}\text{bar}^{-1}$.

The conductivities extrapolated to zero pressure for the three runs were 1.48, 6.9, and 21.3, all times $10^{-6}\text{ohm}^{-1}\text{cm}^{-1}$, values that satisfy the semiconduction equation

$$\sigma = \sigma_0 \exp(-E/kT)$$

if the constants σ_0 and E are taken as $4 \times 10^{5}\text{ohm}^{-1}\text{cm}^{-1}$ and 2.7 eV, respectively. The magnitude of these constants shows the conductivity is ionic. Now,

$$\frac{\partial(\log \sigma)}{\partial p} = \frac{\partial(\log \sigma_0)}{\partial p} - \frac{1}{kT}\frac{\partial E}{\partial p}$$

and it is likely that the first term is small compared with the second. On this assumption, the measurements indicate that the initial increase of E with pressure is $4.8 \times 10^{-6}\text{eV/kg/cm}^2$.

The temperature and pressure at which these measurements were made are approximately those obtaining at the top of the earth's mantle, and we shall assume that the measured decrease of conductivity of 4%/1000 kg/cm^2 holds there, though the uncertainties common in geophysical speculation due to the uncertain composition and phase of the interior must be kept in mind. The pressure increases with depth by 350 bars/km, which, acting alone, would decrease the conductivity by 1.4%/km. But

$$\frac{1}{\sigma}\frac{\partial \sigma}{\partial T} = \frac{E}{kT^2} = 1.6\%/°\text{C}$$

with $E = 2.7$ eV, $T = 1400$°K. Thus, an increasing temperature gradient of about 1°C/km is needed to keep the conductivity constant. However, the conductivity is known to be rapidly increasing at the rate of about 1%/km in the upper part of the mantle, so that the total temperature gradient required is about 1.7°C/km.

At the base of the mantle, the pressure is a factor of a hundred greater than attained in the measurements, so that the large extrapolation required introduces an added uncertainty to the estimated temperature. The measurements merely determined the average value of $(\sigma^{-1}\partial\sigma/\partial p)_T$, or physically $\partial E/\partial p$, in a small temperature-pressure field. In the circumstances, perhaps the most physically reasonable assumption is that the excitation energy E increases at the measured rate for all temperatures and pressures; this ignores the possibly important derivatives of $\partial E/\partial p$ with respect to temperature and pressure, but is a step beyond earlier work where E was treated as a constant. With this model, E is 2.8, 3.7,

and 4.6 eV at 100, 600, and 1000 km depth, and the temperatures required at these depths to give the observed conductivities (Lahiri and Price, 1939, curve *d*) are 1480, 2220, and 3180°K, respectively. At the base of the mantle, E is 9.2 eV and the conductivity inferred from magnetic observations about 10 ohm^{-1} cm^{-1}, necessitating a temperature of 10,000°K, though here, of course, the extrapolation from the measured values is very great.

The advice of Prof. Francis Birch and his support of this work are gratefully acknowledged.

References

Birch, F. (1939); Rev. Sci. Instr., **10**, 137-140.
Garrison, J. B., and A. W. Lawson (1949); Rev. Sci. Instr., **20**, 785-794.
Hughes, H. (1953); Ph.D. thesis, University of Cambridge.
Lahiri, B. H., and A. T. Price (1939); Phil. Trans. R. Soc., A, **237**, 509-540.
Price, A. T. (1953); Nature, **172**, 786-787.

FIRST INVESTIGATION OF AMBIENT POSITIVE-ION COMPOSITION TO 219 KM BY ROCKET-BORNE SPECTROMETER

BY CHARLES Y. JOHNSON AND EDITH B. MEADOWS

Naval Research Laboratory, Washington 25, D. C.

(Received February 28, 1955)

ABSTRACT

The ambient positive-ion composition of the upper atmosphere in the range 8 to 49 atomic mass units (AMU) was measured between 93 and 219 km by means of a Bennett radio-frequency mass spectrometer. The experiment was flown in the Navy Viking 10 rocket, launched from White Sands Proving Ground, Las Cruces, New Mexico, at $10^h\ 00^m$ MST, May 7, 1954. The most prominent ion peaks found between 93 and 124 km on the ascent were at 16, 26, 30, and 32 AMU. Other less prominent peaks occurred at 12, 18, 19, 21, 23, 38, and 45 AMU. From 124 to 219 km, ions of 16 and 32 AMU persisted. The results of this investigation are to be considered preliminary and need further verification, not only because the data were obtained from only one flight, but also because of complications introduced by a charge acquired by the rocket and by the evolution of gas from the rocket.

INTRODUCTION

Data on the ion composition of the ionosphere are of primary importance to an understanding of the physical processes which take place there. This paper reports on the first attempt to make a direct measurement of the ionosphere's positive-ion composition by means of rocket-borne instrumentation.

The ambient positive-ion composition of the upper atmosphere in the range 8 to 49 atomic mass units (AMU) was measured between 93 and 219 km by means of a Bennett radio-frequency mass spectrometer [see 1 of "References" at end of paper]. The experiment was flown in the Navy Viking 10 rocket, launched from White Sands Proving Ground, Las Cruces, New Mexico, at $10^h\ 00^m$ MST, May 7, 1954. Results of this first investigation indicate that in the 93- to 124-km region the most prominent positive ions were of 16, 26, 30, and 32 AMU; above 124 km, ions of 16 and 32 AMU persisted. In addition, a peak at the high end of the mass scale appeared at 100 km, increased rapidly, and persisted to 219 km.

There are several features of the experimental results which have not been fully explained and need to be verified by additional flights. Acquisition by the rocket of a negative charge made the interpretation of the spectra ambiguous and may have upset the ambient ion composition. Gas evolved from the rocket may have become ionized and contaminated the spectra or may have interfered with the collection of ambient ions. Additional flights using this technique are planned in the summer of 1955.

EXPERIMENTAL ARRANGEMENT

Instrumentation for the positive ion experiment was similar to that described by Townsend [2] for gas composition studies in the upper atmosphere, but had no internal ion source, since the source of ions was the ionosphere itself. The spectrometer elements were encased in a stainless steel tube, 6.3 cm in diameter and 15 cm in length; this sturdy construction permitted placing the first grid only 1.9 cm from the rocket skin. The tube was attached to the rocket skin 2.1 meters from the nose-tip and perpendicular to the rocket axis by means of an adapter ring with two O-ring seals to maintain nose-cone pressurization. It was recognized that a metal tube which was open at all times would evolve a considerable amount of gas during the rocket flight. The gases evolved did not attain sufficient density to interfere with the passage of ions through the tube, because the 4.1-cm diameter hole in the rocket skin had a pumping speed of 150 liters/second.

The flight unit, Figure 1, was 25.4 cm long over-all and weighed 2.2 kg. The

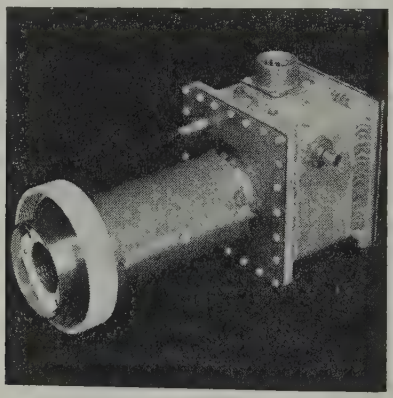

FIG. 1—Radio-frequency ion mass spectrometer for Viking 10

enclosure at the rear of the stainless steel envelope protected the metal to glass seals and facilitated wiring. As a precaution, a mu-metal shield was placed around the tube to reduce any magnetic field effect.

The spectrometer was a modified version of the Bennett 7-5 cycle radio-

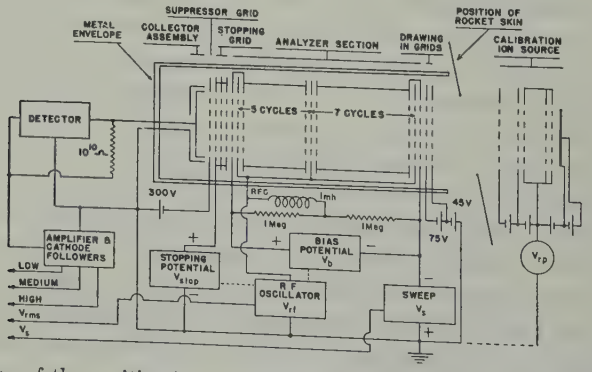

FIG. 2—Diagram of the positive-ion spectrometer instrumentation for Viking 10

frequency mass spectrometer (see Fig. 2). It consisted of a series of accurately-spaced, circular grids of knitted tungsten mesh, and a collector assembly, all supported within the metal envelope by two teflon spacers. Positive ions were drawn into the spectrometer by the negative potential on the first grid and further directed down the tube by the potential on the second grid. After passing the second grid, the ions were accelerated to a velocity depending on their mass by the negative saw-tooth sweep potential, V_s , applied to the analyzer section. Unlike conventional spectrometers, the R.F. spectrometer did not require a magnetic field in its analyzer section, but utilized an R.F. grid system, in which maximum incremental energy was imparted to the desired ion which arrived at the R.F. grids with the proper phase and velocity. A "stopping" field after the analyzer section was used to reject all ions except those receiving this maximum energy. A suppressor grid was used to return secondary electrons released by ions hitting metal surfaces in the collector assembly.

Since the radio frequency potential used in this experiment was not negligible compared to the sweep potential, the equation giving the mass of the singly charged ion receiving maximum incremental energy was [3]

$$M = \frac{0.266(V + 2.05V_{rms})}{s^2 f^2} \quad \ldots\ldots\ldots\ldots\ldots\ldots\ldots\ldots (1)$$

where M is the mass in atomic mass units, V is the negative potential in volts through which the ion has fallen in reaching the first stage, V_{rms} is the root-mean-square value of the radio frequency potential in volts, s is the grid spacing in centimeters, and f is the radio frequency in megacycles. The term, 2.05 V_{rms} , is the potential through which the selected ions fall due to the radio frequency potential in passing through the first stage. To avoid preferential selection with mass number in a multi-stage tube, it was necessary to introduce a bias potential.

If the rocket vehicle containing the spectrometer acquires a charge while it is in the ionosphere, V in equation (1) must be modified to include the effects of such a charge. An apparent rocket potential may be defined as kV_{rp} , where V_{rp} is the potential due to a negative charge and k is the fraction which takes into account the point in the field where the ion was created or where it experienced its last collision. Then V in equation (1) is equal to V_s , the negative sweep potential, plus kV_{rp} , giving for the mass of the selected ion

$$M = \frac{0.266(V_s + kV_{rp} + 2.05V_{rms})}{s^2 f^2} \quad \ldots\ldots\ldots\ldots\ldots\ldots\ldots\ldots (2)$$

When V_{rp} is zero and s, f, and V_{rms} are constants, a linear relationship exists between M and V_s . The mass scale for the spectrometer under these conditions will be called the absolute mass scale.

A negative charge on the rocket would result in a mass scale which is shifted toward lower mass numbers on the absolute mass scale and in an increased ion current due to the effective lowering of the stopping potential by kV_{rp} . Introduction of the uncontrolled parameter, kV_{rp} , made it difficult to determine the proper setting of the stopping potential so the spectrometer would operate at the desired signal level.

Ion current reaching the collector was passed through a 10^{10}-ohm resistor and detected by a 100 per cent negative feedback DC amplifier which saturated at 40 volts. One-ninth of the output was taken from a resistance-voltage divider and telemetered through a cathode follower as LOW, the output of the amplifier was telemetered through another cathode follower as MEDIUM, and the signal was amplified by a factor of seven and telemetered as HIGH. In addition, proportional parts of V_s and V_{rms} were telemetered. All this information was radioed to ground recorders by the NRL AN/DKT-2 telemeter [4].

CALIBRATION

Response of the ion spectrometer to pressure and stopping potential was measured by using an ion source of known characteristics in the experimental arrangement shown in Figure 2. The efficiency of the spectrometer (ratio of the ion current collected to ion current entering the spectrometer) was nearly constant below 10^{-4} mm Hg and decreased to zero at about 10^{-3} mm Hg. Furthermore, the efficiency in the 10^{-3} to 10^{-4} mm Hg range depended upon the composition of the ion.

Typical spectra taken in the laboratory on a longer mass scale are shown in Figure 3. The ions, $N^+(14)$, $O^+(16)$, $OH^+(17)$, $H_2O^+(18)$, $N_2^+(28)$, $O_2^+(32)$, and

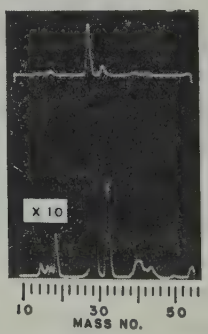

FIG. 3—Laboratory spectra of air

$A^+(40)$, are produced by the ion source from air admitted to the vacuum system. The other ions present are produced from oil contaminants in the vacuum system.

To simulate the effects of rocket potential, a variable potential was introduced between the ion source and the ground point of the analyzer, as indicated in Figure 2; other parameters were held constant. As rocket potential increased, the fundamental peak moved down scale. However, the intercept on the high mass side remained nearly constant, because the potential varied in such a manner that thermal ions were always present. Above a particular rocket potential, harmonic peaks began to appear.

The absolute mass scale was determined prior to flight from spectra of thermal ions and was 8.2 to 49.2 AMU for the flight instrumentation. Deviations in the length of the mass scale were expected, primarily in the high mass end due to changes in V_s as the impedance of the power supply changed. Deviation in the low mass end was due to fluctuations of the ignition point of the thyratron used

n the sweep circuit and was found not to exceed 0.1 AMU with normal B^+ and neater supply variation.

Adjustment of the spectrometer prior to flight was based on the expectation that the rocket would acquire a negative charge. Since the rocket potential due to this negative charge effectively lowers the stopping potential, the stopping potential was set close to that required for complete suppression of ion current. This left an operating range of 10 volts before harmonics would appear.

EXPERIMENTAL DATA

Viking 10 was in powered flight to an altitude of 53 km above sea level and continued under free fall conditions to a peak altitude of 219 km. After powered flight, the rocket was inclined 3° from the vertical along its flight path to the north and was controlled in pitch, roll, and yaw by auxiliary jets. The jets used steam from hydrogen peroxide and operated intermittently as needed. At 115 km, however, roll control was lost, and the rocket proceeded to slowly rotate counterclockwise, as observed from the nose, for one and one-quarter revolutions, until peak was reached. At peak, the rocket was turned toward a horizontal position and then was spun clockwise about its axis with an initial roll rate of 0.64 rev./sec. Following this maneuver, all controls were shut off and the rocket continued to spin on the descent. After the maneuver, the rocket axis described a cone whose included angle was 40°. The axis of this cone was 55° from the vertical and pointed 15° west of north.

A few seconds after spin was introduced, a rupture occurred in the peroxide system and released copious quantities of gas for a period of at least 20 seconds. Furthermore, under the influence of this spin, the excess liquid oxygen in the fuel tank was thrown by centrifugal force to the tank walls, where it evaporated at an accelerated rate. At 207 km on the descent, the pressure within the tank reached the relief valve value and oxygen venting began. Venting was presumed to have continued during the remainder of the flight.

Prior to the rocket flight, ionosphere records taken at White Sands Proving Ground showed normal ionospheric conditions in the E and $F1$ regions, and a mild storm in progress in the $F2$ region. The electron density experiment [5], performed simultaneously, showed that the electron density ranged from 10^4 electrons/cc at 91 km to 10^5 electrons/cc at 101 km, and then slowly increased to 2×10^5 electrons/cc somewhere between 101 and 219 km.

Data from the spectrometer were recorded 100 per cent of the time by the telemeter ground stations. The absolute mass scale for the flight spectra was determined by measuring the sweep potential from the telemetered data. The low mass end was at 8.6 ± 0.5 AMU, and the sweep length was 41 ± 0.2 AMU. As these values are equal within the experimental error to those measured prior to flight, the mass scale, 8.2 to 49.2 AMU, was used as the absolute mass scale for all spectra. The mass number of a particular ion peak was determined by noting the position of the high mass side of the peak on the base-line. The high mass intercept of a peak remained constant in the pressure range covered in this experiment, because there were always ions which had fallen through a negligible portion of the rocket potential after their last collision. Such ions behaved as thermal

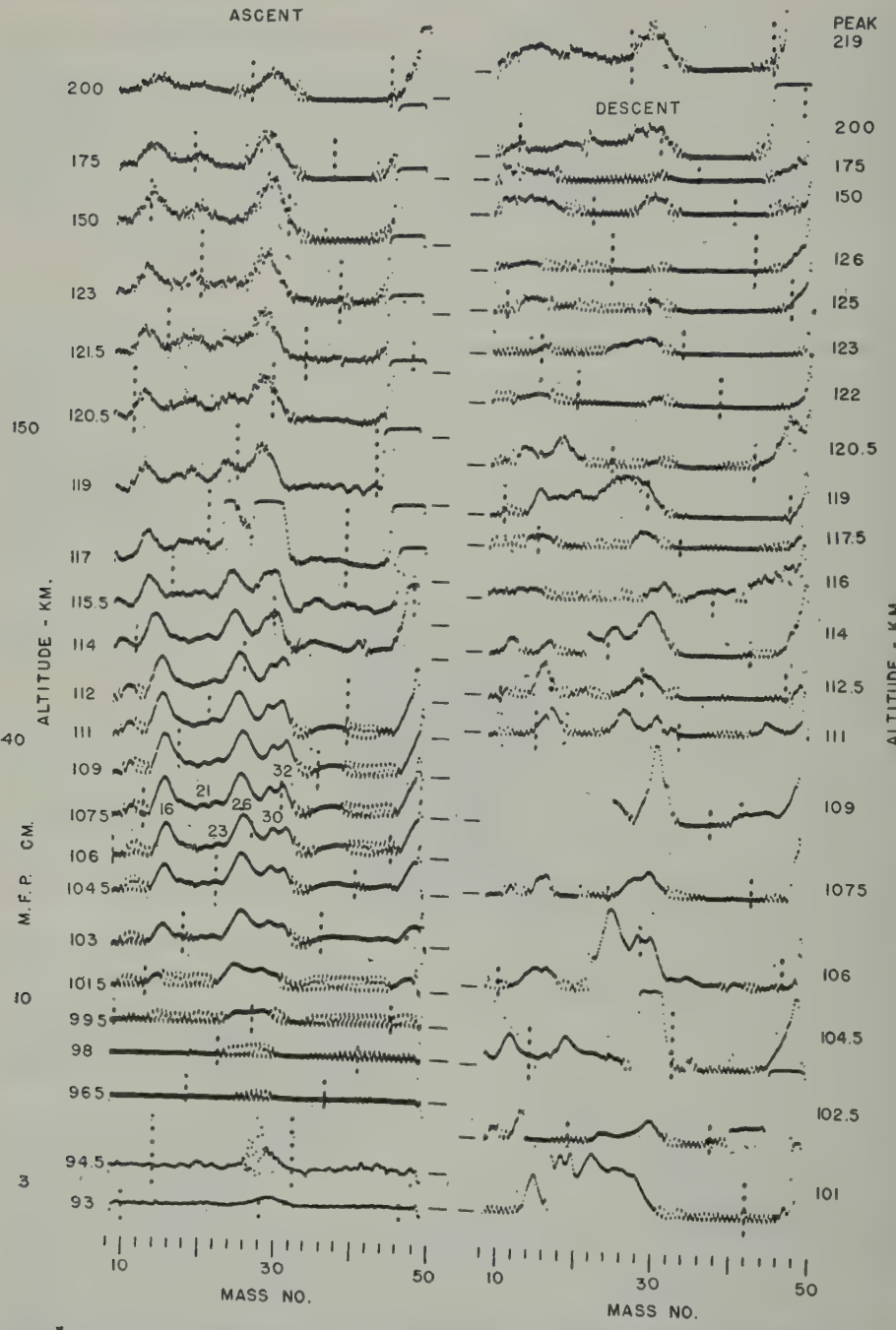

FIG. 4—Positive ion spectra, $10^h\ 00^m$ MST, May 7, 1954, White Sands Proving Ground, New Mexico

ions and were collected at their proper mass number on the absolute mass scale. In the rocket spectra, the ion peak which had its high mass intercept at 33.5 was studied most carefully, since it was not distorted by ion peaks at immediately higher mass numbers; this peak had a mass number of 32 AMU. The amount of shift along the mass scale could then be established for each spectrum and the mass number of the remaining ion peaks determined.

Samples of the spectra obtained are shown in Figure 4. All the spectra shown were recorded on the LOW channel, except the 93- and 94-5-km spectra taken on the ascent, which were recorded on the MEDIUM channel. The left column shows all the mass spectra obtained from 93 to 123 km and typical spectra at higher altitudes on the ascent. The right column shows typical spectra taken on the descent at corresponding altitudes. The spectrum at the top right was obtained at 219 km, the peak of the flight. Altitudes given for each spectrum are mean altitudes to the nearest 0.5 km. Mass scales from 8 to 50 atomic mass units, shown at the bottom of the ascent and descent columns, are based on the absolute mass range previously discussed. Mean free paths in centimeters for nitrogen molecules at several altitudes [6] are indicated on the left of the ascent spectra. Horizontal lines between the two columns of spectra indicate the base-line for each spectrum. The vertical rows of dots are half-second time-markers supplied by the telemeter recorder.

On the ascent, the first spectrum to show a resolved ion-current peak occurred at 93 km. The peak was extremely broad and was identified by its high mass intercept as mass 32. Other ions may have been present at this altitude, but were not detected, since the efficiency of the spectrometer depended on composition below 103 km. On the 99.5-km spectrum, measurable ion current appeared at other mass numbers, notably at mass number 26.

Consider the spectra at 106 and 107.5 km on the ascent, where the shift of the peaks on the mass scale indicated that the rocket potential, kV_{rp} , was at a minimum. Beginning from the left or low mass end, the spectra showed positive ion peaks at masses 12, 16, 21, 23, 26, 30, 32, and 48(?). Other less prominent ion peaks which have been identified on these spectra were of masses 18, 19, 38, and 45. The mass of the peak at 48 was difficult to determine, since its high mass intercept was off scale. However, from the 101.5- to 104.5-km spectra, its mass number appeared to be 48, although it could be as high as 50 AMU. This peak does not appear to be an instrumental effect, but its presence has not been explained.

It was interesting to note the behavior of the various peaks with altitude on the ascent. The amplitudes of the peaks of mass number 16, 26, 30, and 32 *vs* altitude have been plotted in Figure 5. The peaks of mass number 26 and 30 increased with altitude to a maximum in the region of 113 to 120 km, and then decreased or were obscured, until by 124 km they were no longer recognizable as peaks. The other peaks of mass number 18, 19, 21, 38, and 45 either disappeared in the same manner or were obscured by noise. The peak of mass 12 was shifted off scale as the rocket acquired charge and did not appear after 115.5 km. At the same time, the peak at the high mass end of the scale, 48(?), which appeared by 101.5 km, increased rapidly in amplitude with altitude and saturated the detector amplifier by 114 km. Peaks at 16, 23, 32, and 48(?) persisted to 219 km. Above

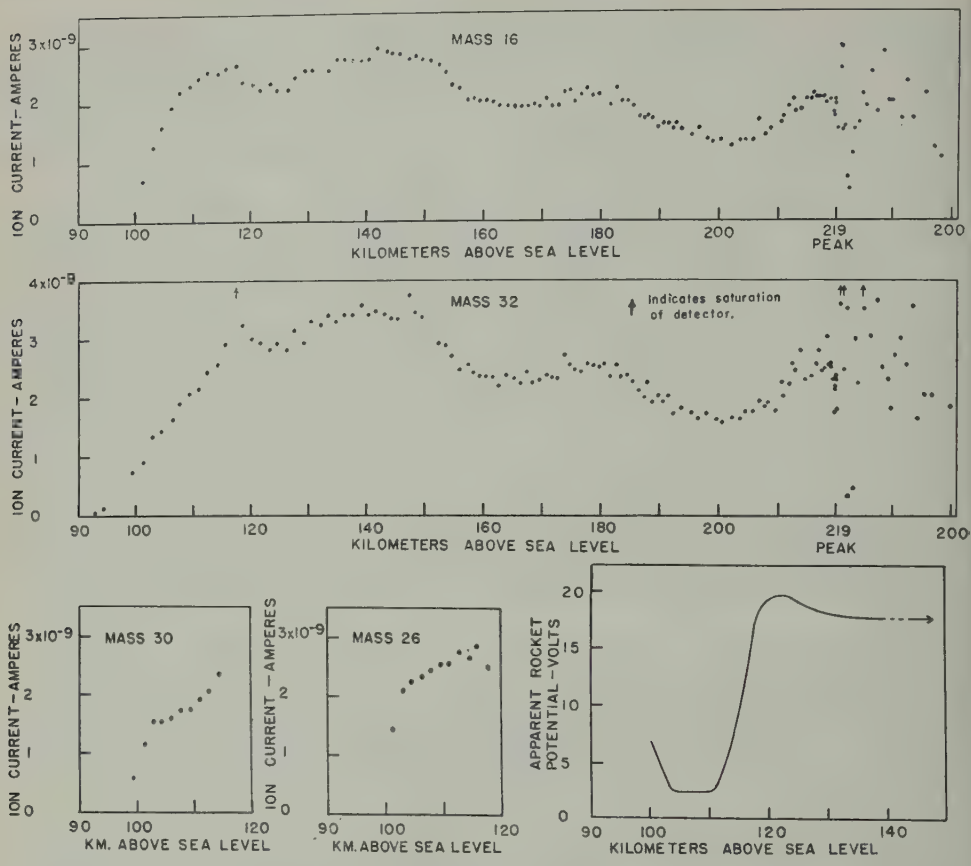

FIG. 5—Ion current of ions of 16, 26, 30, and 32 AMU, and apparent rocket potential *vs* altitude

160 km, ion current in the region 34 to 44 AMU approached zero, even on the HIGH channel. Above 120 km, harmonic peaks were expected to appear due to the rocket potential. The lower harmonic for the peak at mass 32 was at 23.8 and for 48 was at 35.6. Since there was no peak near 35.6, it was doubtful that the peak at 23 was the lower harmonic of 32. Between mass numbers 16, 23, and 32, there was ion current, but the peaks were too small and broad to permit their identification.

Measurements on the mass separation between the peaks of mass number 16 and 32 showed their average separation above 124 km to be 15.3 AMU instead of 16. This shift of 0.7 AMU was associated with the rocket potential, as it did not occur on spectra where the rocket potential was low.

A striking feature of the spectra was the shift of the position of the ion peaks with respect to the absolute mass scale. The shift was at a minimum at about 107 km and had a constant value above 130 km. In Figure 5, the shift of the ion peaks was plotted as an apparent rocket potential, wherein the potential plotted was the change in position of the ion peak on the mass scale in volts of accelerating

potential. Because the spectrometer measured the velocity which the ion had upon entering the tube, the potential plotted was less than the actual potential on the rocket by an undetermined factor. This factor depended on the position of the ion in the rocket field when it was created or when it experienced its last collision before entering the tube.

DISCUSSION

The clarity of the flight spectra was impaired by the presence of oscillations and noise and by the broadness of the peaks. The regular oscillations occurred only when the ion current was in a certain range and for this reason may have been instrumental in origin. The irregular type of noise above 120 km may have been due to random fluctuations in the rocket potential, to non-uniformities in the surrounding cloud of rocket gas, or to variations in the ion density of the ionosphere. The ion peaks were very broad due to the shift they experience from the rocket potential. Consequently, peaks differing in mass number by one or two AMU contributed to each other, and a large ion peak tended to obscure the presence of any small ion peak of adjacent mass number. In Figure 5, no corrections have been made for this overlapping. Above 100 km, any additional ions in the mass range 10 to 35 AMU having a concentration of at least one part in 65 would have been identified.

At various times during the ascent and during the maneuver at peak, described in a previous section, the control jets, located at the rear of the rocket, were turned on. Except during the maneuver, a jet was on for less than 0.3 second. Sometimes there appeared to be a slight enhancement of the spectra when a jet was on, but at other times the operation of a jet could not be detected in the spectra. Philips gages located on the nose-cone above the spectrometer detected a change in pressure whenever a jet was on [7].

Upon introduction of the maneuver, the amplitude of the peaks gradually decreased during the period that the tumble jets were on. When the roll jets were turned on, the spectra were enhanced, and were further enhanced when the rupture in the peroxide system occurred. Then the resulting gas cloud which formed around the rocket apparently interfered with ions approaching the rocket and caused the spectra to diminish. As the cloud dissipated, the spectra reappeared and resembled the ascent spectra.

During the descent below 207 km, a series of abrupt, roll sensitive disturbances appeared simultaneously on the records of three of the experiments carried in the rocket. They were seen as noise-free regions on the record of the radio propagation experiment, as either an increase or decrease in pressure indicated by the Philips gages, and as a corresponding increase or decrease in the ion current detected by the mass spectrometer. The disturbance was in the medium outside the rocket, but its cause and nature have not been explained.

After oxygen venting commenced, the spectra decreased in amplitude and remained depressed to about 120 km, as can be seen in Figure 4. Here the velocity of the rocket and the ambient pressure were high enough to make the oxygen stream out behind the rocket instead of enveloping the rocket in a cloud. Because the rocket was on its side and spinning, the mean free path in the spectrometer

varied. When the mean free path was approximately 30 cm or less, the efficiency of the spectrometer was reduced; hence, the spectra were distorted at lower altitudes and depended on the spatial position of the rocket. The portions of the spectra taken near ambient pressure conditions tended to confirm spectra taken on the ascent, for example, the center portion of the spectrum at 106 km.

Sunlight entered the spectrometer at various times during the flight, depending upon the spatial position of the rocket. On the ascent, sunlight entered the tube between 175 and 211 km (see Fig. 5). In this region, the over-all ion current showed a decrease, which can be correlated with the depth of penetration of the sunlight into the spectrometer. Apparently, the decrease in ion current was due to an abundance of photoelectrons produced in the tube and possibly around the mouth of the spectrometer.

Several theories have been advanced concerning the source of the negative rocket potential. It was apparently due to electrons striking the rocket with energies greater than 20 electron volts. The electrons might have acquired their energy from the R.F. field around the antenna of the radio propagation experiment at 7.754 Mc[5]. Or, they might have been the result of photoelectric absorption of the sun's high energy X-rays by the gas around the rocket. Further study is needed to explain the presence and magnitude of the rocket potential.

In either case, the presence of electrons with this energy would have been sufficient to ionize the gas in the region of the rocket and might have contaminated the spectra. However, it is believed that ions so produced were not a major part of the ions entering the spectrometer for the following reasons. Assuming that ions produced were collected before secondary processes occurred, ions of nitrogen would be expected. Also, above 135 km, rocket gas predominated and ions of water vapor would be expected. However, throughout the flight, peaks at 14, 17, 18, and 28 due to water vapor and nitrogen were not prominent. Furthermore, when oxygen venting occurred on the descent, no increase in the peaks at mass numbers 16 and 32 was detected. Instead, the entire spectrum was nearly blanked out, although gas density at these altitudes, 207 to 125 km on the descent, was

TABLE 1

Mass number	Chemical composition
12*	Carbon (C)
16*	Oxygen (O)
18*	Water vapor (H_2O)
19*	Fluorine (F), (H_3O)
21	—— —— ——
23	Sodium (Na)
26*	Cyanogen (CN), acetylene (C_2H_2)
30*	Nitric oxide (NO)
32*	Oxygen (O_2)
38*	—— —— ——
45	—— —— ——
48(?)	—— —— ——

* Peaks of these mass numbers were detected in the gas composition experiment of Townsend, Meadows, and Pressly [8].

low enough for proper spectrometer operation. On the other hand, the facts that above 124 km on the ascent the pattern of the spectra remained essentially constant and also that above 135 km Philips gages indicated that the pressure in the immediate vicinity of the rocket was constant at about 2×10^{-5} mm Hg[7] make it conceivable that the spectral pattern here depended upon the rocket gas. It may be that secondary processes between ambient ions and rocket gas, such as charge transfer, did occur in sufficient number to give the spectra obtained. However, below 115 km, the density of the rocket gas was small compared to that of the atmosphere. Spectra obtained under this condition should depend primarily on the ambient ions in the ionosphere.

Possible chemical compositions of the ions detected are given in Table 1.

ACKNOWLEDGMENTS

The authors extend their thanks to Mr. John W. Townsend, Jr., for generously contributing to the ion composition experiment the electronic equipment and instrumentation space of his gas composition experiment originally scheduled to be flown in Viking 10, and for his suggestions on spectrometry. Dr. J. P. Heppner assisted in the post-flight experimentation and discussion, especially in regard to the rocket potential. In addition, we wish to thank Drs. R. J. Havens and H. E. Newell for their encouragement and helpful discussions, Messrs. C. R. Trent and D. E. Rudert for the construction of the spectrometer tube assembly, and Mr. M. W. Rosen and members of the Rocket Development Branch for their services in connection with Viking 10.

References

[1] W. H. Bennett, J. Appl. Phys., **21**, 143 (1950).
[2] J. W. Townsend, Jr., Rev. Sci. Instr., **23**, 538 (1952).
[3] W. H. Bennett, private communication.
[4] N. R. Best, Electronics, **23**, No. 8, 82 (1950).
[5] J. C. Seddon, A. D. Pickar, and J. E. Jackson, J. Geophys. Res., **59**, 513 (1954).
[6] The Rocket Panel, Phys. Rev., **88**, 1027 (1952).
[7] H. E. LaGow, private communication.
[8] J. W. Townsend, Jr., E. B. Meadows, and E. C. Pressly, Rocket exploration of the upper atmosphere, edited by R. L. F. Boyd and M. Seaton, Interscience Publishers, Inc., New York, pp. 169-188 (1954).

PHOTOMETRY OF THE AURORA

BY EDWARD V. ASHBURN

Geophysical Institute, University of Alaska, College, Alaska

(Received March 7, 1955)

ABSTRACT

Simultaneous measurements of the 5577A line and the 3914A line in the aurorae are described. The measurements were made with a scanning photoelectric photometer. The 3914A line was present toward the north during the entire period of observation. The 3914A line usually showed a larger increase relative to the night-sky background than did the 5577A line. In a pulsating aurora, the 3914A line showed many small pulsations, whose period was 1 to 2 seconds, in addition to the large pulsations.

INTRODUCTION

The intensities of aurorae at College, Alaska (latitude 64° 52′ north, longitude 147° 49′ west) were measured with two recording photoelectric photometers. One photometer was used to measure the intensity of the auroral green line (5577A) and the other to measure the intensity of a band centered at 3914A. The telescopes of the photometers were in an alt-azimuth mount.

The principal advantage of a photoelectric photometer in auroral work lies in the ease with which instantaneous measurements may be made of weak or rapidly changing aurorae. Photographic methods require long exposures for the weak aurorae. This paper will present a summary of measurements that could not have been made with photographic techniques.

PHOTOELECTRIC PHOTOMETER

The scanning photoelectric photometer used was described by St. Amand [see 1 of "References" at end of paper]. The field of view of the telescope was changed to a rectangle, whose one-half intensity width on the vertical was approximately 0°.3 (full width, 0°.6) and whose horizontal width was 5°. Baird interference filters were used in combination with appropriate Corning filters to isolate a band centered on 5577A for one telescope and a band centered on 3914A for the second telescope. The half intensity width of the filters was approximately 150A. The measurements were made from the roof of the Geophysical Institute Building at College, Alaska.

PULSATING AURORA

Figures 1 and 2 illustrate portions of the records obtained from a pulsating aurora in the zenith. In general, the 3914A light showed many small pulsations superimposed upon the major pulsations. The small oscillations usually had periods

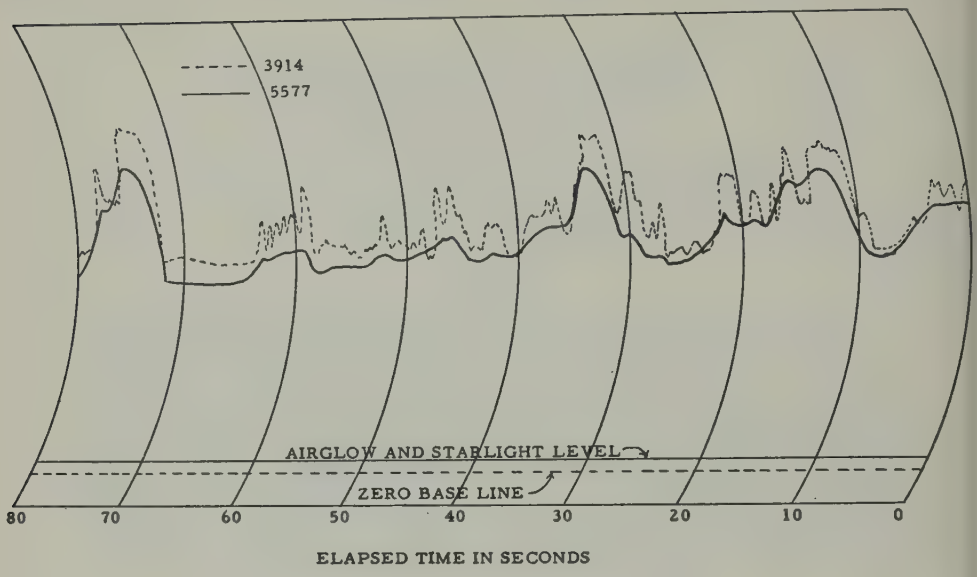

Fig. 1—Pulsating aurora, $00^h\ 48^m$, February 22, 1955

of 1 to 2 seconds. There were indications also of shorter period pulsations, but the recorder was too slow to follow them. In contrast to this, the 5577A light showed very few pulses of 1 to 2 seconds duration. All the major pulsations of the 3914A were matched quite closely by changes in 5577A. The 5577A large pulses lagged behind the 3914A pulses by about one-half second. In general, the large pulses showed a rise time that was near the limit of the recorder to follow (one-half

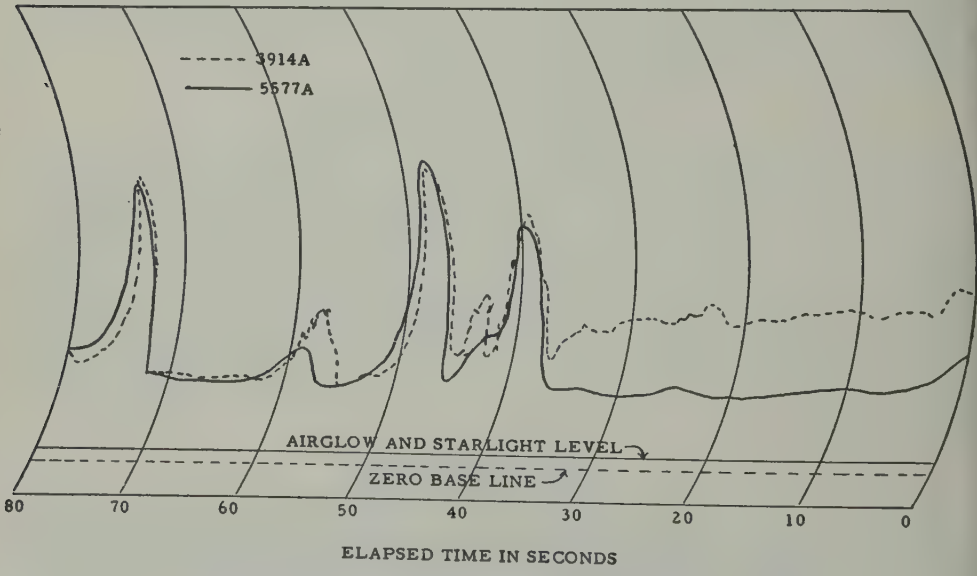

Fig. 2—Pulsating aurora in zenith, $01^h\ 57^m$, February 22, 1955

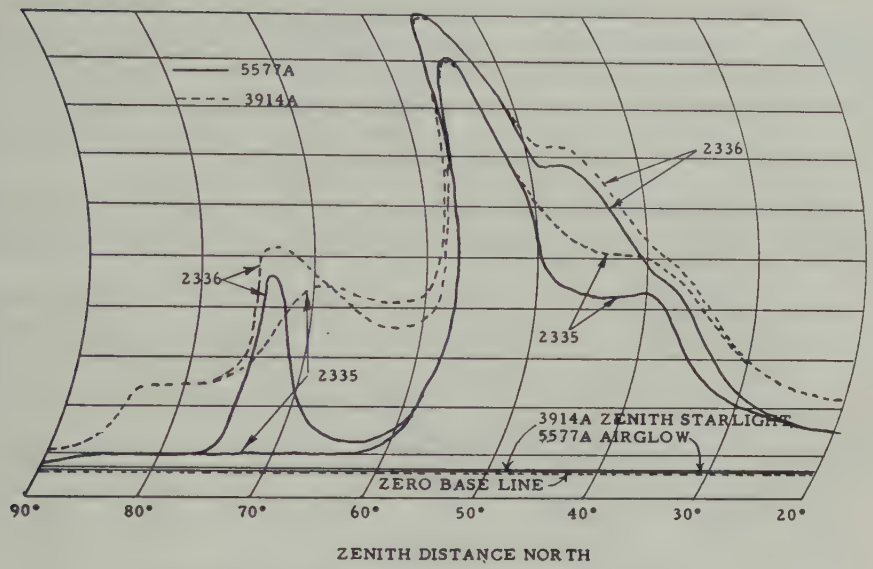

FIG. 3—Auroral intensities, February 21, 1955

second). The decline was usually less rapid. The interval between pulses was seldom less than the duration of the pulse. During the period of these measurements, the air was exceptionally clear and there was no moonlight.

RAYED BANDS

Figures 3, 4, and 5 are typical results of scans across rayed bands. The telescopes were moved from the horizon on the azimuth of the magnetic pole to the

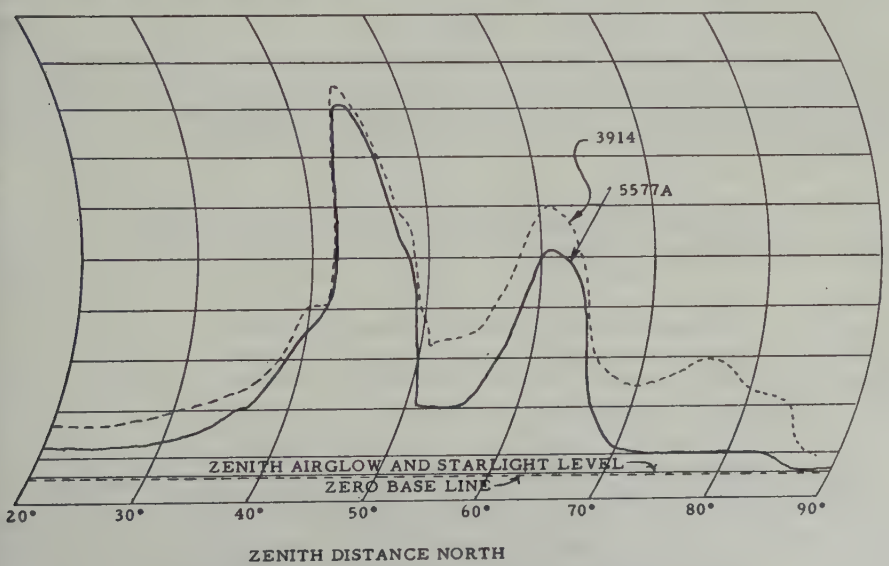

FIG. 4—Auroral intensities, $00^h\ 16^m$, February 22, 1955

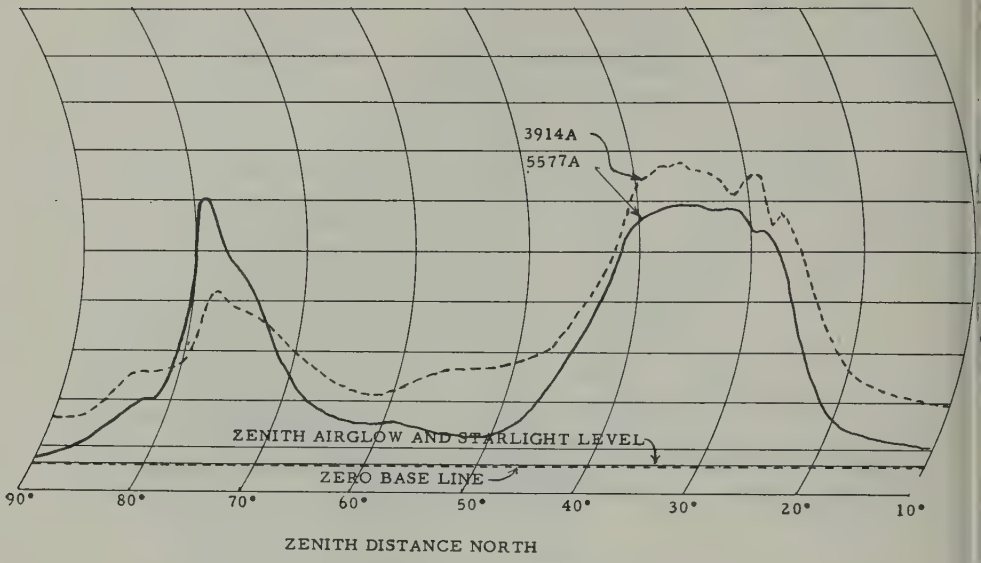

FIG. 5—Auroral intensities, $00^h\ 40^m$, February 22, 1955

opposite horizon at the rate of 60° per minute. Figure 3 shows clearly that the 3914A line can be relatively intense while the 5577A remains at a low level of intensity. Approximately one minute later, the 5577A line showed a large increase in intensity at 74° zenith distance. Figure 4 shows a rayed band at 84° zenith distance for 3914A but not for 5577A. In the five partial nights of observation, every significant peak for the 5577A line was accompanied by a peak for the 3914A line.

The relative intensities of the light emitted in the two bands can be obtained from the records illustrated above by applying a correction for extinction and for multiple scattered light. Extinction coefficients of 0.20 for 5577A and 0.50 appear to be reasonable values for the relatively clear air. If the correction for extinction alone is used, the readings on the charts should be multiplied by the values given in Table 1.

TABLE 1—*Correction-factors due to extinction by the atmosphere below the aurora*

Wavelength	0	30	60	70	75	80	85
5577A	1.22	1.26	1.49	1.79	2.16	3.07	8.00
3914A	1.65	1.79	2.72	4.30	6.90	16.5	181

These corrections when used alone yield erroneous results for large zenith distances. The errors would be much larger for 3914A than for 5577A. Ashburn [2] has shown that in the interpretation of the airglow measurements, the correction for multiple scattered light is significant. For 3914A, the light coming from large

zenith distances is principally multiple scattered light. The calculation of the magnitude of multiple scattered light due to non-uniform aurorae is outside the scope of this paper, but the same general method used in reference [2] could be used as a relatively good approximation.

DIFFUSE SURFACES AND GLOW

Figure 6 shows copies of two records of scans across diffuse surfaces. It is to be noted that there is no evidence of a distinct boundary. These records were

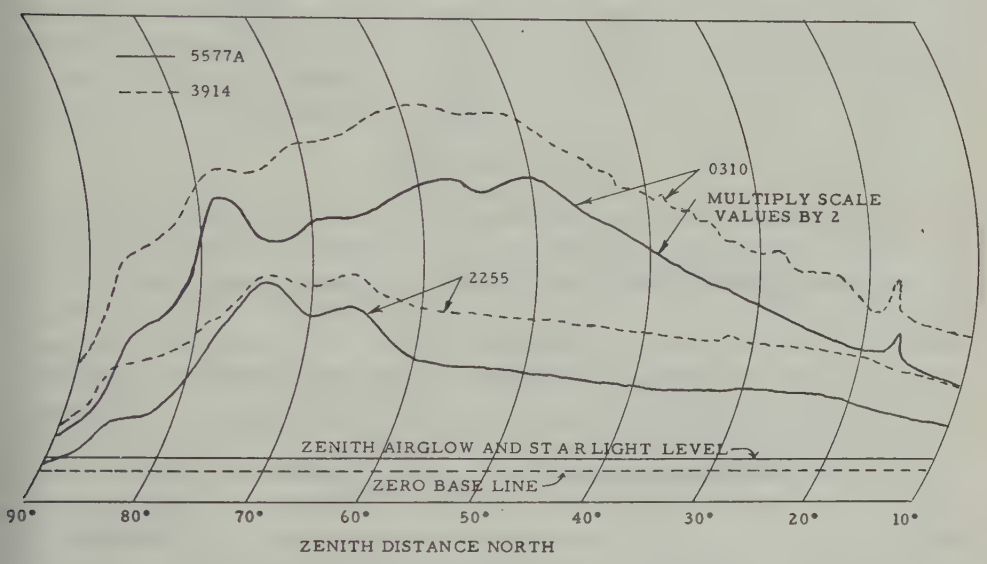

FIG. 6—Auroral intensities, February 21-22, 1955

taken on a clear moonless night. Observations made on a night with a full moon and very thin ice-fog showed the same general character, except the entire level of light intensity was higher. During the period of observation, in February 1955 and February 1954, the intensity of the 5577A and the 3914A light was always greater toward the north than toward the south during periods of no apparent aurora or of a weak glow. The aurora is usually identified and distinguished from airglow by the presence of the 3914A line. With this criterion, there was no observation made when aurora was not present toward the north.

BRIGHTNESS OF A HORIZONTAL SURFACE

Figure 7 shows a simplified copy of three records of the brightness of a white horizontal surface as seen by a photoelectric photometer with a 5577A filter. The largest measured range of brightness of the surface was a factor of 50. The maximum range was greater than this, but was not measured because of an incorrect setting of the gain control of the amplifier. In the three nights of record, the brightness of the horizontal surface at astronomical twilight in the morning was significantly greater than at astronomical twilight in the evening.

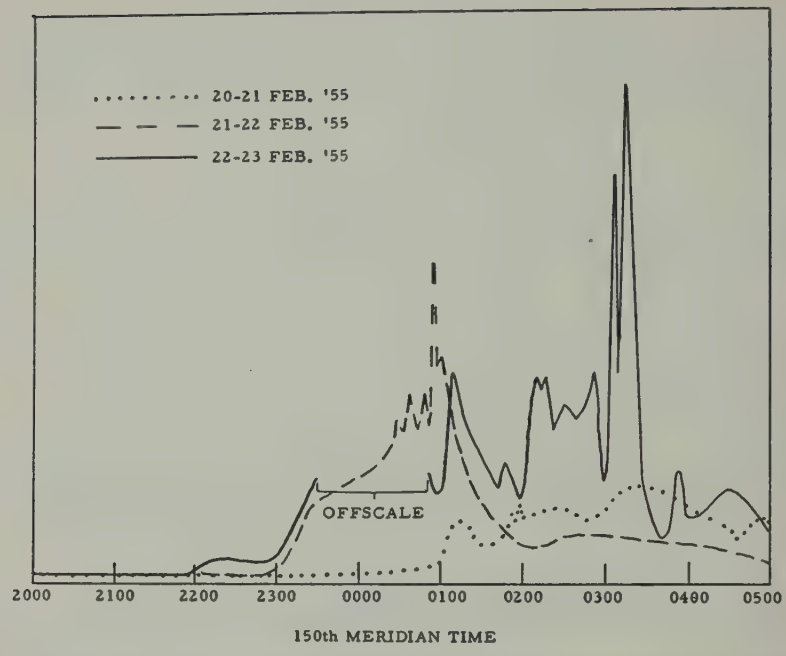

FIG. 7—Brightness of a horizontal surface illuminated by auroral green line from entire sky

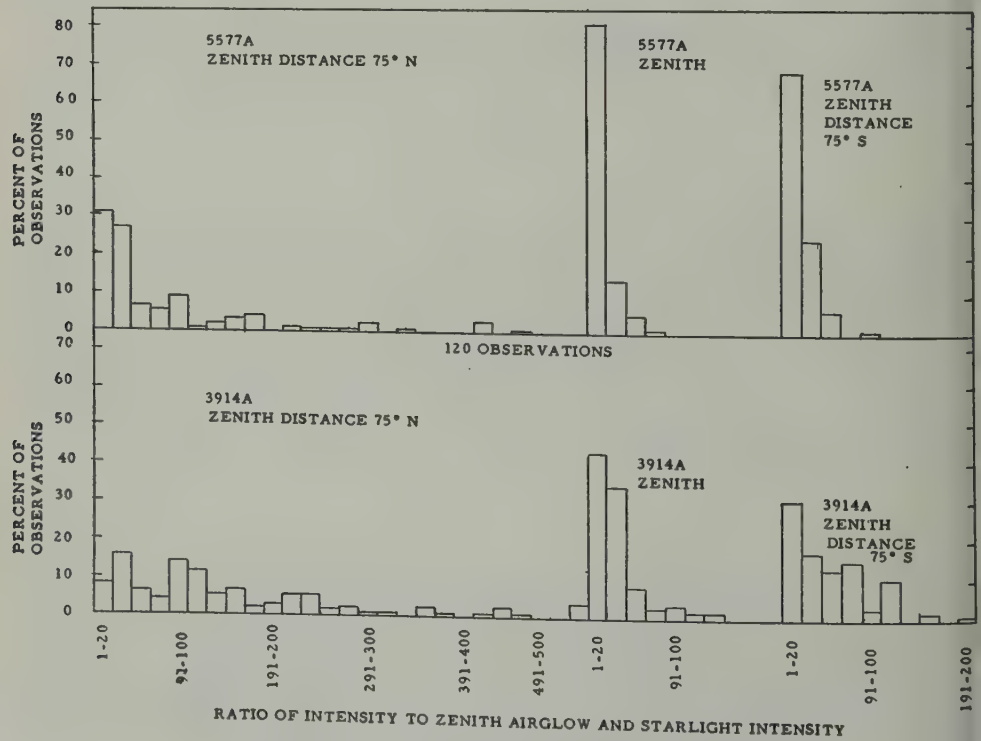

FIG. 8—Frequency distribution of auroral intensities

FREQUENCY DISTRIBUTION OF AURORAL INTENSITIES

Figure 8 illustrates the frequency distribution of the intensities at zenith distances 75° north, 0°, and 75° south. The unit is the lowest observed value of the zenith intensity corrected for extinction. This unit is larger in terms of energy for 5577A and for 3914A, because there is no airglow at 3914. The values for 75° zenith distance were corrected for extinction but not multiple scattering. The correction for multiple scattering would decrease the range of intensities, but for purposes of a rough comparison Figure 8 is probably satisfactory. The principle features to be noted are that the range of intensities is greater for 3914A than for 5577A, and the range for 75° north is much greater than for 75° south. The number of observations should be increased and the correction for multiple scattering should be applied before more quantitative conclusions can be drawn from the frequency distribution curves.

LUMINOSITY CURVES

Harang [3] discussed the penetration of electrons into the atmosphere and the resulting distribution of luminosity in homogeneous arcs. Bates and Griffing [4] called attention to the fact that Harang's work was based on false assumptions and they computed luminosity curves for aurorae produced by protons. More recently, Chamberlain [5, 6] extended the work of Bates and Griffing. The computed luminosity curves do not fit the observed luminosity curves as published by Harang [3]. Most of the data given by Harang were taken from photographs made without the use of filters. Some photographs were made with broad pass-band filters. Harang pointed out that the simultaneous photographs made with the use of filters showed a significant difference in the luminosity curves. The photometric observations described in the present paper did not have adequate angular resolution to justify publishing luminosity curves, but the measurements did indicate important differences in the luminosity curves for 5577A and 3914A.

It appears to the author that before any satisfactory comparison of the theory with observations may be made that the observations should be improved in the following manner:

(1) The auroral arcs should be scanned in one second or less with photometers with very narrow pass filters.
(2) If the arcs are within 20° of the horizon, precautions should be used to insure that the arc is not a double one.
(3) The angular resolution of the telescope should be adequate for the comparison of the observations with theory.
(4) The change of the luminosity curve of the arc with time should be determined.

The photometer that has been developed for Roach's [7] night airglow studies would be excellent for the auroral luminosity studies.

The author wishes to acknowledge the assistance given to him by the staff of the Geophysical Institute. Special thanks are due to Wallace Murcray for his help with the installation of the photometers.

References

[1] P. St. Amand, Doctoral thesis, California Institute of Technology, Pasadena, Calif. (1953).
[2] E. V. Ashburn, J. Atmos. Terr. Phys., **5**, 83-91 (1954).
[3] L. Harang, Geofys. Pub., Oslo, **16**, No. 6 (1944-46).
[4] D. R. Bates and G. W. Griffing, J. Atmos. Terr. Phys., **3**, 212-216 (1953).
[5] J. W. Chamberlain, Astroph. J., **120**, 360-366 (1954).
[6] J. W. Chamberlain, Astroph. J., **120**, 566-571 (1954).
[7] F. E. Roach, private conversation, 1954.

OBSERVATIONS OF A VARIABLE RADIO SOURCE ASSOCIATED WITH THE PLANET JUPITER

By B. F. Burke and K. L. Franklin

Department of Terrestrial Magnetism, Carnegie Institution of Washington, Washington 15, D. C.

(Received April 15, 1955)

ABSTRACT

A source of variable 22.2-Mc/sec radiation has been detected with the large "Mills Cross" antenna of the Carnegie Institution of Washington. The source is present on nine records out of a possible 31 obtained during the first quarter of 1955. The appearance of the records of this source resembles that of terrestrial interference, but it lasts no longer than the time necessary for a celestial object to pass through the antenna pattern. The derived position in the sky corresponds to the position of Jupiter and exhibits the geocentric motion of Jupiter. There is no evident correlation between the times of appearance of this phenomenon and the rotational period of the planet Jupiter, or with the occurrence of solar activity. There is evidence that most of the radio energy is concentrated at frequencies lower than 38 Mc/sec.

During the months of January, February, and March 1955, the large 22-Mc/sec "Mills Cross" of the Carnegie Institution of Washington was used for detailed observations in declination strips containing the Crab Nebula (M1). This antenna system, inspired by a design of Mills and Little [see 1 of "References" at end of paper] and utilizing the phase-switching principle first described by Ryle [2], will be discussed more fully in a subsequent paper.

The antenna may be briefly described as a pair of 66-dipole linear arrays, each 2,047 feet in length, arranged to form a slightly flattened X. The intersection of the fan-beams of the two arrays defines the effective beam position. By phasing the dipoles of the arrays, the direction of the fan-beams and hence the direction of the effective pencil-beam can be changed. Normally, the two arrays are phased identically, in which case the antenna is used as a meridian transit instrument. By tapering the dipole feeds in each array, all side-lobe responses have been reduced to roughly one one-hundreth that of the main beam. A slightly elliptical beam is produced, measuring $1°.6 \times 2°.4$ at half-power points, with the larger dimension in declination. Figure 1 shows a trace taken at declination $+ 22°.3$, with M1 and IC443 both showing prominently. Since the Crab Nebula has an angular size of about 5′, it exhibits the antenna response to a point-source traversing the beam, in this instance, $0°.3$ south of the beam center. The upper trace is from the phase-switching receiver, while the lower trace is a record of total power received; the latter is required to make corrections for interaction between the two arrays

comprising the cross. Calibration marks interrupt the traces every hour. It should be noted on the total power record that the Crab Nebula contributes an amount of noise power that is very small compared to the total noise power received from the galactic background.

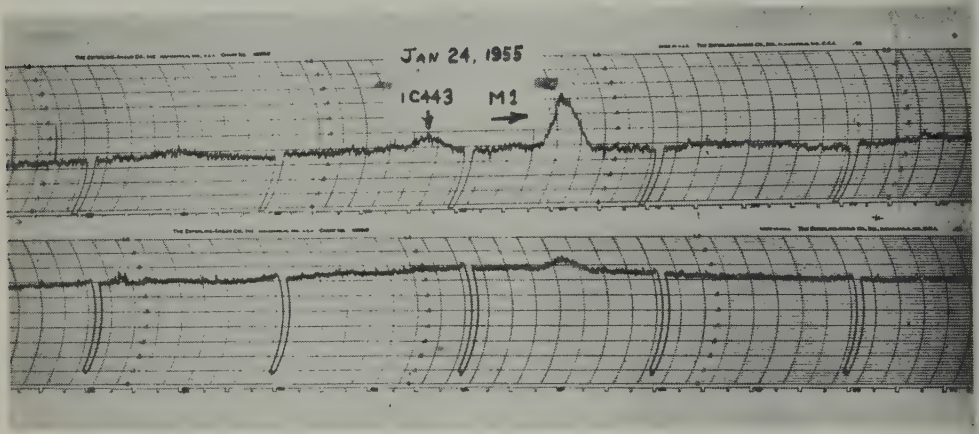

FIG. 1—Phase-switching (upper) and total power records showing Crab Nebula (M1) and IC443 passing through the antenna pattern

Inspection of a number of records obtained at or close to the declination of the Crab Nebula revealed that on a number of occasions interference appeared for a brief time, the duration of which was about the same as the length of time required for a point-source at this declination to go through the antenna pattern. Six such occurrences are given in Figure 2. In all cases, the bursts occurred during the night hours, at times when terrestrial interference was rare. In fact, of the 31 records obtained in this region of the sky, nine show the bursts at approximately the same sidereal time, while only one record showed interference of this intensity at any other time during the night. In view of such absence of interference at other times, it appears unlikely that terrestrial interference, approximately at the same sidereal time, should persist for nearly three months.

The noise bursts exhibited one puzzling feature: The dependence on sidereal time was not exact, but showed a slow drift in right ascension. The apparent right ascension (using the Crab Nebula as a reference point) of the beginning and ending of the burst has been plotted as a function of time in Figure 3. The short vertical lines indicate our estimate of the position where the burst amplitude reaches approximately twice the noise level. In one case, March 10, which appears in Figure 2, it was difficult to assign a position for the beginning. Not all side-lobes of the antenna have been suppressed, and it may be that the initial negative bursts represent unusually intense events occurring just before the source enters the main beam. We have chosen the time at which all bursts are clearly positive as the significant position, but the March 10 example is not as clearly defined as the other instances.

If a variable point-source passing through the beam is responsible for the observed signals, its true position should lie about half-way between beginning

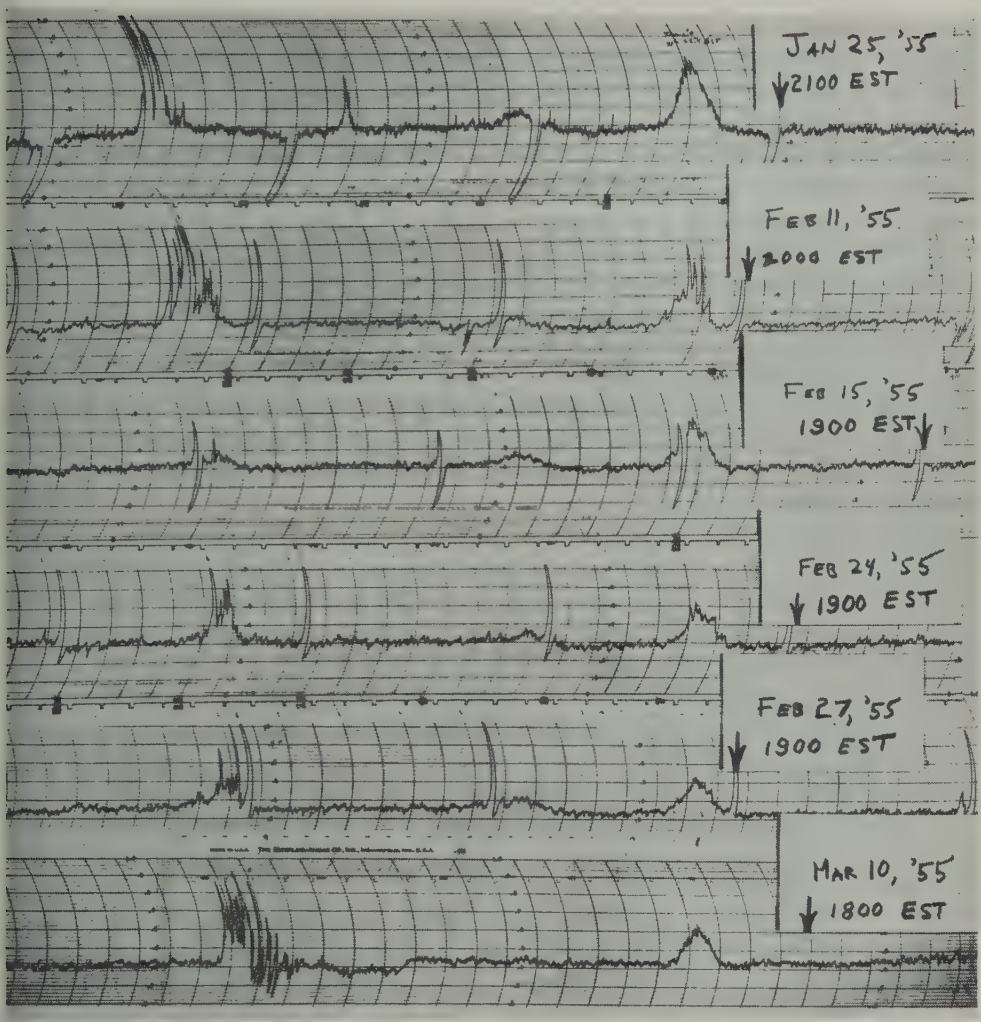

FIG. 2—Phase-switching records showing the appearance of the variable source

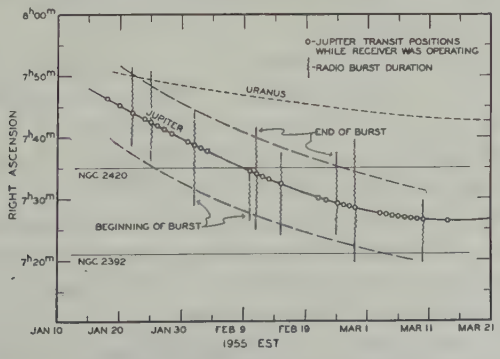

FIG. 3—Comparison of right ascension and duration of bursts with positions of Jupiter, Uranus, and two galactic objects

and ending of the disturbance, although the uncertainty would be greater than for a steady source of noise such as M1. From Figure 3, it can be seen that the mean position of the disturbance agrees closely with the position of the planet Jupiter throughout this period. The planet Uranus was initially near Jupiter, but by March 10 was far outside the range of position indicated by the bursts. The regular apparent motion of the fluctuating source renders highly improbable any identification of the source with a fixed object, such as the galactic cluster NGC2420 or the planetary nebula NGC2392. We have concluded, therefore, that the source of radio noise must be associated with the planet Jupiter.

The character of the bursts is interesting, for large fluctuations in intensity occur during the brief period while the source is in the antenna beam. The larger, more persistent peaks may result from the superposition of many shorter bursts, but this has not been clearly demonstrated as yet. The integrating time-constant of the receiver is 15 seconds, and, since several bursts sometimes occur within a minute, it appears that the duration of each smaller burst may be shorter than 15 seconds. Measurements with receivers having shorter time-constants should establish the single burst duration.

Although the peak intensity of the burst cannot be determined until we are certain that the receiver time-constant is considerably shorter than the burst duration, an order of magnitude estimate can be made, comparing the apparent burst height to the trace of the Crab Nebula. Of the nine events seen so far, seven reach apparent peak intensities that exceed M1, and on two occasions, February 11 and February 15, the peak intensities remain less than M1 for the entire period of observation. It appears that rather violent outbursts are favored, reaching a peak intensity at least as great as that of the Crab Nebula. Our determination of the flux per unit bandwidth for M1 at this frequency (22.2 Mc/sec) is 5.2×10^{-23} w.m.$^{-2}$ sec, including both polarization components. If we assume that the bursts we associate with Jupiter are also randomly polarized, the peak intensities are at least as great as this, and occasionally are several times larger. If the bursts originate from Jupiter, which was between 4.25 and 4.67 astronomical units (AU) from the earth during the period of observation, and if we assume that the source is an isotropic radiator, we can estimate the peak power per unit bandwidth generated at this frequency. Taking a distance of 4.5 AU, for example, the peak power per burst must be at least as great as 300 watts per cps of bandwidth.

The possibility that the occurrence of the bursts was correlated with a region on the surface of Jupiter was investigated. No obvious periodicity related to the rotational period of the planet has been found. Furthermore, there does not appear to be any clear correlation with either radio or optical solar activity.

Information about the spectrum of the bursts is limited to a single observation obtained with interferometers having much lower antenna gain. During the month of June 1954, simultaneous interferometer records were obtained at frequencies of 22.2 and 38.7 Mc/sec. On one occasion, June 6, 1954, an intense radio source of fluctuating intensity was observed with the 22.2-Mc/sec interferometer, which consisted of two 4-dipole arrays, spaced 67.4 wavelengths along an east-west line. For nearly two hours, the source was prominent, moving through the interferometer lobes at a sidereal rate, with an intensity that was occasionally more than

ten times greater than that of the Crab Nebula. From the rate of passage of the source through the interferometer lobes, and from the change of this rate with time, an approximate position was deduced which agreed with the position of Jupiter at that time, within the experimental uncertainty of 5°. At the same time, the 38.7-Mc/sec interferometer, which consisted of a pair of antennas having twice the gain of the lower-frequency arrays, failed to show any detectable trace of such a source. Since the Crab Nebula gave a trace having an amplitude 15 times the noise level, it would appear, from this single observation, that most of the radio noise is concentrated in the low-frequency range, below 38 Mc/sec.

We take pleasure in acknowledging the work of Dr. F. G. Smith, of the Cavendish Laboratory, Cambridge, England, who played an important and active role in the design and construction of the large antenna with which this work was done. We also wish to thank our colleagues at the Department of Terrestrial Magnestism for many valuable discussions and for their assistance in the construction and maintenance of the instrument.

References

[1] B. Y. Mills and A. G. Little, Aust. J. Phys., **6**, 272 (1953).
[2] M. Ryle, Proc. R. Soc., A, **211**, 351 (1952).

GEOMAGNETIC AND SOLAR DATA

INTERNATIONAL DATA ON MAGNETIC DISTURBANCES, FOURTH QUARTER, 1954

This report continues the series which has appeared regularly in this JOURNAL since Vol. 54, No. 3, 295 (1949). Please refer to that first report for an explanation of the data given, and to Vol. 59, No. 3, 423 (1954) for the definition of Ap.

Short Comment on Magnetic Activity in 1954

As a year of minimum in the solar cycle (the last minimum was 1944), 1954 was notable for the absence of strong magnetic storms. The highest Kp recorded was 7+. During a succession of 81 days, beginning April 28, 1954, not a single Kp exceeded 4+. No clear sudden-storm commencement occurred from April 12 to October 22, for nearly half a year.

Judged by the number of three-hour intervals with $Kp = 6-$ or higher, 1954 was the least disturbed year of the whole Kp-series starting in 1937: there were only 23 such intervals in 1954 as compared with the annual numbers in the last minimum, 41 in 1944, 42 in 1945. (The highest numbers were 151 in 1947, 177 in 1951, 180 in 1952. In these counts, the total number of three-hour intervals has been reduced to 240 per month, 2880 per year.)

However, judged by the number of three-hour intervals with small Kp-indices (0o to 1+), the year 1954 as a whole appears by no means outstandingly quiet; with 991 such intervals, it ranks inferior to 1944 (with 1272) and 1945 (with 1352). But the month of June 1954 taken alone, with 152 such intervals out of 240, compares well with the record month of November 1944 with 158 intervals. None of the last minima seems to have reached the prolonged low level of the years around 1901.

For further statistical aspects, see this JOURNAL, Vol. 55, No. 2, 158, and No. 4, 431 (1950); also the forthcoming IAGA (formerly IATME) Bulletin for 1954.

A noteworthy event was the occurrence of 11 successive intervals with $Kp = 0o$ around October 12, 1954. But although such a long quiet level of 33 hours is unprecedented in the available series of more than 50,000 Kp-indices, it should be kept in mind that $Kp = 0o$ means nothing more than that the ranges at most stations remained below the limit set for $K = 0$, for instance, 5γ for Cheltenham. In fact, at least one clear pulsation (world-wide?) occurred at Göttingen on October 12 between $01^h\ 21^m$ and $01^h\ 26^m$ UT. A special solar and geophysical study of that day, especially for stations within the auroral zone, would seem promising.

Preliminary Report on Sudden Commencements

S.c.'s given by five or more stations are in italics. Times given are mean values, with special weight on data from quick-run records.

DAYS IN SOLAR ROTATION INTERVAL
ROT-NR.
1954
1650
1651
1652
1653
1654
1655
1656
Jan
Feb
Mch
Apr
May
Jun
Jul

FIG. 1A

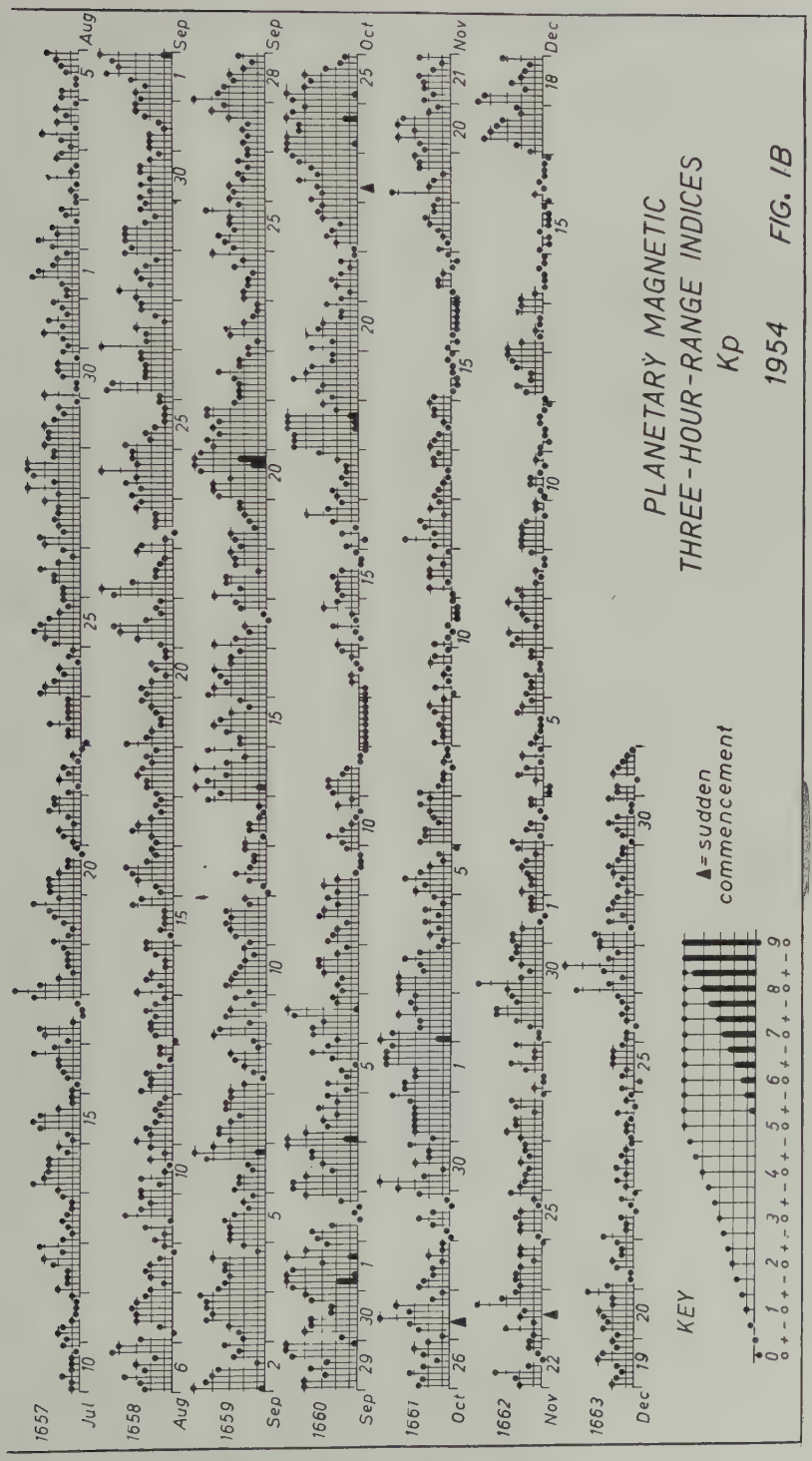
1657
Jul
Aug
1658
Aug
Sep
1659
Sep
Sep
1660
Sep
Oct
1661
Oct
Nov
1662
Nov
Dec
1663
Dec
KEY
0 + - 1 + - 2 + - 3 + - 4 + - 5 + - 6 + - 7 + - 8 + - 9
▲= sudden commencement
PLANETARY MAGNETIC
THREE-HOUR-RANGE INDICES
Kp
1954 FIG. 1B

Sudden commencements followed by a magnetic storm or a period of storminess (s.s.c.)

1954 October *23d 07h 22m:* sixteen.—*27d 07h 47m:* twenty-one.
1954 November *23d 11h 45m:* twelve.
1954 December 17d 06h 18m: Ch Tu.

Sudden commencements of polar or pulsational disturbances (p.s.c.)

1954 October *01d 16h 59m:* ten.—*02d 21h 05:* twelve.—02d 21h 37: CF Eb Hr.—04d 00h 50: SM Bi.—*04d 01h 15:* five.—*05d 19h 50:* ten.—*08d 22h 26:* nine.—09d 21h 06: So Eb Bi.—*09d 23h 45:* ten.—*10d 18h 52:* five.—*13d 22h 53:* six.—13d 23h 18: CF Ta El.—*14d 20h 08:* six.—*14d 20h 16:* eight.—*15d 23h 55:* five.—16d 14h 30: SM Ka Am.—17d 22h 57: Le Wn Tl SF.—18d 00h 38: SJ Hr.—*18d 22h 48:* eleven.—20d 21h 54: Ci Ta.—*21d 19h 27:* fifteen.—23d 18h 10: Tr So Do.—24d 03h 58: Ta Bi.—24d 16h 20: Ka Qu Tn.—25d 18h 13: Do Wn.—*28d 00h 25:* seven.—28d 21h 13: So Ma Eb.—*29d 22h 07:* five.—30d 03h 30: Ci Ta.—31d 20h 30: SM Ta Qu.

1954 November 01d 14h 32m: Ka Qu Am.—01d 19h 42: Do Wn Bi El.—03d 23h 36: CF Ta.—*04d 23h 58:* twelve.—*06d 00h 17:* nine.—*06d 18h 00:* seven.—06d 23h 52: Wn Ma CF Ta.—07d 01h 08: CF Tl SF Ta.—08d 00h 50: CF Tl.—*08d 20h 07:* eight.—09d 15h 34: Ka Qu Hr To.—*10d 00h 21:* five.—12d 18h 47: Tr So.—13d 21h 07: Tr Eb.—13d 21h 22: Tl El.—14d 12h 56: Ka Qu Ap.—14d 23h 00: Ci Ta.—16d 00h 52: CF Bi.—*17d 23h 12:* six.—18d 22h 00: Bi El.—*19d 03h 16:* seven.—21d 21h 40: Tr Bi.—21d 23h 16: CF Bi.—22d 07h 54: Am Ap.—*22d 22h 21:* six.—24d 19h 05: Fu Ta Qu El.—25d 03h 21: CF Ta.—25d 22h 38: Es Ma Tl.—25d 22h 52: CF Fu Ta.—*27d 18h 45:* seventeen.—28d 18h 58: Tr So.—*28d 23h 08:* six.—29d 14h 28: Ci Ka Qu To.—29d 18h 54: Ta Bi El Ap.—30d 04h 34: CF Ta.—*30d 23h 17:* eleven.

1954 December 01d 17h 01m: So Qu.—01d 23h 26: Bi El.—01d 23h 36: Bi El.—*02d 23h 27:* eleven.—03d 20h 06: Tr Wn IK.—05d 22h 18: SM Eb Ta.—06d 19h 52: CF Bi.—06d 20h 10: So El.—*07d 00h 13:* nine.—07d 18h 38: Do Wn CF Qu.—*07d 22h 23:* five.—09d 19h 24: CF Qu Bi El.—11d 19h 22: Eb Bi El.—12d 22h 09: SM Ta.—13d 17h 53: So Qu.—17d 00h 08: Eb IK El.—*17d 22h 28:* seven.—*18d 00h 22:* seven.—*18d 21h 49:* eleven.—*18d 22h 00:* nine.—*19d 19h 34:* six.—*20d 21h 42:* thirteen.—*20d 21h 51:* six.—21d 00h 50: IK Ta.—*22d 00h 34:* six.—22d 00h 45: CF SM Ci El.—*22d 18h 30:* eight.—24d 19h 01: Tr CF Bi.—25d 00h 02: Eb Tl SF Bi.—25d 00h 18: CF IK Ta.—27d 00h 23: SM Ci IK.—*27d 22h 09:* twenty.—28d 03h 42: CF SM.—30d 22h 18: CF Eb Bi.

TABLE 1—*Geomagnetic planetary three-hour-range indices Kp, preliminary magnetic character-figures C, average amplitudes Ap (unit 2_γ), and final selected days, October to December, 1954*

E	October 1954									November 1954								
	1	2	3	4	5	6	7	8	Sum	1	2	3	4	5	6	7	8	Sum
1	5 −	6 +	5 +	5 +	3o	6 −	4o	3 −	36 +	4 −	4 −	3o	3o	5 −	5 −	5 −	4 +	32 −
2	3 +	4 −	2 +	0 +	1 −	0 +	2 −	4o	16 +	6o	4 +	3 −	3 −	4o	3o	3 +	3o	29o
3	5 −	5 −	4o	2 +	3o	4 −	4 −	5o	31o	4o	4o	4o	2 +	3 −	4 −	3 −	1 +	25 −
4	6o	4o	3 −	3o	2o	3 +	2o	3 −	26 −	1o	2o	1 +	2 +	1 +	2 +	1o	2 −	13o
5	1 +	3 −	1 +	2 −	1 −	2 +	4 −	3 −	16 +	3o	2 +	4 −	3 −	2o	1o	1 +	0o	16o
6	2o	4 −	4 −	3o	5 −	5 +	2o	2 +	27 −	3 −	2 +	2 +	1 +	2 −	2o	3 −	2o	17o
7	2 −	2o	2 −	3o	3 −	3 +	2o	1 +	18 +	3 −	1 +	1o	1o	0 +	1o	1 −	1 −	9 −
8	3 −	2 +	2o	1 +	3 +	3o	2o	3 −	19 +	2 −	1o	1o	1 +	1o	2 −	2o	1o	11 −
9	2o	3o	2o	1 −	0 +	0 +	0 +	1 +	10o	0 +	2 −	1 −	1o	1 −	2o	2 −	1 −	9 −
10	2 −	3 −	2 −	1o	1 −	0 +	2o	1o	11o	2 −	1 −	0 +	1 −	0o	0o	0o	0 +	4 −
11	2 +	3 −	3 −	2 −	1 +	0 +	0 +	0o	11 +	0 +	2o	1 −	2o	2o	1o	2o	1 −	11 −
12	0o	0o	0o	0o	0o	0o	0o	0o	0o	2 −	4 −	2 −	2 +	3 −	1o	2o	1 +	16 +
13	0o	0o	1o	1o	0 +	1 −	1o	2 −	6 −	2 −	1 +	1o	1 −	1 −	2 −	2 −	1 +	10o
14	2o	0 +	1 −	2 +	1 −	1o	3o	2o	12o	2o	2 −	1 +	1 −	1o	2 −	2 −	2o	12o
15	2 −	2o	2o	2 +	2 −	0 +	0 +	1 −	11o	2 −	0 +	0o	0o	0 +	0 +	1 −	0 +	4 −
16	1 +	0o	2 −	1 −	2 +	4o	3 −	2 −	14 +	1 −	0o	0 +	0o	0o	0o	0o	0o	1o
17	2o	2 +	1 +	2 −	1 +	1 +	2o	3 +	15 +	0o	0 +	1 +	1 +	1o	0 +	0o	1 −	5o
18	5 −	5 −	5 −	5 +	5 +	6 −	2o	3o	35 +	1 +	1 −	1o	1 +	2o	2 +	2 −	2 −	12o
19	2 +	3 +	3o	5 −	4o	4 −	2 +	2 +	26 −	1 +	4 +	2o	2 −	1o	3 −	3 −	3o	19 −
20	4 −	2 +	4o	3 +	3o	2 −	2 −	3 −	22 +	2 +	3 −	4o	3o	4o	4 −	2o	1 +	23o
21	2 −	1o	2o	2 +	2 −	1o	2 −	1 −	12o	2 +	2 −	2 +	2 +	3 −	2 −	1o	3 −	17 −
22	1 −	2o	3 −	2 +	2 −	3o	3 +	3o	19 −	2o	2 +	4 −	1 +	0 +	1 −	1 +	1 +	13o
23	4 −	3o	3 +	4 +	3 +	4 −	4 +	5 −	30 +	1o	3o	1o	2o	2 −	5 −	3 +	2 +	19o
24	5o	5 +	5o	4 +	4 +	6o	5 −	4o	39 −	2o	2 +	2 +	2o	1o	2o	2o	0 +	14o
25	5 −	5 +	4o	4 −	4o	3 −	2 −	1 +	27 +	1 −	2o	2o	2 +	2o	1 −	1o	3 −	13 +
26	3 −	2 +	3 +	2 +	1 +	2 +	3o	2o	19 +	2o	2 −	2 −	1 +	2o	1 +	2 −	2 −	13 +
27	1o	3 −	3 +	5o	3 +	4o	2 −	1o	22o	2o	3o	2 +	2 +	1o	2 +	3 −	0 +	16o
28	3 −	2 +	2 −	2 −	1o	2o	1o	1o	13 +	1o	0 +	0 +	2 −	3 −	1o	1o	2 +	10 +
29	0 +	1 −	2 −	3 −	2 −	0 +	1 −	3 −	11 −	1 −	1 −	1 +	2 +	4 −	4 −	2 +	3 −	17 +
30	4o	5o	2 +	1o	3o	2o	2o	3 +	23 −	3o	5 −	2o	1 +	2o	3 −	2 +	2 +	20 +
31	2 −	3o	3o	3o	3o	3o	3 +	4 +	24 +									

E	December 1954								
	1	2	3	4	5	6	7	8	Sum
1	3 −	3 −	2o	1 −	0 +	1 +	1 +	1 +	12 +
2	2o	1 +	1 +	2 −	2o	2 −	1o	2 +	13 +
3	3 −	1 −	2 −	1 +	0 +	1 −	1 +	1 +	10o
4	0o	0o	1o	2 +	2 −	1 −	2o	1 −	8 +
5	1 +	1o	1 −	1 −	1 −	2 +	2o	1 +	10o
6	2 −	1 +	1 +	2 −	1 −	1 −	1 +	1 +	10o
7	3 −	2 +	3o	1o	2 −	2o	2 +	3o	18o
8	2o	2 +	1o	1 −	1o	0 +	0 +	1 +	9o
9	2o	2o	2o	2o	2 −	0 +	1o	1o	12o
10	0 +	1 −	1 +	1 +	1 −	0 +	1o	1 −	6 +
11	1 −	0o	0 +	0 +	1 −	1 −	0 +	0o	3o
12	0 +	2 −	2 +	1 +	1 +	2 +	3 −	3o	15o
13	3o	2o	1 −	1o	1 −	1 −	2 +	2o	12 +
14	2o	1o	0 +	0 +	1 −	0 +	0 +	5 +	
15	1 −	0o	0o	1 −	0o	0o	0o	0 +	2 −
16	0o	1o	0 +	1 −	0 +	0 +	0 +	0o	3o
17	1 +	2 +	4 +	4o	4 −	3 +	2o	2 +	23 +
18	5 −	4 +	2 −	3 −	2o	2 −	1 +	3 +	22 −
19	2o	2 −	1 +	2 −	3o	3 −	2 −	2o	16o
20	2 −	3 −	2 +	3 −	3o	2o	2o	4 −	20o
21	2 +	1 −	1 −	2 −	2o	1 +	1 +	2 −	12 −
22	3 −	1o	1o	1 +	0 +	1 −	1 +	0 +	9 −
23	1o	2 −	1o	2 −	1o	1 +	1o	1 −	9 +
24	1 −	1o	1o	1 −	2 −	0 +	1o	1 −	7o
25	1 +	0o	1 +	1o	2o	2o	2o	1 +	11o
26	1o	1o	0 +	1o	1 +	1o	1 +	2 −	9 −
27	4 +	2 +	1 +	3 −	5o	2 +	2 −	3o	23 −
28	3o	3 +	1 −	2 +	1 +	2 +	2o	2 −	17 −
29	1o	2 −	1 +	2o	2 +	2 −	1 +	1 +	13 −
30	1 −	1 +	2 −	2 +	2 −	1 −	1 −	2 +	11 +
31	2 −	2 −	0 +	2o	2 −	1 +	1o	1 −	10 +

	Preliminary *C*, 1954			Average amplitude *Ap*		
	Oct.	Nov.	Dec.	Oct.	Nov.	Dec.
1	1.4	1.5	0.3	44	28	6
2	0.8	1.3	0.3	11	26	6
3	1.3	1.0	0.2	28	18	5
4	1.2	0.3	0.3	22	6	4
5	0.7	0.5	0.4	9	9	5
6	1.2	0.8	0.2	22	8	5
7	0.8	0.2	0.8	10	5	10
8	0.7	0.4	0.0	11	5	4
9	0.1	0.1	0.4	5	4	6
10	0.1	0.0	0.0	6	2	3
11	0.1	0.4	0.0	6	5	2
12	0.0	0.6	0.6	0	9	8
13	0.1	0.3	0.5	3	5	6
14	0.5	0.3	0.0	6	6	3
15	0.2	0.0	0.0	5	2	1
16	0.6	0.0	0.0	8	1	2
17	0.5	0.1	1.1	8	3	16
18	1.5	0.4	0.9	40	6	16
19	1.0	0.8	0.6	18	12	8
20	0.8	0.9	1.0	14	16	11
21	0.3	0.6	0.4	6	8	6
22	0 9	0.4	0.2	11	7	5
23	1.3	1.2	0.1	25	13	3
24	1.5	0.5	0.0	45	6	4
25	1.1	0.6	0.3	24	6	5
26	0.7	0.4	0.3	10	6	4
27	1.1	0.7	1.2	17	8	17
28	0.1	0.4	0.5	6	5	9
29	0.2	0.8	0.3	6	11	6
30	0.9	0.8	0.4	17	13	6
31	1.0		0.2	16		5

Table 1—(Concluded)—*Final selected days, October to December, 1954*

Month	Five quiet days	Ten quiet days	Five disturbed days
October	9 10 12 13 15	9 10 11 12 13 14 15 21 28 29	1 3 18 23 24
November	9 10 15 16 17	7 8 9 10 11 13 15 16 17 28	1 2 3 20 30
December	10 11 14 15 16	4 6 10 11 14 15 16 22 23 24	7 17 18 20 27

Sudden impulses found in the magnetograms (s.i.)

1954 October 23d 08h 50m: Ci Ka Tn.

1954 November *12d 02h 02m:* five.—17d 09h 01: Qu Tn Hr.—*18d 17h 33:* twenty-one.—23d 15h 15: CF Am.—27d 12h 00: El Hr.

1954 December *07d 08h 07m:* six.—08d 22h 25: Ta Tn Am.—17d 08h 45: Le El Tn.—28d 19h 01: Ta Hu.—30d 09h 23: Qu El Tn.

Preliminary Report on Solar-Flare Effects

None of these effects was confirmed by ionospheric or solar observations.

1954 October 02d 14h 10m–14h 20m: Gt.—02d 16h 14–16h 18: Ch.—13d 10h 48–10h 55: Ch.—14d 18h 00–18h 04: Ch.—19d 10h 20–10h 28: SM.—22d 14h 59–15h 06: Eb.

1954 November 14d 10h 28m: Hr.—23d 11h 46m–11h 52m: Ch.—26d 12h 22: El Hr.

1954 December 06d 03h 52m: El.

Ionospheric or solar disturbances without clear geomagnetic effect

None.

Minor disturbances reported by one station only are listed in the De Bilt quarterly circular, but omitted here.

Table 2—*Mean values of Ci, Cp, and Ap for months and year 1954*

(*Ci* = preliminary international *C*-figure, *Cp* = planetary character-figure derived from *Kp*, and *Ap* = average amplitude-figure derived from *Kp* (see IATME Bulletin No. 12e, pp. 109-137)

Index	Jan.	Feb.	Mar.	Apr.	May	June	July	Aug.	Sep.	Oct.	Nov.	Dec.	Year
Mean *Ci*	0.49	0.80	0.81	0.71	0.44	0.36	0.51	0.61	0.88	0.74	0.54	0.37	0.60
Mean *Cp*	0.45	0.79	0.83	0.70	0.37	0.25	0.39	0.53	0.83	0.69	0.42	0.29	0.54
Mean *Ap*	9	16	16	14	7	6	8	10	17	15	9	6	11

Committee on Characterization of Magnetic Disturbances

J. Bartels, *Chairman*
University
Göttingen, Germany

J. Veldkamp
Kon. Nederlandsch Meteorologisch Instituut
De Bilt, Holland

PROVISIONAL SUNSPOT-NUMBERS FOR JANUARY TO MARCH, 1955

(Dependent on observations at Zurich Observatory and its stations at Locarno and Arosa)

Day	Jan.	Feb.	Mar.
1	22	19	23
2	17	28	20
3	11	32	16
4	19	34	15
5	32	32	8
6	22	32	8
7	23	34	8
8	29	24	8
9	31	28	7
10	36	27	0
11	33	27	0
12	31	26	0
13	28	28	0
14	27	10	0
15	18	8	0
16	16	16	0
17	15	7	0
18	10	0	0
19	9	0	0
20	7	0	0
21	8	0	0
22	8	9	0
23	8	19	0
24	19	28	0
25	21	28	0
26	25	30	0
27	25	30	7
28	19	26	0
29	16		0
30	12		17
31	22		10
Means.....	20.0	20.8	4.7
No. days.....	31	28	31

Mean for quarter: 15.0 (90 days)

M. Waldmeier

Swiss Federal Observatory
Zurich, Switzerland

CHELTENHAM THREE-HOUR-RANGE INDICES K FOR JANUARY TO MARCH, 1955

[$K9 = 500\gamma$; scale-values of variometers in γ/mm: $D = 5.4$; $H = 2.4$; $Z = 4.3$]

Gr. day	January 1955		February 1955		March 1955	
	Values K	Sum	Values K	Sum	Values K	Sum
1	1113 1112	11	0010 1011	4	1100 0110	4
2	2122 1112	12	1111 1132	11	1111 0010	5
3	0121 2112	10	4421 1112	16	0221 1010	7
4	4223 2132	19	1235 3344	25	1211 0022	9
5	1110 1122	9	4222 3233	21	3322 1223	18
6	2411 2221	15	2423 2334	23	4223 2232	20
7	2122 2222	15	3422 3321	20	4333 1353	25
8	1120 0023	9	2112 2333	17	4232 2343	23
9	3342 3332	23	2343 1231	19	3442 2243	24
10	2111 1120	9	1231 1112	12	3354 4334	29
11	3111 4234	19	1111 2244	16	3343 4232	24
12	5210 0021	11	3332 2223	20	4433 3333	26
13	3443 3322	24	4213 2220	16	3222 2233	19
14	2212 1130	12	2222 2223	17	4212 2233	19
15	0100 0000	1	3342 1010	14	3443 2133	23
16	2112 1322	14	0002 2122	9	3421 1233	19
17	1333 6555	31	3111 1011	9	4245 2223	24
18	6751 2333	30	2311 0023	12	2133 3432	21
19	6665 4435	39	2220 1122	12	2120 0121	9
20	4421 1134	20	2322 2121	15	2131 1114	14
21	4321 0123	16	3432 2222	20	3222 2122	16
22	3311 1111	12	3334 2222	21	2235 5433	27
23	3123 3232	19	4334 3333	26	2121 3244	19
24	1110 0111	6	2223 3122	17	4432 2121	19
25	1210 1111	8	4313 1103	16	1122 0222	12
26	1121 0000	5	4412 1122	17	1343 3113	19
27	0022 2334	16	0111 1223	11	1223 2232	17
28	3232 0113	15	5633 5312	28	2131 1012	11
29	1111 1123	11			2111 1001	7
30	2211 2222	14			2112 2244	18
31	2110 0002	6			6655 3344	36

J. B. Campbell
Observer-in-Charge

Cheltenham Magnetic Observatory
Cheltenham, Maryland, U.S.A.

PRINCIPAL MAGNETIC STORMS

(Advance knowledge of the character of the records at some observatories as regards disturbances)

Observatory (Observer-in-Charge)	Greenwich date	Storm-time GMT of begin.	Storm-time GMT of ending[1]	Sudden commencement Type[2]	Amplitudes[3] D	H	Z	C-figure, degree of activity[4]	Maximal activity on K-scale 0 to 9 Gr. day	Gr. 3-hr. period	K-index	Ranges D	H	
(1)	(2)	(3)	(4)	(5)	(6)	(7)	(8)	(9)	(10)	(11)	(12)	(13)	(14)	(
	1955	*h m*	*d h*		′	γ	γ					′	γ	
College	Jan. 17	03 24	20 07	s.c.*	−3	+28	+2	ms	17	5,6,7	7	410	1500	20
(C. J. Beers)									19	2,3,4,5	7			
	Mar. 30	10 35	1 16	.....	....	....	....	ms	31	3	7	210	1450	7
									1	4	7			
Sitka	Jan. 17	10 00	20 07	.....	....	....	....	s	18	2	9	122	1720	6
(T. L. Skillman)	Feb. 23	08 15	9 22	.....	....	....	....	ms	23	5	7	54	454	3
	Feb. 27	23 00	28 23	.....	....	....	....	ms	28	2,5	6	43	477	5
	Mar. 9	05 00	11 17	.....	....	....	....	ms	10	3	6	75	339	4
									11	4,5	6			
	Mar. 22	07 07	8 01	.....	....	....	....	s	22	5,6	8	172	972	6
	Mar. 30	07 50	1 14	.....	....	....	....	ms	31	3	7	115	546	6
Cheltenham	Jan. 11	12 19	12 04	s.c.	+1	−4	0	m	12	1	5	23	71	
(J.B. Campbell)	Jan. 17	03 27	20 06	.....	....	....	....	ms	18	2	7	56	214	1
	Feb. 27	22 ..	28 18	.....	....	....	....	ms	28	2	6	25	114	
	Mar. 9	05 45	12 22	s.c.	0	+2	0	m	10	3	5	23	109	
	Mar. 22	07 ..	23 02	.....	....	....	....	m	22	4,5	5	28	149	
	Mar. 30	11 ..	.. ..	.....	....	....	....	ms	31	1,2	6	35	117	1
		(*Note:* Storm still in progress at end of March)												
Tucson	Jan. 17	11 30	20 06	.....	....	....	....	ms	18	1,2	7	35	187	
(M. L. Cleven)	Feb. 28	01 00	28 18	.....	....	....	....	m	28	1,2	5	12	127	
	Mar. 30	11 00	1 08	.....	....	....	....	ms	31	1,2	6	18	100	
San Juan	Jan. 17	03 22	18 08	.....	....	....	....	ms	17	8	6	10	130	
(P. G. Ledig)	Feb.	None												
	Mar.	None												
Honolulu	Jan. 17	10 00	19 15	.....	....	....	....	ms	18	1	7	8	195	
(R. F. White)	Feb.	None												
	Mar. 30	10 40	1 08	.....	....	....	....	ms	31	1	6	6	103	
Instituto	Jan. 8	18 27	9 21	.....	....	....	....	m	9	6,7	5	7	243	
Geofísico de	Jan. 17	03 21	20 04	s.c.	+1	+37	−3	ms	17	6	7	13	394	
Huancayo	Feb. 4	08 33	5 02	s.c.	−1	+12	−2	m	4	6,7	5	8	214	
(A. A. Giesecke,	Feb. 28	00 52	28 18	s.c.	+1	+28	−5	ms	28	5	7	7	230	
Jr.)	Mar. 9	05 43	10 23	s.c.	0	+35	−3	m	9	7	5	6	202	
	Mar. 22	08 08	23 23	.....	....	....	....	m	22	4,5,6	5	5	136	
	Mar. 30	10 40	31 21	.....	....	....	....	m	30	7	5	5	237	
	1954													
Vassouras	Oct.	None												
(Lelio I. Gama)	Nov.	None												
	Dec.	None												
	1955													
Apia	Jan. 17	03 ..	18 08	.....	....	....	....	ms	17	5	6	2	108	
(A. L. Burrows)	Jan. 17	18 52	18 08	s.c.	2	34	−10	ms	18	1	6	4	150	
		(*Note:* No range in *Z* because no record)												
	Feb. 28	01 ..	28 16	.....	....	....	....	m	28	1,2	5	3	143	
	Mar. 22	09 ..	24 06	.....	....	....	....	m	22	4	5	1	55	
	Mar. 30	10 40	1 05	.....	....	....	....	m	31	1,2,3	5	2	81	

[1]Approximate time of ending of storm construed as the time of cessation of reasonably marked disturbance movements in t traces; more specifically, when the *K*-index measure diminished to 2 or less for a reasonable period.

[2]s.c. = sudden commencement; s.c.* = small initial impulse followed by main impulse (the amplitude in this case is that of t *main impulse only*, neglecting the initial brief pulse; . . . = gradual commencement.

[3]Signs of amplitudes of *D* and *Z* taken algebraically; *D* reckoned positive if towards the east and *Z* reckoned positive if ve cally downwards.

[4]Storm described by three degrees of activity: *m* for moderate (when *K*-index as great as 5); *ms* for moderately severe (wh *K* = 6 or 7); *s* for severe (when *K* = 8 or 9)

PRINCIPAL MAGNETIC STORMS—Concluded

Observatory (Observer-in-Charge)	Greenwich date	Storm-time GMT of begin.	Storm-time GMT of ending[1]	Sudden commencement Type[2]	Amplitudes[3] D	H	Z	C-figure, degree of activity[4]	Maximal activity on K-scale 0 to 9 Gr. day	Gr. 3-hr. period	K-index	Ranges D	H	Z
(1)	(2)	(3)	(4)	(5)	(6)	(7)	(8)	(9)	(10)	(11)	(12)	(13)	(14)	(15)
	1955	*h m*	*d h*		′	γ	γ					′	γ	γ
ermanus	Jan. 17	03 21	20 03	s.c.	0	+28	+19	ms	17	5	6	31	152	102
..M.vanWijk)	Jan. 27	08 52	28 03	s.c.?	0	+3	0	m	27	6	5	22	62	92
	Feb. 11	15 ..	12 01	.....	.....	.....	.....	m	11	8	5	17	62	81
	Feb. 23	06 ..	23 21	.....	.....	.....	.....	m	23	7	5	17	73	61
	Feb. 27	23 38	28 17	s.c.	.....	.....	.....	m	28	5	5	21	109	54
	Mar. 7	15 ..	7 21	(Large polar bay, 19h 59m to 21h)				m	7	7	5	12	65	56
	Mar. 9	12 ..	11 01	.....	.....	.....	.....	m	9	7,8	5	17	94	85
	Mar. 22	05 ..	24 05	.....	.....	.....	.....	ms	22	4	6	32	182	152
	Mar. 30	10 ..	31 23	.....	.....	.....	.....	m	30	8	5	16	106	94
									31	1,3,7	5			
Vatheroo	Jan. 17	03 25	20 04	s.c.	.....	+14	.....	ms	17	5	7	30	153	200
A. F. Tillott)	Feb.	None												
	Mar. 22	09 ..	22 19	.....	.....	.....	.....	m	22	4,5,6	5	14	122	93
	Mar. 30	18 30	31 20	.....	.....	.....	.....	m	31	1,3,6	5	(15)	(112)	88
mberley	Jan. 13	01 ..	13 15	.....	.....	.....	.....	m	13	2	5	11	121	25
A L.	Jan. 17	03 ..	18 09	.....	.....	.....	.....	ms	17	5	7	27	245	122
Cullington)									18	1,2	6			
	Jan. 18	21 ..	19 20	.....	.....	.....	.....	ms	19	2	6	16	165	85
	Feb.	None												
	Mar. 6	20 ..	13 09	.....	.....	.....	.....	m	10	5	5	13	130	40
									11	4,5	5			
	Mar. 22	01 ..	24 16	.....	.....	.....	.....	m	22	4,5	5	22	97	57
	Mar. 26	04 ..	27 17	.....	.....	.....	.....	m	27	4	5	14	114	37
	Mar. 30	11 ..	.. ..	.....	.....	.....	.....	m	31	1,3,4	5			
	(*Note:* Storm still in progress at end of March)													
	Reports added in page-proof:													
	1955													
Vitteveen	Jan. 8	18 00	9 21	.....	.....	.....	.....	ms	9	6	6	25	130	40
D. vanSabben)	Jan. 11	21 37	12 05	s.c.	−3	+14	0	ms	11	8	6	30	110	20
	Jan. 17	09 31	20 04	s.c.	−1	+7	0	ms	17	5	7	55	280	140
									18	1	7			
	Feb. 11	15 00	12 03	.....	.....	.....	..M	ms	11	7	6	25	125	40
	Feb. 23	08 00	8 24	.....	.....	.....	.....	ms	23	7	6	25	125	40
	Feb. 28	00 00	28 18	.....	.....	.....	.....	m	28	1,2	5	20	110	75
	Mar. 7	15 00	7 24	.....	.....	.....	.....	ms	7	7	7	25	245	50
	Mar. 22	08 00	23 02	.....	.....	.....	.....	ms	22	6	6	30	130	185
	Mar. 30	10 40	31 24	s.c.	−1	+3	0	ms	30	8	6	35	265	95
									31	8	6			
uetta	Jan.l 17	03 23	20 04	s.c.	−2	+23	−4	ms	17	5,6,7	6	10	182	25
S.A.A. Kazmi)	Feb. 23	06 25	26 05	s.c.	.....	+9	.....	m	23	4,5	5	5	90	22
	Mar. 22	09 20	24 01	.....	.....	.....	.....	ms	22	4,5	6	11	192	25
	Mar. 30	10 35	1 03	.....	.....	.....	.....	ms	31	3	6	6	129	25
lisabethville	Jan. 17	03 22	19 24	s.c.	−1	+33	0	s	17	4 to 8	...	1 3	177	33
Al Alexandre)	Feb.	None												
	Mar. 22	03 20	22 24	s.c.	0	−8	+1	ms	22	4,5	...	10	264	33
inza	Jan. 11	11 20	12 04	s.c.	0	+20	−1	m	11	7,8	...	7	79	20
J. Leroy and	Jan. 17	03 22	20 03	s.c.	−1	+35	+3	ms	17	5,6,7,8	...	8	197	36
h. Staes)	Feb.	None												
	Mar.	None												

ON THE ANALYSIS OF EXPERIMENTAL RECOMBINANCE DATA USING A NON-UNIFORM RECOMBINANCE MODEL PROPOSED BY CHAPMAN

A height variation in recombinance, α, given by $\alpha = \alpha_0 (1 + e^{-cz})$, where α_0 and c are positive constants, and z is height measured in units of scale height from a *recombinance datum* level, has been proposed by Chapman.[1]

Values of these constants have been fitted to the mean experimental values of α for the range 65 to 110 km given by Mitra and Jones,[2] the best fit being obtained with $c = 1.2$ and the recombinance datum at 98 km. Figure 1 presents

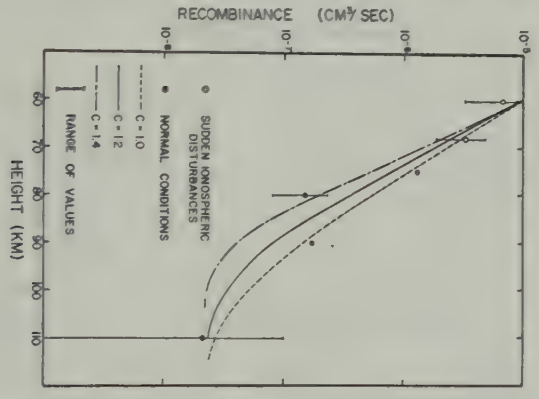

FIG. 1—Results of fitting $\alpha = \alpha_0(1 + e^{-cz})$ to the experimental recombinance values compiled by Mitra and Jones, for the range 65 to 110 km

the mean values of α from Mitra and Jones, the range of values considered by them (where given), and fitted curves for three values of c.

Using $c = 1$ and $c = 2$, and assuming a plane exponential atmosphere, values of $n_{em}(\chi)/n_{em}(0)$, where $n_{em}(\chi)$ is the maximum density of electrons when χ is the zenith angle of the sun, have been calculated as a function of $\cos \chi$ for various values of z_0, the height of the maximum absorption for $\chi = 0$, measured in scale height units from the recombinance datum.

These values for $c = 1$ are given in Table 1.

Log $n_{em}(\chi)/n_{em}(0)$ is plotted as a function of log $\cos \chi$ for $c = 1$, $c = 2$ in Figure 2. There seems to be a nearly linear relationship between log $n_{em}(\chi)/n_{em}(0)$ and log $\cos \chi$ over most of the range of χ for $c = 1$. This approximate relationship also seems to hold for $c = 2$, $z_0 = 1$, but there is more noticeable curvature for lesser values of z_0. For a constant recombinance, $n_{em}(\chi)/n_{em}(0) = (\cos \chi)^s$, where

[1]S. Chapman, Proc. Phys. Soc. (London), **67**, 717 (1954). Prof. Chapman asks us to notify corrections as follows: Equation (5), $c = bH$; equation (10), omit sec χ or alternatively change the suffixes χ to zero; in Figure 2, the ordinates are 0. 1, 0. 2, etc.

[2]A. P. Mitra and R. E. Jones, J. Geophys. Res., **59**, 391 (1954).

TABLE 1—*Values of* $n_{em}(\chi)/n_{em}(0)$ *for* $c = 1$ *as a function of* cos χ

χ	cos χ	$n_{em}(\chi)/n_{em}(0)$		
		$z_0 = 0$	$z_0 = 1$	$z_0 = -1$
0	1.00	1.00	1.00	1.00
15	0.97	0.98	0.99	0.98
30	0.87	0.95	0.95	0.95
45	0.71	0.90	0.87	0.91
60	0.50	0.79	0.75	0.83
68.5	0.37	0.70	0.66	0.76
75	0.26	0.62	0.56	0.68
85	0.09	0.38	0.33	0.44
89	0.02	0.15	0.15	0.20

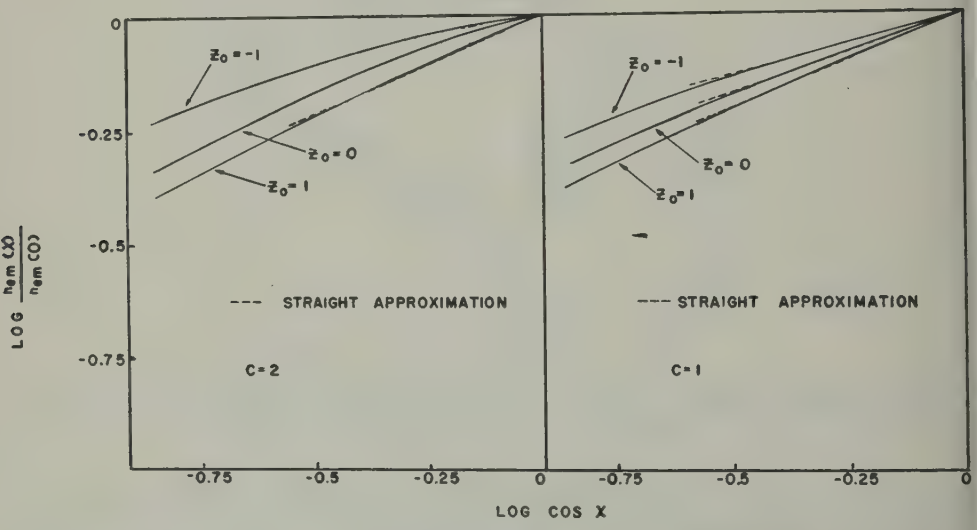

FIG. 2—$n_{em}(\chi)/n_{em}(0)$ as a function of cos χ for three values of z_0, using a non-uniform recombinance model

$s = 0.5$. Hence, it would be expected that, for larger z_0, the curves would tend more toward a straight line with $s = 0.5$. Straight-line approximations for the range 0° to 60° are also given in Figure 2. In the $c = 1$ case, the approximate s for $z_0 = -1$ is 0.28; for $z_0 = 0$, 0.36; and for $z_0 = 1$, 0.43. For $c = 1$, $z_0 = 1$, the approximation has $s = 0.46$.

We wish to thank Prof. Chapman for suggesting this problem and for his advice and encouragement.

CHONG CHOL KIM
CHARLES DICKERMAN

DEPARTMENT OF PHYSICS,
STATE UNIVERSITY OF IOWA,
Iowa City, Iowa, January 31, 1955
(Received February 16, 1955)

A RELATIONSHIP BETWEEN THE GEOMAGNETIC SECULAR VARIATION RATES

An interesting and valuable relationship between the secular variation of the horizontal field ($\dot{H}$) and the space gradient of the secular variation of the vertical intensity ($\dot{Z}$) has recently been noticed by Lundbak (private communication).[1] He shows that, if l is a distance in kilometers along a great circle on the earth's surface and $\dot{H}_l$ is the component of $\dot{H}$ in the direction l, then the ratio $(\mathrm{d}\dot{Z}/\mathrm{d}l)/\dot{H}_l$ over much of the earth's surface is about $+ 1/1400$ km^{-1}. As is usual in geomagnetism, Z is taken as positive downwards. He explains this in terms of the representation by Lowes and Runcorn (1951)[2] of the geomagnetic secular-variation field as a number of radial dipoles near the interface of the earth's mantle and core. A general derivation by spherical harmonics is given in this short note.

We suppose that the geomagnetic secular variation field near the earth's surface may be expressed as a scalar potential $\dot{V}$. Then

$$\frac{\mathrm{d}\dot{Z}}{\mathrm{d}l} \Big/ \dot{H}_l = -\left(\frac{\mathrm{d}^2\dot{V}}{\mathrm{d}r\,\mathrm{d}l} \Big/ \frac{\mathrm{d}\dot{V}}{\mathrm{d}l}\right)_{r=R}$$

If the origin of the field is external to the earth, $\dot{V}$ at a point (r, θ, ϕ) may be expressed as a series of terms $\sum (r/R)^n S_n(\theta, \phi)$, where S_n are surface harmonics of degree n and R is the radius of the earth. If the field is of internal origin, a series of terms $\sum (R/r)^{n+1} S_n(\theta, \phi)$ is taken. For a field which is well expressed by one harmonic term, Lundbak's ratio is $+ (n + 1)/R$ if of internal origin and $- n/R$ if of external origin, at all points on the surface of the earth. If the field potential is the sum of a number of harmonics, then Lundbak's ratio will vary over the surface, giving a mean value of n weighted in favour of the higher harmonics. From Lundbak's expression, we find $n = 3.5$, while Vestine, Laporte, Lange, and Scott (1947)[3] give $n = 2$ and $n = 3$ as the predominant spherical harmonics in the secular variation.

[1] A. Lundbak, unpublished dissertation (Copenhagen).

[2] F. J. Lowes and S. K. Runcorn, Phil. Trans., **243**, 525-546 (1951).

[3] E. H. Vestine, L. Laporte, I. Lange, and W. E. Scott, Carnegie Institution of Washington, Pub. No. 580 (1947).

S. K. Runcorn

Department of Geodesy and Geophysics,
University of Cambridge,
Downing Place, Cambridge, England, February 15, 1955
(Received February 21, 1955)

NOTES

(13) *Publication of second volume of "The solar system, the earth as a planet," edited by Gerard P. Kuiper*—The University of Chicago Press published early in 1955 the second volume in the series of four books. Volume II, like Volume I, is priced at $12.50. Forthcoming volumes in the series are III—Planets and comets, Part 1: Planets and satellites; and IV—Planets and comets, Part 2: Asteroids, meteorites and meteors, comets, problems and origins.

(14) *Release of total-intensity aeromagnetic map*—The United States Geological Survey has placed in open file for inspection a preliminary total-intensity aeromagnetic map of the Laramie Range, Albany County, Wyoming. The purpose of the airborne magnetometer survey by the Geological Survey was to determine possible correlation between magnetic and geologic features, especially with respect to the location of magnetite-ilmenite bodies, and the extent of and variations within the anorthosite in the area.

(15) *Annual meeting of the Society of Exploration Geophysicists*—The twenty-fifth annual meeting of the Society of Exploration Geophysicists is to be held at the Shirley Savoy Hotel in Denver, Colorado, October 3-6, 1955. The technical program will include papers on all phases of petroleum and mining geophysics. The Society's twenty-fifth year will also feature a silver anniversary celebration to honor the charter members.

(16) *High-altitude research laboratories and observatories*—The first comprehensive survey of the world's high-altitude research stations was issued in the form of a 100-page report on January 19, 1955, by the Research Division of New York University College of Engineering, which made the study for the Joint Commission on High Altitude Research Stations, an agency of the International Union of Biological Sciences and the International Council of Scientific Unions. "High altitude" is defined in the report as about 7,500 feet or above, and there are at least 42 such laboratories and observatories, it was found. There are seven in the United States. The highest station covered in the report is the 18,000-foot Chacaltaya cosmic-ray laboratory in Bolivia. Cosmic rays, radio astronomy, meteorology, astrophysics, botany, terrestrial magnetism, and solar radiation are a few of the fields which benefit from research at high altitudes.

(17) *Antarctic expeditions planned by France*—Definite plans for a series of French antarctic expeditions during the next three years, including establishment of an observation post at the South Magnetic Pole primarily for magnetic measurements and a possible 1800-mile overland snow-tractor project to the South Pole, have recently been announced. They will be under the general direction of Paul Emile Victor, who has led numerous French arctic and antarctic expeditions. The first party is expected to leave Rouen in October 1955 under the command of Robert Guillard. A primary station will be established at Cape Geologie on the coast of Adélie Land, the narrow sector of Antarctica claimed as French territory.

The expeditions will be connected with the 1957-58 International Geophysical Year.

(18) *Viking rocket reaches 144-mile altitude*—On February 5, 1955, at the White Sands Proving Grounds, New Mexico, United States Navy scientists sent a Viking rocket, the twelfth in the single-stage series, to a height of 144 miles (232 km) into the air, in order to obtain information on the thermal barrier itself and its effect on an earth-launched rocket. The thermal barrier, unlike the sound barrier, becomes more and more of a problem as an aircraft's speed increases. When aircraft reach certain high speeds, they become dangerously overheated. This situation is most acute for a rocket when it returns to the earth's atmosphere.

(19) *Center of Milky Way galaxy determined*—Using radio waves of various lengths, measurements made by scientists at the U.S. Naval Research Laboratory, at Ohio State University, and by Australian and Dutch astronomers have been combined to give a new precise location of the center of the Milky Way galaxy. The center of the Milky Way galaxy, it is concluded, is 8,500 parsecs from the sun, or 166,260,000,000,000,000 miles, at a right ascension of 17 hours, 42 minutes and 40 seconds, and a declination of minus 28 degrees, 50 minutes and 55 seconds. This confirms previous less-exact positions that also put the galactic center in the constellation of Sagittarius, the archer, which becomes visible low in the southeast sky in May. The position is based on the variations in intensity of the different radio-wave frequencies at the center, and is a weighted average of the different measurements at four institutions. The exact location of the nucleus of our galaxy had long been sought by optical astronomers, but it is hidden from view by vast clouds of interstellar dust. Radio waves, however, penetrate these dust clouds, even though light waves do not.

(20) *Radiometric sextant*—As the first practical application in a man-made gadget of the new science of radio astronomy, the United States Office of Naval Research reported the development of a "radiometric sextant" which within certain limitations can track automatically the sun and moon under any weather conditions. It consists of a highly directional antenna and very sensitive receiving equipment to pick up the continuous radio-wave emission (noise) of the two heavenly bodies. Because of its highly directional antenna and operation on a very high frequency, it is not likely to be disturbed by local or man-made static. The United States Navy has been conducting tests on the use of the sextant for navigation of surface ships. Although the present sextant cannot be used on stars, the ultimate aim is to track on either sun or stars.

(21) *Special geomagnetic number of the Indian Journal of Meteorology and Geophysics*—To commemorate the Golden Jubilee of the Alibag Magnetic Observatory, Bombay, India, a special geomagnetic number (Vol. 5, Dec., 1954) of the Indian Journal of Meteorology and Geophysics was published recently. The unusually large issue, containing 240 pages, has an appropriate golden cover. In addition to historical accounts of geomagnetic observations in India, some 26 well-known geophysicists throughout the world contributed papers. The publication will serve as a permanent tribute to India's long participation in studies of geomagnetism, of which she may well be proud.

(22) *Geomagnetic activities of the United States Coast and Geodetic Survey*—

Two volumes of the MHV series of publications were issued, giving magnetic hourly values and reproductions of magnetograms for Honolulu, 1951, and for Sitka, 1952.

Lt. Rojana Hongprasith and Capt. Vera Suvannus of Thailand have been studying the methods and procedures of the U.S. Coast and Geodetic Survey in office and field work in geomagnetism.

(23) *Personalia*—The Royal Astronomical Society of Great Britain has recently awarded the Gold Medal to Prof. *Dirk Brouwer*, director of the Yale University Observatory, for outstanding contributions to celestial mechanics; and the Eddington Medal to Prof. *H. C. van de Hulst*, of Leyden Observatory, for his prediction of the 21-cm line radiation of neutral hydrogen, and for his share in its detection and observation and in the theoretical interpretation of the observations. Prof. Brouwer will go to England this spring for a presentation ceremony and to deliver the Darwin lectures.

Among the 25 new members elected to fellowship in the Royal Society on March 17, 1955, were Prof. *A. C. B. Lovell*, professor of radio astronomy, University of Manchester, and Prof. *D. R. Bates*, professor of applied mathematics, The Queen's University, Belfast.

It is with regret that we have learned of the death of Prof. *Erich Regener*, director of the Max-Planck-Institut für Physik der Stratosphäre in Weissenau (near Stuttgart, Germany), after a brief illness on February 27, 1955, at the age of 74. He will be remembered for his work on atmospheric physics, in particular for his pioneer observations on ozone.

Under the auspices of the Smithsonian Institution, Washington, D.C., Sir *Harold Spencer Jones*, the Astronomer Royal of Great Britain, delivered on April 27, 1955, the twenty-second annual James Arthur lecture on the sun, entitled "Solar activity and its terrestrial effects."

LIST OF RECENT PUBLICATIONS

By W. E. Scott

Department of Terrestrial Magnetism,
Carnegie Institution of Washington,
Washington, D. C.

(Received March 31, 1955)

A—Terrestrial Magnetism

Bartels, J., and J. Veldkamp. International data on magnetic disturbances, third quarter, 1954. J. Geophys. Res., **60**, No. 1, 105-107 (1955).

Bullard, E., and H. Gellman. Homogeneous dynamos and terrestrial magnetism. Phil. Trans. R. Soc., A, **247**, 213-278 (Nov. 30, 1954).

Campbell, J. B. Cheltenham three-hour-range indices *K* for October to December, 1954. J. Geophys. Res., **60**, No. 1, 108 (1955).

Copenhagen, Det Danske Meteorologiske Institut. Magnetisk Årbog. 1ste del: Danmark (undtagen Grönland)—Annuaire magnétique, 1ere partie: Le Danemark (excepté le Groenland), 1953. Köbenhavn, 27 pp. (1954). 32 cm.

Cullington, A. L. The geomagnetic field in New Zealand at epoch 1950.5. Department of Scientific and Industrial Research, Geophys. Mem. 2, Wellington, R. E. Owen, Govt. Printer, 32 pp. + 7 isomagnetic charts (1954). 28 cm.

Dauvillier, A. IV—Le magnétisme des corps célestes. Tome troisième: Les aurores polaires et la luminescence nocturne. Paris, Hermann et Cie, 143 pp. + 52 figs. (1954). 25 cm. [Actualités scientifiques et industrielles, No. 1210.]

Gaibar-Puertas, C. Variación secular del campo geomagnético. Observatorio del Ebro, Mem. No. 11, 475 pp. + 55 tables + 80 figs. (1953). 25 cm.

Grenet, G. Explication qualitative du début de certaines perturbations magnétiques polaires au moyen de la théorie de Chapman et Ferraro. Paris, C.-R. Acad. sci., **240**, No. 4, 448–450 (1955).

Grenet, G., Y. Kato, J. Ossaka, and M. Okuda. Pulsations in terrestrial magnetic field at the time of bay disturbances. Sci. Rep. Tôhoku Univ., Ser. 5, Geophysics, **6**, No. 1, 1-10 (1954).

Heppner, J. P. Notes on the occurrence of world-wide s.c.'s during the onset of negative bays at College, Alaska. J. Geophys. Res., **60**, No. 1, 29-32 (1955).

Hospers, J., and H. A. K. Charlesworth. The natural permanent magnetization of the lower basalts of Northern Ireland. Mon. N. R. Astr. Soc., Geophys. Sup., **7**, No. 1, 32-43 (1954).

Hospers, J. Rock magnetism and polar wandering. J. Geol., **63**, No. 1, 59-74 (1955).

International Association of Terrestrial Magnetism and Electricity. Enquête sur les appareils enregistreurs des variations rapides du champ magnétique terrestre. Committee on Observational Technique, Rapport technique No. 1, 46 pp., mim. (rec'd March 15, 1955).

Kawai, N., S. Kume, and S. Sasajima. Magnetism of rocks and solid phase transformation in ferromagnetic minerals. II. Proc. Japan Acad., **30**, No. 9, 864-868 (1955).

Kazmi, S. A. A., and K. A. Wienert. Magnetic observations during the total sun eclipse of 30th June 1954, at the magnetic observatory of Quetta. J. Geophys. Res., **60**, No. 1, 95-96 (1955).

Lewis, R. P. W., D. H. McIntosh, and R. A. Watson. Annual variation of the magnetic elements. J. Geophys. Res., **60**, No. 1, 71-74 (1955).

Lovö. Ergebnisse der Beobachtungen des magnetischen Observatoriums zu Lovö (Stockholm) im Jahre 1951. Von Nils Ambolt. Stockholm, Kungl. Sjökarteverket, 30 pp. (1953). 31 cm.

Lovö. Ergebnisse der Beobachtungen des magnetischen Observatoriums zu Lovö (Stockholm) im Jahre 1952. Von Folke Eleman und Kjell Borg. Stockholm, Kungl. Sjökarteverket, 30 pp. (1954). 31 cm.

Matsuzaki, H., K. Kobayashi, and K. Momose. On the anomalously strong natural remanent

magnetism of the lava of Mt. Utsukushi-ga-hara. Kyoto, J. Geomag. Geoelectr., **6**, No. 2, 53-56 (1954).

Mauritius, Royal Alfred Observatory. Results of magnetical and meteorological observations for the months of July to December 1950 (v. 35, pts. 7 to 12). Port Louis, J. E. Félix, Govt. Printer, each part 14 to 16 pp. (May 1954 to Sept. 1954). 34 cm.

Mauritius, Colony of. Annual report of the Observatory Department for the year 1953. Port Louis, J. E. Félix, Govt. Printer, No. 32 (July 1954). 25 cm. [Contains mean values of the magnetic elements for 1953 derived from eye observations.]

Morais, J. C. Algunas observações do magnetismo terrestre nos Açores. Mem. Not. Public. Mus. Lab. Min. Geol. Univ. Coimbra, No. 37, 1-19 (1954).

Nagamiya, T., K. Yosida, and R. Kubo. Antiferromagnetism. Adv. Phys., **4**, No. 13, 1-112 (1955).

Nagata, T. Umgekehrte Magnetisierung eruptiver Gesteine. Naturwiss., **42**, Heft 3, 62-64 (1955).

Nagata, T., and S. Uyeda. Interaction of two constituents in ferromagnetic materials showing reverse thermo-remanent magnetism. Nature, **175**, 35-36 (Jan. 1, 1955). [Letter to Editor.]

Ota, M. An analysis on the diurnal variation of the terrestrial magnetism, especially on the daytime-variation of geomagnetically quiet days. Kyoto, J. Geomag. Geoelectr., **6**, No. 2, 83-98 (1954).

Pecker, J.-C., and W. O. Roberts. Solar corpuscles responsible for geomagnetic disturbances. J. Geophys. Res., **60**, No. 1, 33-44 (1955).

Procopiu, S. Le moment magnétique de la Terre a commencé à croître. J. Geophys. Res., **60**, No. 1, 114 (1955). [Letter to Editor.]

Roquet, J. Sur les rémanences magnétiques des oxydes de fer et leur intérêt en géomagnétisme. Ann. Géophys., **10**, No. 3, 226-247, and No. 4, 282-325 (1954).

Runcorn, S. K. Recent progress in the theory of the main geomagnetic field. Sci. Prog., **43**, No. 169, 13-27 (1955).

Scholte, J. G., and J. Veldkamp. Geomagnetic and geoelectric variations. J. Atmos. Terr. Phys., **6**, No. 1, 33-45 (1955).

Shimazaki, T. Correlation between the solar corona and the geomagnetism for the remarkable *M*-regions in 1950-1953. J. Radio Res. Labs. Japan, **1**, No. 5, 51-61 (1954).

Smyth, M. J. Photoelectric investigations of solar corpuscular radiation, I. Mon. Not. R. Astr. Soc., **114**, No. 2, 137-153 (1954).

Thiruvengadathan, A. Diurnal variation of horizontal magnetic force at Kodaikanal. Indian J. Met. Geophys., **5**, No. 3, 267-271 (1954).

Toledo, Observatorio Central Geofísico. Geomagnetismo, año 1949. [Prepared by J. Sancho de San Roman.] Madrid, Instituto Geografico y Catastral, 76 pp. + 14 graphs (1953). 24 cm.

United States Coast and Geodetic Survey. Magnetograms and hourly values, Honolulu, T.H., 1951. Washington, D.C., U.S. Coast Geod. Surv., No. MHV-Ho51, 140 pp. (1954). 25 cm.

United States Coast and Geodetic Survey. Magnetograms and hourly values, Sitka, Alaska, 1952. Washington, D.C., U.S. Coast Geod. Surv., No. MHV-Si52, 159 pp. (1954). 25 cm.

Valentia Observatory. Magnetic observations at Valencia Observatory 1941-1953 with an account of observations made since 1888. Dublin, Dept. of Industry and Commerce, Meteorological Service, 45 pp., mim. (Sept. 1954). 33 cm.

Vassouras, Observatório Magnético de. Observações da amplitude diurna da componente horizontal do camp magnético na Ilha de Fernando de Noronha. Rio de Janeiro, Ministério da Educação e Cultura, Pub. No. 2, 8 pp. (1953).

Wingst Observatorium. Ergebnisse der erdmagnetischen Beobachtungen im Observatorium Wingst in den Jahren 1949 und 1950. D. Hydrogr. Inst., Hamburg, Jahrb. No. 7, 163 pp. (1954). 25 cm.

Witteveen Magnetic Observatory. Yearbook 1950. B—Geomagnetism(K. Nederlands Met. Inst. No. 98). 's-Gravenhage, iv + 28 pp. (1953). 34 cm. [Contains hourly values of the magnetic elements for 1950 at Witteveen.]

B—Terrestrial Electricity

Bruce, C. E. R. The leader strokes of the lightning and spark discharges. J. Inst. Elec. Eng., **1** (new series), No. 1, 38 (1955). [Correspondence.]

Gunn, R. The electrification of mist and rain in the lower atmosphere. J. Geophys. Res., **60**, No. 1, 23-27 (1955).

Harris, D. L. Effects of radioactive debris from nuclear explosions on the electrical conductivity of the lower atmosphere. J. Geophys. Res., **60**, No. 1, 45-52 (1955).

Hess, V. F. The role of eddy diffusion in the distribution of ions in the atmosphere near the ground. Nuovo Cimento, **1** (new series), No. 1, 51-62 (1955).

Hess, V. F., and W. D. Parkinson. On the contribution of alpha rays from the ground to the total ionization of the lower atmosphere. Trans. Amer. Geophys. Union, **35**, No. 6 (Pt. 1), 869-871 (1954).

Kano, M. A note on the Workman-Reynolds' theory of thunderstorm charge generation. Pap. Met. Geophys., **5**, No. 1, 47-53 (1954).

Malan, D. J. Les décharges orageuses intermittentes et continues de la colonne de charge négative. Ann. Géophys., **10**, No. 4, 271-281 (1954).

Venkiteshwaran, S. P., B. K. Gupta, and B. B. Huddar. Measurement of the electrical potential gradient in the atmosphere by radiosonde. Indian J. Met. Geophys., **5**, No. 3, 253-256 (1954)

C—Cosmic Rays

Alfvén, H. On the origin of cosmic radiation. Tellus, **6**, No. 3, 232-253 (1954).

Bachelet, F., and A. M. Conforto. Time variations of cosmic ray intensity. Nuovo Cimento, **12**, No. 6, 923-929 (1954).

Brunberg, E.-Å., and A. Dattner. Variations of the cosmic ray intensity during magnetic storms. Tellus, **6**, No. 3, 254-259 (1954).

Chaloupka, P. Influence of the geomagnetic field on the extensive air showers. Phys. Rev., **96**, No. 6, 1709 (1954). [Letter to Editor.]

Chasson, R. L. Cosmic-ray intensity fluctuations at sea level. Phys. Rev., **96**, No. 4, 1116-1123 (1954).

Chupp, E. L. Cosmic ray time variations. Berkeley, University of California, 29 pp. + 11 figs., mim. (Feb. 1, 1955). 28 cm.

Heidmann, J. Sur un schéma de théorie de l'origine des rayons cosmiques. Paris, C.-R. Acad. sci., **240**, No. 5, 511-513 (1955).

Heidmann, J. Sur une théorie de l'origine des rayons cosmiques. Paris, C.-R. Acad. sci., **240**, No. 6, 618-620 (1955).

Maeda, K., and M. Wada. Atmospheric temperature effect upon the cosmic-ray intensity at sea level. J. Sci. Res. Inst., Tokyo, **48**, No. 1350, 71-79 (1954).

McClure, G. W. Composition of the primary cosmic radiation at $\lambda = 10°$ N. Phys. Rev., **96**, No. 5, 1391-1400 (1954).

Meyer, P., and J. A. Simpson. Changes in amplitude of the cosmic-ray 27-day intensity variation with solar activity. Phys. Rev., **96**, No. 4, 1085-1088 (1954).

Parker, E. N. The propagation of hydromagnetic waves and the acceleration of cosmic rays. Salt Lake City, University of Utah, Tech. Rep. No. 13, 21 pp., mim. (Jan. 12, 1955). 28 cm.

Pomerantz, M. A. Primary alpha particles in the cosmic radiation near the geomagnetic equator. J. Frank. Inst., **258**, No. 6, 443-459 (1954).

Wada, M., and S. Kudō. The relation between cosmic-ray intensities and heights of isobar levels. II—On the positive temperature effect. J. Sci. Res. Inst., Tokyo, **48**, No. 1370, 245-259 (1954).

D—Upper Air Research

Appleton, E. Storms in the ionosphere. Endeavour, **14**, No. 53, 24-28 (1955).

Ashburn, E. V. Measurements of the specific intensities of the auroral green line at College, Alaska. J. Atmos. Terr. Phys., **6**, No. 1, 57-60 (1955).

Banerji, R. B. The autocorrelogram of randomly fading waves. J. Atmos. Terr. Phys., **6**, No. 1, 50-56 (1955).

Bonnet, G. Une particularité de la couche *F*2 à Lwiro. Ann. Géophys., **10**, No. 4, 348-350 (1954).

Booker, H. G., C. W. Gartlein, and B. Nichols. Interpretations of radio reflections from the aurorae. J. Geophys. Res., **60**, No. 1, 1-22 (1955).

Bray, W. J., H. G. Hopkins, F. A. Kitchen, and J. A. Saxton. Review of long-distance radio-wave propagation above 30 Mc/s. Proc. Inst. Elec. Eng., B, **102**, No. 1, 87-95 (1955).

Budden, K. G. The numerical solution of differential equations governing reflexion of long radio waves from the ionosphere. Proc. R. Soc., A, **227**, No. 1171, 516-537 (1955).

Chamberlain, J. W. The ultraviolet airglow spectrum. Astroph. J., **121**, No. 1, 277-286 (1955).

Davies, K., and E. L. Hagg. Ionospheric absorption measurements at Prince Rupert. J. Atmos. Terr. Phys., **6**, No. 1, 18-32 (1955).

Donahue, T. M., and A. Foderaro. The effect of resonance absorption on the determination of the height of airglow layers. J. Geophys. Res., **60**, No. 1, 75-86 (1955).

Dyce, R. More about V.H.F. auroral propagation—Recent findings and suggestions for improved results. QST, **39**, No. 1, 11-15 (1955).

Eyfrig, R., E. Harnischmacher, et K. Rawer. Informations obtenues à l'aide des cartes d'ionisation. Paris, C.-R. Acad. sci., **240**, No. 4, 446-448 (1955).

Fan, C. Y., and D. H. Schulte. Variations in the auroral spectrum. Astroph. J., **120**, No. 3, 563-565 (1954).

Ghosh, M. Geomagnetic control of the $F1$ region of the ionosphere. J. Geophys. Res., **60**, No. 1, 115-116 (1955). [Letter to Editor.]

Giovanelli, R. G. The attenuation of light by meteoric dust in the upper atmosphere. Aust. J. Phys., **7**, No. 4, 641-648 (1954).

Gordon, W. E. Radio scattering in the troposphere. Proc. Inst. Radio Eng., **43**, No. 1, 23-28 (1955).

Gough, M. W. Some features of V.H.F. tropospheric propagation. Proc. Inst. Elec. Eng., B, **102**, No. 1, 43-58 (1955).

Harnischmacher, E. Sur une influence lunaire relative à l'ionisation maximum de la couche ionosphérique *E*. Paris, C.-R. Acad. sci., **240**, No. 5, 553-555 (1955).

Hartsfield, W. L. Observations of distant meteor-trail echoes followed by ground scatter. J. Geophys. Res., **60**, No. 1, 53-56 (1955).

Jones, R. E. The development of an *E*-region model consistent with long wave phase path measurements. J. Atmos. Terr. Phys., **6**, No. 1, 1-17 (1955).

Kaiser, T. R. A symposium on meteor physics at Jodrell Bank. Observatory, **74**, No. 882, 195-208 (1954).

Kamiyama, H. Ion production rate in an atmosphere of exponentially rising temperature with height. Sci. Rep. Tôhoku Univ., Ser. 5, Geophysics, **6**, No. 1, 11-18 (1954).

Koster, J. R., and L. R. O. Storey. An attempt to observe whistling atmospherics near the magnetic equator. Nature, **175**, 36-37 (Jan. 1, 1955). [Letter to Editor.]

Kundu, M. R. Velocity of movement of sporadic *E* clouds. Science and Culture, **20**, No. 6, 303 (1954).

Larsen, S. H. H. Vertical distribution of atmospheric ozone at Longyearbyen, Spitzbergen (78°N). J. Atmos. Terr. Phys., **6**, No. 1, 46-49 (1955).

Leak, W. M. Rocket research at NRL. Washington, D.C., Naval Research Laboratory, NRL Rep. No. 4441, 26 pp. (Nov. 12, 1954). 27 cm.

Lejay, P., and D. Lepechinsky. Influence de l'inclinaison du champ magnétique terrestre sur l'absorption des ondes radioélectriques dans la couche *D*. Paris, C.-R. Acad. sci., **240**, No. 2, 136-138 (1955).

Lepechinsky, D., and J. Durand. Sur les conditions de réflexion verticale dans l'ionosphère en présence des chocs et du champ magnétique terrestre. Cas de la couche *E*. Paris, C.-R. Acad. sci., **240**, No. 3, 333-336 (1955).

Lovell, A. C. B. Meteor astronomy. Oxford, Clarendon Press, xiv + 463 (1954). 24 cm. [Comprehensive study of meteors by photography and radio; price 60 sh. net.]

Maxwell, A. Turbulence in the upper ionosphere. Phil. Mag., **45**, No. 371, 1247-1254 (1954).

McNamara, A. G., and B. W. Currie. Polarization of radio echoes from aurorae. Nature, **174**, 1153-1154 (Dec. 18, 1954). [Letter to Editor.]

Meek, J. H. East-west motion of aurorae. Astroph. J., **120**, No. 3, 602-603 (1954). [Note.]

Mitra, A. P. Ionospheric ionization associated with sudden ionospheric disturbances. Pennsylvania State University, Ionosphere Res. Lab., Sci. Rep. No. 60, 62 pp., mim. (March 30, 1954). 28 cm.

Mitra, A. P. Nocturnal recombination processes in the lower ionosphere. Pennsylvania State University, Ionosphere Res. Lab., Sci. Rep. No. 68, 76 pp., mim. (Sept. 1, 1954). 28 cm.

Obayashi, T. On the world-wide disturbance in $F2$-region. Kyoto, J. Geomag. Geoelectr., **6**, No. 2, 57-67 (1954).

Ochs, A. Über die Messung der Dämpfung in der Ionosphäre. Archiv Elektr. Uebertrag., **8**, Heft 12, 535-544 (1954).

Pettit, H. B., H. E. Roach, P. St. Amand, and D. R. Williams. A comprehensive study of atomic emissions in the nightglow. Ann. Géophys., **10**, No. 4, 326-347 (1954).

Ramachandra Rao, B., and E. Bhagiratha Rao. A continuous radio wave method of studying travelling disturbances in the ionosphere. J. Sci. Industr. Res., New Delhi, **13**, No. 10, 462-466 (1954).

Rawer, K. Sur l'interpretation des mesures de la couche ionosphérique F_1. Paris, C.-R. Acad. sci., **240**, No. 3, 331-333 (1955).

St. Amand, P., and E. V. Ashburn. The frequency distribution of the intensity of aurorae and the night airglow for 5577[OI]. J. Geophys. Res., **60**, No. 1, 112-113 (1955). [Letter to Editor.]

Sen Gupta, P. K. Periodic influx of interplanetary dust particles into the terrestrial atmosphere. Indian J. Met. Geophys., **5**, No. 3, 272-276 (1954).

Shimazaki, T. The effect of the solar tides and the temperature change on the daily variation in electron density and height of the $F2$-layer. Kyoto, J. Geomag. Geoelectr., **6**, No. 2, 68-82 (1954).

Sinno, K. On the variation of the $F2$ layer accompanying geomagnetic storms (second report)—On the relations between the grade of geomagnetic activity and the ionospheric $F2$ disturbance. J. Radio Res. Labs. Japan, **1**, No. 6, 127-133 (1954). [This report is a sequel of Rep. Ionosphere Res. Japan, **7**, 7 (1953).]

Švestka, Z. The problem of a meteoritic dust layer in the earth atmosphere. Bull. Astron. Inst. Czechosl., **5**, No. 5, 91-98 (1954).

Toman, K. Movement of the F-region. J. Geophys. Res., **60**, No. 1, 57-70 (1955).

Uyeda, H., and Y. Nakata. Continuous sweep frequency traces, their properties and applications. J. Radio Res. Labs. Japan, **1**, No. 6, 17-30 (1954).

Wait, J. R., and C. Froese. Reflection of a transient electromagnetic wave at a conducting surface. J. Geophys. Res., **60**, No. 1, 97-103 (1955).

Whale, H. A. Widespread diurnal variations of effective slope of the ionosphere. Nature, **175**, 77-78 (Jan. 8, 1955).

Yerg, D. G. Viscosity in the high atmosphere. J. Geophys. Res., **60**, No. 1, 87-94 (1955).

E—Radio Astronomy

Bracewell, R. N. Using cosmic radio waves to study solar flares. Observatory, **74**, No. 881, 155-157 (1954).

Bracewell, R. N., and J. A. Roberts. Aerial smoothing in radio astronomy. Aust. J. Phys., **7**, No. 4, 615-640 (1954).

Chvojková, A., et F. Link. Echos lunaires sur 20 MHZ et structure de l'ionosphère. Bull. Astron. Inst. Czechosl., **5**, No. 5, 99-104 (1954).

Hanbury Brown, R. The remnants of supernovae as radio sources in the Galaxy. Observatory, **74**, No. 882, 185-194 (1954).

Kraus, J. D., and H. C. Ko. A detailed radio map of the sky. Nature, **175**, 159-161 (Jan. 22, 1955). [Letter to Editor.]

Kraus, J. D., H. C. Ko, and S. Matt. Galactic and localized source observations at 250 megacycles per second. Astr. J., **59**, No. 11, 439-443 (1954).

Kwee, K. K., C. A. Muller, and G. Westerhout. The rotation of the inner parts of the galactic system. Bull. Astron. Inst. Netherlands, **12**, No. 458, 211-222 (1954).

Pawsey, J. L. A catalogue of reliably known discrete sources of cosmic radio waves. Astroph. J., **121**, No. 1, 1-5 (1955).

Reber, G. Radio astronomy in Hawaii. Nature, **175**, 78-79 (Jan. 8, 1955).

Reber, G. Fine structure of solar radio transients. Nature, **175**, 132 (Jan. 15, 1955).

Takahashi, T., M. Onoue, and K. Kawakami. Character of 200 Mc noise observation equipment installed at Hiraiso Radio Wave Observatory. J. Radio Res. Labs. Japan, **1**, No. 6, 41-53 (1954).

F—Earth's Crust and Interior

Båth, M. The elastic waves Lg and Rg along Euroasiatic paths. Ark. Geofys., **2**, No. 13, 295-342 (1954).

Deutsche Geodätische Kommission. Beitrag zum deutschen Schweregrundnetz und zur Geoidbestimmung aus Schwere-Anomalien. München, D. Geodätischen Forschungsinst., No. 19, 67 pp. + map (1954). 30 cm.

Hershberger, J. Recent developments in strong-motion analysis. Bull. Seis. Soc. Amer., **45**, No. 1, 11-21 (1955).

Liubimova, Ye. A. Effect of radioactive decay on the thermal regime of the earth and the role of thermal conductivity in the thermal regime of the earth. Ottawa, Defence Research Board, No. T145R, 19 pp. + 6 figs., mim. (Nov., 1954). 27 cm. [English translations from Izvest. Akad. Nauk SSSR, Sér. Géofiz., No. 2, 3-14, 1952, and No. 6, 523-525, 1953.]

Nuttli, O. W. The P wave and the earth's core. Trans. Amer. Geophys. Union, **35**, No. 6 (Pt. 1), 962-968 (1954).

Patterson, C., G. Tilton, and M. Inghram. Age of the earth. Science, **121**, 69-75 (Jan. 21, 1955).

Perri, E. Sopra un'onda lenta superficiale provocata da esplosione vicina: I. Geofisica pura e appl., **27**, 7-29 (1954).

Shimazu, Y. Equation of state of materials composing the earth's interior, Part II. J. Earth Sci. Nagoya Univ., **2**, No. 2, 95-172 (Sept. 1954).

Shor, G. G., Jr. Deep reflections from Southern California blasts. Trans. Amer. Geophys. Union, **36**, No. 1, 133-138 (1955).

Suzuki, Z., and H. Sima. On forms of seismic waves generated by explosion, I. Sci. Rep. Tôhoku Univ., Ser. 5, Geophysics, **6**, No. 1, 85-94 (1954).

Toledo, Observatorio Central Geofísico. Corrientes telúricas, año 1951. [Prepared by Luis. de Miguel y González Miranda.] Madrid, Instituto Geografico y Catastral, 50 pp. + 13 figs, (1954). 24 cm.

Toledo, Observatorio Central Geofísico. Saltos bruscos en corrientes telúricas y su relación con los impulsos bruscos del campo magnético terrestre. [By Luis de Miguel y González Miranda.] Madrid, Instituto Geografico y Catastral, 17 pp. (1954). 24 cm.

Volchok, H. L., and J. L. Kulp. The ionium method of age determination. Columbia University, Lamont Geological Observatory, 167 pp., mim. (Jan. 1955). [Final technical report, Office of Naval Research contract.]

G—Miscellaneous

Babcock, H. W., and H. D. Babcock. The sun's magnetic field and corpuscular emission. Nature, **175**, 296 (Feb. 12, 1955).

Chapman, S. The International Geophysical Year, 1957-58. Nature, **175**, 55-56 (Jan. 8, 1955).

Ewing, A. International look at earth. Science News Letter, **67**, No. 3, 42-43 (1955). [Regarding International Geophysical Year 1957-58.]

Ferraro, V. C. A. Geophysical aspects of solar flares. Nature, **175**, 242-244 (Feb. 5, 1955). [Subject of geophysical discussion held at the Royal Astronomical Society, November 26, 1954, with Prof. Ferraro in the chair.]

Geophysical Commission. Geophysical Research in Norway 1953-54. Bergen, Annual Report No. 4 (1/7 1953—30/6 1954), 22 pp. (January 1955). 22 cm.

Plumpton, C., and V. C. A. Ferraro. On toroidal magnetic fields in the sun and stars. Astroph. J., **121**, No. 1, 168-174 (1955).

NOTICE

When available, single unbound volumes can be supplied at $6 each and single numbers at $2 each, postpaid.

Charges for reprints and covers

Reprints can be supplied, but prices have increased considerably and costs depend on the number of articles per issue for which reprints are requested. It is no longer possible to publish a schedule of reprint charges, but if reprints are requested approximate estimates will be given when galley proofs are sent to authors. Reprints without covers are least expensive; standard covers (with title and author) can be supplied at an additional charge. Special printing on covers can also be supplied at further additional charge.

Fifty reprints, without covers, will be given to institutions paying the publication charge of $8 per page.

Alterations

Major alterations made by authors in proof will be charged at cost. Authors are requested, therefore, to make final revisions on their typewritten manuscripts.

Orders for back issues and reprints should be sent to Editorial Office, 5241 Broad Branch Road, N.W., Washington 15, D.C., U.S.A.

Subscriptions are handled by The Editorial Office, 5241 Broad Branch Road, N.W., Washington 15, D.C., U.S.A.

CONTENTS—Concluded